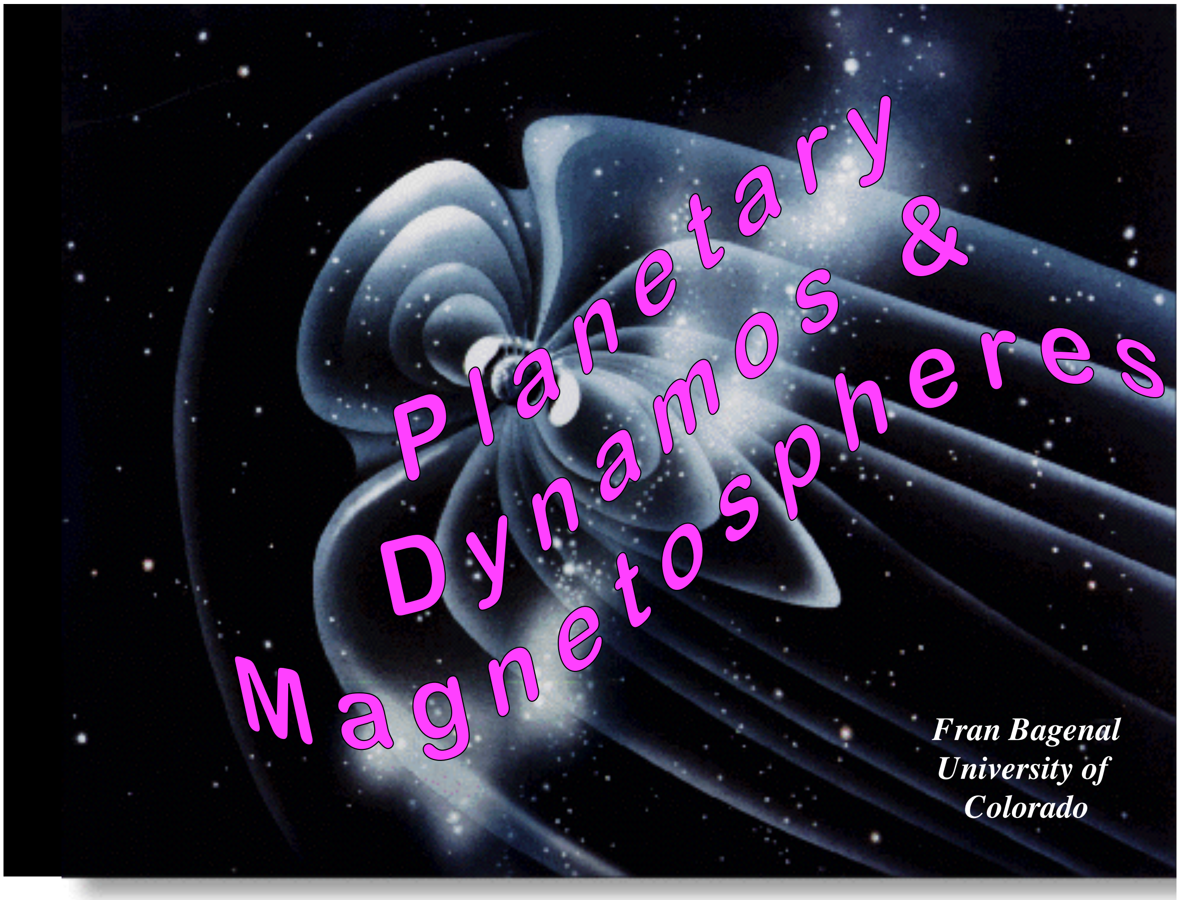


Which topic is (probably, at this point in time) your primary interest?

1. Solar physics
2. Heliosphere
3. Earth ionosphere/magnetosphere
4. Planetary space physics

# Planetary Dynamos & Magnetospheres

See vol. III ch. 7 & vol. I ch. 13

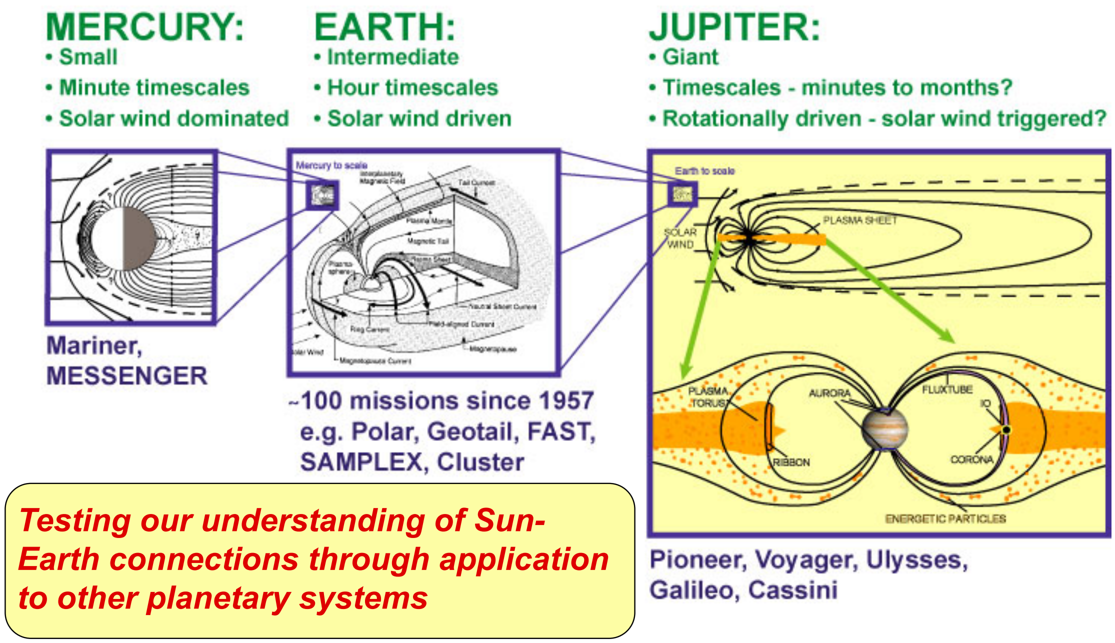


Table 3 Planetary Magnetic Fields

| | Ganymede | Mercury | Earth | Jupiter | Saturn | Uranus | Neptune |
|---|---|---|---|---|---|---|---|
| $B_{Dipole}{}^{a}$ (nT) | 719 | 170-270 | 30,600 | 430,000 | 21,400 | 22,800 | 14,200 |
| Maximum / Minimum[b] | 2 | ~2 | 2.8 | 4.5 | 4.6 | 12 | 9 |
| Dipole Tilt and Sense[c] | -4° | ~+10° | +9.92° | -9.4° | -0.0° | -59° | -47° |
| Dipole offset[d] ($R_P$) | - | - | - | 0.119 | 0.038 | 0.352 | 0.485 |
| Obliquity[e] | 0° | 0° | 23.5° | 3.1° | 26.7° | 97.9° | 29.6° |
| Range in Solar Wind Angle[f] | 90° | 90° | 67-114° | 87-93° | 64-117° | 8-172° | 60-120° |

[a] Surface field at dipole equator. Values derived from modeling the magnetic field as an offset, tilted dipole (OTD).

[b] Ratio of maximum surface field to minimum (equal to 2 for a centered dipole field). This ratio increases with larger non-dipolar components and tends to increase with the planet's oblateness.

[c] Angle between the magnetic and rotation axes. Positive values correspond to magnetic field directed north at the equator.

[d] Values for the giant planets come from dipole (OTD) models of Connerney (1993). The Earth's dipole is from the International Geomagnetic Reference Field while the magnetic dip poles of the Earth's field are located (in 2010) at 85°N and 64°S latitudes and moving over 10 degrees per century (Finlay et al. 2010).

[e] The inclination of a planet's spin equator to the ecliptic plane.

[f] Range of angle between the radial direction from the sun and the planet's rotation axis over an orbital period. In Ganymede's case, the angle is between the corotational flow and the moon's spin axis.

Vol. I Ch. 13 (updated as *Bagenal 2011*)

# Tilts and Obliquities

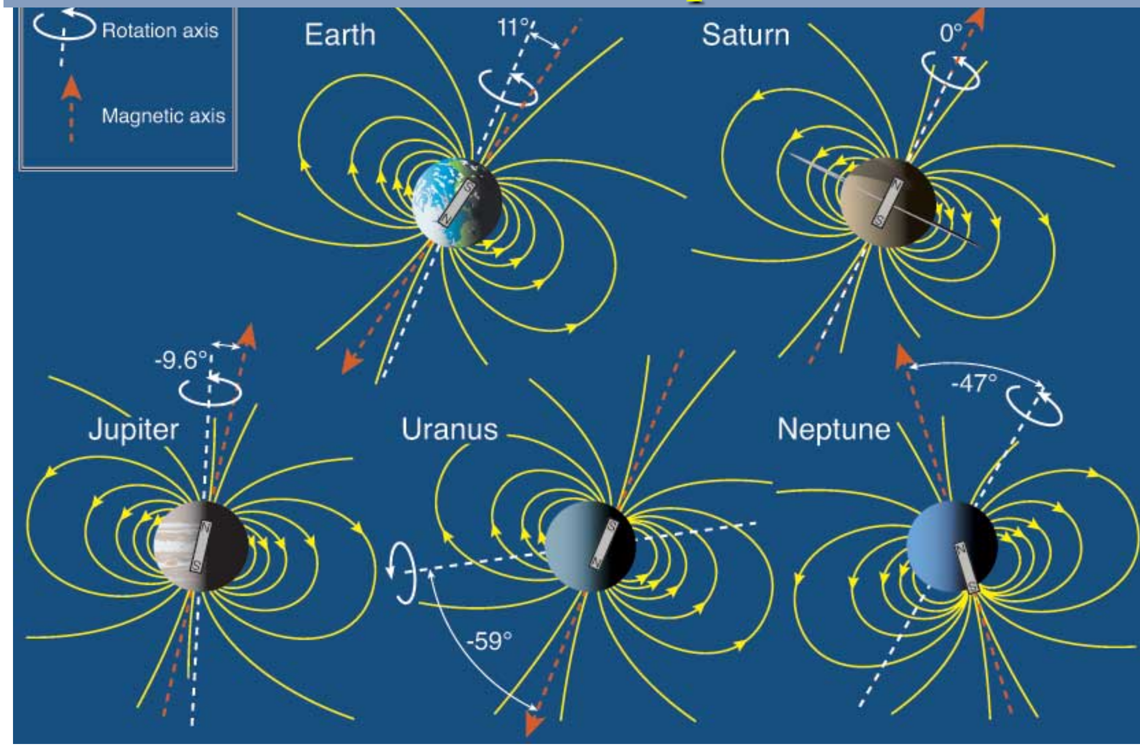


Offset Tilted Dipole (poor) Approximation

*Stanley & Glatzmaier 2010*

$B_{radial}$ @ surface

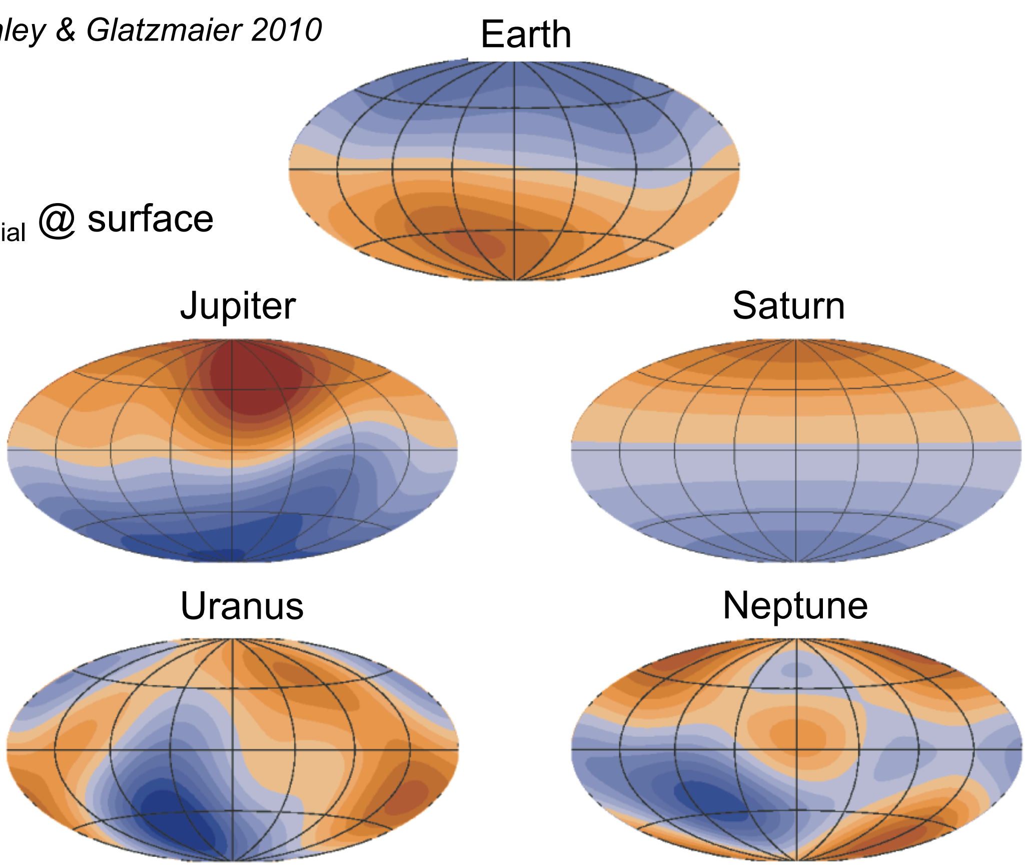

# Magnetic Potential
# 3-D harmonics

$$\mathbf{B} = -grad\ V$$

$$V = R_p \sum_{n=1}^{\infty} \sum_{m=0}^{n} \left(\frac{R_p}{r}\right)^{n+1} P_n^m(\cos\theta)\left(g_n^m \cos m\lambda + h_n^m \sin m\lambda\right), \qquad (7.1)$$

coefficients - constants

functions

$$P_0^0(\cos\theta) = 1$$
$$P_1^0(\cos\theta) = \cos\theta$$
$$P_1^1(\cos\theta) = -\sin\theta$$
$$P_2^0(\cos\theta) = \tfrac{1}{2}(3\cos^2\theta - 1)$$
$$P_2^1(\cos\theta) = -3\cos\theta\sin\theta$$
$$P_2^2(\cos\theta) = 3\sin^2\theta$$
$$P_3^0(\cos\theta) = \tfrac{1}{2}(5\cos^3\theta - 3\cos\theta)$$

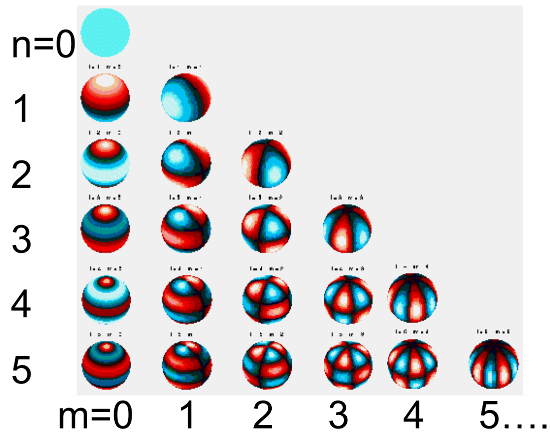


Same technique used to model cosmic microwave background

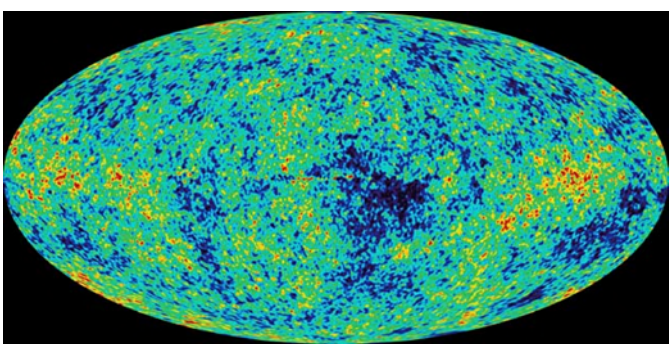

or interior of Sun with Helioseismology…


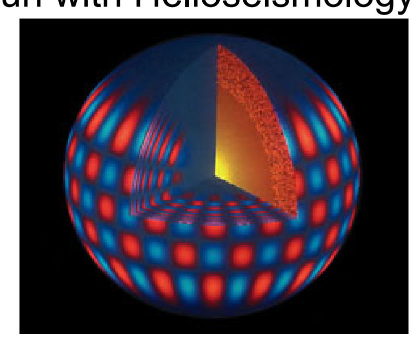

# Earth - International Geomagnetic Reference Field

Complexity ↓

\# 11th Generation International Geomagnetic Reference Field Schmidt semi-normalised spherical harmonic coefficients, degree n=1,13
\# in units nanoTesla for IGRF and definitive DGRF main-field models (degree n=1,8 nanoTesla/year for secular variation (SV))

| g/h | n | m | IGRF 1900.0 | IGRF 1905.0 | IGRF 1910.0 | IGRF 1915.0 | IGRF 1920.0 | IGRF 1925.0 | IGRF 1930.0 | IGRF 1935.0 | IGRF 1940.0 | DGRF 1945.0 | DGRF 1950.0 | DGRF 1955.0 | DGRF 1960.0 | DGRF 1965.0 | DGRF 1970.0 | DGRF 1975.0 | DGRF 1980.0 | DGRF 1985.0 | DGRF 1990.0 | DGRF 1995.0 | DGRF 2000.0 | DGRF 2005.0 | IGRF 2010.0 | SV 2010-15 |
|---|---|---|---|---|---|---|---|---|---|---|---|---|---|---|---|---|---|---|---|---|---|---|---|---|---|---|
| g | 1 | 0 | -31543 | -31464 | -31354 | -31212 | -31060 | -30926 | -30805 | -30715 | -30654 | -30594 | -30554 | -30500 | -30421 | -30334 | -30220 | -30100 | -29992 | -29873 | -29775 | -29692 | -29619.4 | -29554.63 | -29496.5 | 11.4 |
| g | 1 | 1 | -2298 | -2298 | -2297 | -2306 | -2317 | -2318 | -2316 | -2306 | -2292 | -2285 | -2250 | -2215 | -2169 | -2119 | -2068 | -2013 | -1956 | -1905 | -1848 | -1784 | -1728.2 | -1669.05 | -1585.9 | 16.7 |
| h | 1 | 1 | 5922 | 5909 | 5898 | 5875 | 5845 | 5817 | 5808 | 5812 | 5821 | 5810 | 5815 | 5820 | 5791 | 5776 | 5737 | 5675 | 5604 | 5500 | 5406 | 5306 | 5186.1 | 5077.99 | 4945.1 | -28.8 |
| g | 2 | 0 | -677 | -728 | -769 | -802 | -839 | -893 | -951 | -1018 | -1106 | -1244 | -1341 | -1440 | -1555 | -1662 | -1781 | -1902 | -1997 | -2072 | -2131 | -2200 | -2267.7 | -2337.24 | -2396.6 | -11.3 |
| g | 2 | 1 | 2905 | 2928 | 2948 | 2956 | 2959 | 2969 | 2980 | 2984 | 2981 | 2990 | 2998 | 3003 | 3002 | 2997 | 3000 | 3010 | 3027 | 3044 | 3059 | 3070 | 3068.4 | 3047.69 | 3026.0 | -3.9 |
| h | 2 | 1 | -1061 | -1086 | -1128 | -1191 | -1259 | -1334 | -1424 | -1520 | -1614 | -1702 | -1810 | -1898 | -1967 | -2016 | -2047 | -2067 | -2129 | -2197 | -2279 | -2366 | -2481.6 | -2594.50 | -2707.7 | -23.0 |
| g | 2 | 2 | 924 | 1041 | 1176 | 1309 | 1407 | 1471 | 1517 | 1550 | 1566 | 1578 | 1576 | 1581 | 1590 | 1594 | 1611 | 1632 | 1663 | 1687 | 1686 | 1681 | 1670.9 | 1657.76 | 1668.6 | 2.7 |
| h | 2 | 2 | 1121 | 1065 | 1000 | 917 | 823 | 728 | 644 | 586 | 528 | 477 | 381 | 291 | 206 | 114 | 25 | -68 | -200 | -306 | -373 | -413 | -458.0 | -515.43 | -575.4 | -12.9 |
| g | 3 | 0 | 1022 | 1037 | 1058 | 1084 | 1111 | 1140 | 1172 | 1206 | 1240 | 1282 | 1297 | 1302 | 1302 | 1297 | 1287 | 1276 | 1281 | 1296 | 1314 | 1335 | 1339.6 | 1336.30 | 1339.7 | 1.3 |
| g | 3 | 1 | -1469 | -1494 | -1524 | -1559 | -1600 | -1645 | -1692 | -1740 | -1790 | -1834 | -1889 | -1944 | -1992 | -2038 | -2091 | -2144 | -2180 | -2208 | -2239 | -2267 | -2288.0 | -2305.83 | -2326.3 | -3.9 |
| h | 3 | 1 | -330 | -357 | -389 | -421 | -445 | -462 | -480 | -494 | -499 | -499 | -476 | -462 | -414 | -404 | -366 | -333 | -336 | -310 | -284 | -262 | -227.6 | -198.86 | -160.5 | 8.6 |
| g | 3 | 2 | 1256 | 1239 | 1223 | 1212 | 1205 | 1202 | 1205 | 1215 | 1232 | 1255 | 1274 | 1288 | 1289 | 1292 | 1278 | 1260 | 1251 | 1247 | 1248 | 1249 | 1252.1 | 1246.39 | 1231.7 | -2.9 |
| h | 3 | 2 | 3 | 34 | 62 | 84 | 103 | 119 | 133 | 146 | 163 | 186 | 206 | 216 | 224 | 240 | 251 | 262 | 271 | 284 | 293 | 302 | 293.4 | 269.72 | 251.7 | -2.9 |
| g | 3 | 3 | 572 | 635 | 705 | 778 | 839 | 881 | 907 | 918 | 916 | 913 | 896 | 882 | 878 | 856 | 838 | 830 | 833 | 829 | 802 | 759 | 714.5 | 672.51 | 634.2 | -8.1 |
| h | 3 | 3 | 523 | 480 | 425 | 360 | 293 | 229 | 166 | 101 | 43 | -11 | -46 | -83 | -130 | -165 | -196 | -223 | -252 | -297 | -352 | -427 | -491.1 | -524.72 | -536.8 | -2.1 |
| g | 4 | 0 | 876 | 880 | 884 | 887 | 889 | 891 | 896 | 903 | 914 | 944 | 954 | 958 | 957 | 957 | 952 | 946 | 938 | 936 | 939 | 940 | 932.3 | 920.55 | 912.6 | -1.4 |
| g | 4 | 1 | 628 | 643 | 660 | 678 | 695 | 711 | 727 | 744 | 762 | 776 | 792 | 796 | 800 | 804 | 800 | 791 | 782 | 780 | 780 | 780 | 786.8 | 797.96 | 809.0 | 2.0 |
| h | 4 | 1 | 195 | 203 | 211 | 218 | 220 | 216 | 205 | 188 | 169 | 144 | 136 | 133 | 135 | 148 | 167 | 191 | 212 | 232 | 247 | 262 | 272.6 | 282.07 | 286.4 | 0.4 |
| g | 4 | 2 | 660 | 653 | 644 | 631 | 616 | 601 | 584 | 565 | 550 | 544 | 528 | 510 | 504 | 479 | 461 | 438 | 398 | 361 | 325 | 290 | 250.0 | 210.65 | 166.6 | -8.9 |
| h | 4 | 2 | -69 | -77 | -90 | -109 | -134 | -163 | -195 | -226 | -252 | -276 | -278 | -274 | -278 | -269 | -266 | -265 | -257 | -249 | -240 | -236 | -231.9 | -225.23 | -211.2 | 3.2 |
| g | 4 | 3 | -361 | -380 | -400 | -416 | -424 | -426 | -422 | -415 | -405 | -421 | -408 | -397 | -394 | -390 | -395 | -405 | -419 | -424 | -423 | -418 | -403.0 | -379.86 | -357.1 | 4.4 |
| h | 4 | 3 | -210 | -201 | -189 | -173 | -153 | -130 | -109 | -90 | -72 | -55 | -37 | -23 | 3 | 13 | 26 | 39 | 53 | 69 | 84 | 97 | 119.8 | 145.15 | 164.4 | 3.6 |
| g | 4 | 4 | 134 | 146 | 160 | 178 | 199 | 217 | 234 | 249 | 265 | 304 | 303 | 290 | 269 | 252 | 234 | 216 | 199 | 170 | 141 | 122 | 111.3 | 100.00 | 89.7 | -2.3 |
| h | 4 | 4 | -75 | -65 | -55 | -51 | -57 | -70 | -90 | -114 | -141 | -178 | -210 | -230 | -255 | -269 | -279 | -288 | -297 | -297 | -299 | -306 | -303.8 | -305.36 | -309.2 | -0.8 |
| g | 5 | 0 | -184 | -192 | -201 | -211 | -221 | -230 | -237 | -241 | -241 | -253 | -240 | -229 | -222 | -219 | -216 | -218 | -218 | -214 | -214 | -214 | -218.8 | -227.00 | -231.1 | -0.5 |
| g | 5 | 1 | 328 | 328 | 327 | 327 | 326 | 326 | 327 | 329 | 334 | 346 | 349 | 360 | 362 | 358 | 359 | 356 | 357 | 355 | 353 | 352 | 351.4 | 354.41 | 357.2 | 0.5 |
| h | 5 | 1 | -210 | -193 | -172 | -148 | -122 | -96 | -72 | -51 | -33 | -12 | 3 | 15 | 16 | 19 | 26 | 31 | 46 | 47 | 46 | 46 | 43.8 | 42.72 | 44.7 | 0.5 |
| g | 5 | 2 | 264 | 259 | 253 | 245 | 236 | 226 | 218 | 211 | 208 | 194 | 211 | 230 | 242 | 254 | 262 | 264 | 261 | 253 | 245 | 235 | 222.3 | 208.95 | 200.3 | -1.5 |
| h | 5 | 2 | 53 | 56 | 57 | 58 | 58 | 58 | 60 | 64 | 71 | 95 | 103 | 110 | 125 | 128 | 139 | 148 | 150 | 150 | 154 | 165 | 171.9 | 180.25 | 188.9 | 1.5 |
| g | 5 | 3 | 5 | -1 | -9 | -16 | -23 | -28 | -32 | -33 | -33 | -20 | -20 | -23 | -26 | -31 | -42 | -59 | -74 | -93 | -109 | -118 | -130.4 | -136.54 | -141.2 | -0.7 |
| h | 5 | 3 | -33 | -32 | -33 | -34 | -38 | -44 | -53 | -64 | -75 | -67 | -87 | -98 | -117 | -126 | -139 | -152 | -151 | -154 | -153 | -143 | -133.1 | -123.45 | -118.1 | 0.9 |
| g | 5 | 4 | -86 | -93 | -102 | -111 | -119 | -125 | -131 | -136 | -141 | -142 | -147 | -152 | -156 | -157 | -160 | -159 | -162 | -164 | -165 | -166 | -168.6 | -168.05 | -163.1 | 1.3 |
| h | 5 | 4 | -124 | -125 | -126 | -126 | -125 | -122 | -118 | -115 | -113 | -119 | -122 | -121 | -114 | -97 | -91 | -83 | -78 | -75 | -69 | -55 | -39.3 | -19.57 | 0.1 | 3.7 |
| g | 5 | 5 | -16 | -26 | -38 | -51 | -62 | -69 | -74 | -76 | -76 | -82 | -76 | -69 | -63 | -62 | -56 | -49 | -48 | -46 | -36 | -17 | -12.9 | -13.55 | -7.7 | 1.4 |
| h | 5 | 5 | 3 | 11 | 21 | 32 | 43 | 51 | 58 | 64 | 69 | 82 | 80 | 78 | 81 | 81 | 83 | 88 | 92 | 95 | 97 | 107 | 106.3 | 103.85 | 100.9 | -0.6 |
| g | 6 | 0 | 63 | 62 | 62 | 61 | 61 | 61 | 60 | 59 | 57 | 59 | 54 | 47 | 46 | 45 | 43 | 45 | 48 | 53 | 61 | 68 | 72.3 | 73.60 | 72.8 | -0.3 |
| g | 6 | 1 | 61 | 60 | 58 | 57 | 55 | 54 | 53 | 53 | 54 | 57 | 57 | 57 | 58 | 61 | 64 | 66 | 66 | 65 | 65 | 67 | 68.2 | 69.56 | 68.6 | -0.3 |
| h | 6 | 1 | -9 | -7 | -5 | -2 | 0 | 3 | 4 | 4 | 4 | 6 | -1 | -9 | -10 | -11 | -12 | -13 | -15 | -16 | -16 | -17 | -17.4 | -20.33 | -20.8 | -0.1 |
| g | 6 | 2 | -11 | -11 | -11 | -10 | -10 | -9 | -9 | -8 | -7 | 6 | 4 | 3 | 1 | 8 | 15 | 28 | 42 | 51 | 59 | 68 | 74.2 | 76.74 | 76.0 | -0.3 |
| h | 6 | 2 | 83 | 86 | 89 | 93 | 96 | 99 | 102 | 104 | 105 | 100 | 99 | 96 | 99 | 100 | 100 | 99 | 93 | 88 | 82 | 72 | 63.7 | 54.75 | 44.2 | -2.1 |
| g | 6 | 3 | -217 | -221 | -224 | -228 | -233 | -238 | -242 | -246 | -249 | -246 | -247 | -247 | -237 | -228 | -212 | -198 | -192 | -185 | -178 | -170 | -160.9 | -151.34 | -141.4 | 1.9 |
| h | 6 | 3 | 2 | 4 | 5 | 8 | 11 | 14 | 19 | 25 | 33 | 16 | 33 | 48 | 60 | 68 | 72 | 75 | 71 | 69 | 69 | 67 | 65.1 | 63.63 | 61.5 | -0.4 |
| g | 6 | 4 | -58 | -57 | -54 | -51 | -46 | -40 | -32 | -25 | -18 | -25 | -16 | -8 | -1 | 4 | 2 | 1 | 4 | 4 | 3 | -1 | -5.9 | -14.58 | -22.9 | -1.6 |
| h | 6 | 4 | -35 | -32 | -29 | -26 | -22 | -18 | -16 | -15 | -15 | -9 | -12 | -16 | -20 | -32 | -37 | -41 | -43 | -48 | -52 | -58 | -61.2 | -63.53 | -66.3 | -0.5 |
| g | 6 | 5 | 59 | 57 | 54 | 49 | 44 | 39 | 32 | 25 | 18 | 21 | 12 | 7 | -2 | 1 | 3 | 6 | 14 | 16 | 18 | 19 | 16.9 | 14.58 | 13.1 | -0.2 |
| h | 6 | 5 | 36 | 32 | 28 | 23 | 18 | 13 | 8 | 4 | 0 | -16 | -12 | -12 | -11 | -8 | -6 | -4 | -2 | -1 | 1 | 1 | 0.7 | 0.24 | 3.1 | 0.8 |
| g | 6 | 6 | -90 | -92 | -95 | -98 | -101 | -103 | -104 | -106 | -107 | -104 | -105 | -107 | -113 | -111 | -112 | -111 | -108 | -102 | -96 | -93 | -90.4 | -86.36 | -77.9 | 1.8 |
| h | 6 | 6 | -69 | -67 | -65 | -62 | -57 | -52 | -46 | -40 | -33 | -39 | -30 | -24 | -17 | -7 | 1 | 11 | 17 | 21 | 24 | 36 | 43.8 | 50.94 | 54.9 | 0.5 |

.......... 4 pages later.....

| | | | | | | | | | | | | | | | | | | | | | | | | | | |
|---|---|---|---|---|---|---|---|---|---|---|---|---|---|---|---|---|---|---|---|---|---|---|---|---|---|---|
| g | 13 | 12 | 0 | 0 | 0 | 0 | 0 | 0 | 0 | 0 | 0 | 0 | 0 | 0 | 0 | 0 | 0 | 0 | 0 | 0 | 0 | 0 | 0.0 | -0.10 | -0.3 | 0.0 |
| h | 13 | 12 | 0 | 0 | 0 | 0 | 0 | 0 | 0 | 0 | 0 | 0 | 0 | 0 | 0 | 0 | 0 | 0 | 0 | 0 | 0 | 0 | -0.5 | -0.57 | -0.5 | 0.0 |
| g | 13 | 13 | 0 | 0 | 0 | 0 | 0 | 0 | 0 | 0 | 0 | 0 | 0 | 0 | 0 | 0 | 0 | 0 | 0 | 0 | 0 | 0 | 0.1 | -0.18 | -0.3 | 0.0 |
| h | 13 | 13 | 0 | 0 | 0 | 0 | 0 | 0 | 0 | 0 | 0 | 0 | 0 | 0 | 0 | 0 | 0 | 0 | 0 | 0 | 0 | 0 | -0.9 | -0.82 | -0.8 | 0.0 |

Time →

g 13 13
h 13 13

http://www.ngdc.noaa.gov/IAGA/vmod/igrf.html
http://onlinelibrary.wiley.com/doi/10.1111/j.1365-246X.2010.04804.x/full

Declination $D$ in degrees in 2010

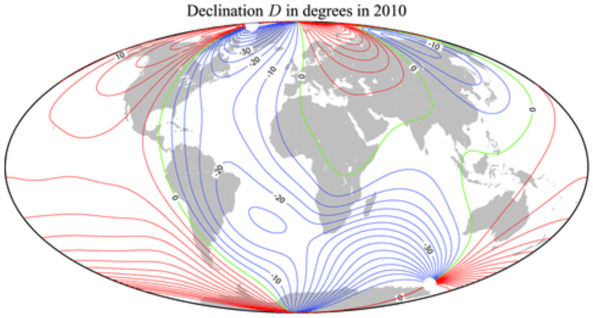

## International Geomagnetic Reference Field

Inclination $I$ in degrees in 2010

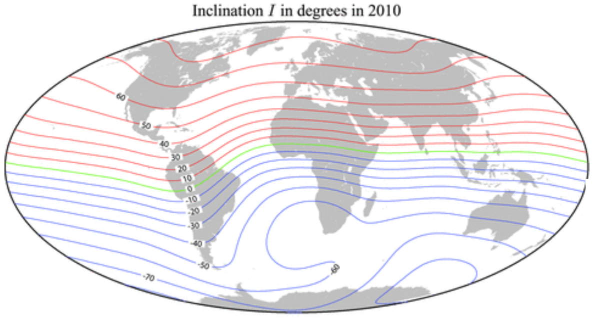

Total Intensity $F$ in nT in 2010

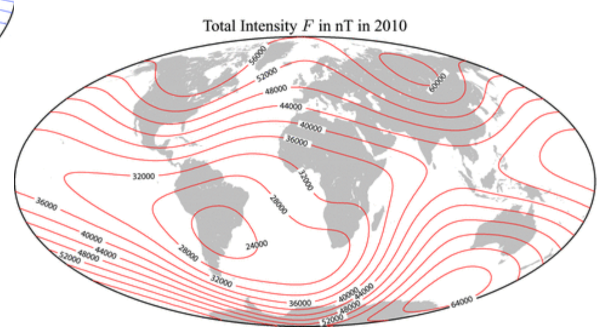

*vol. III ch. 7*

Br surface

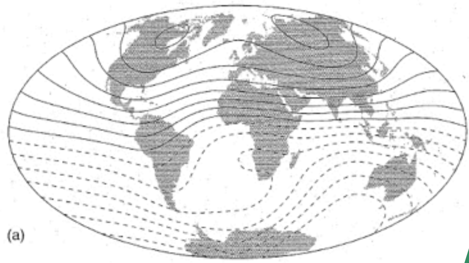


Br core-mantle boundary

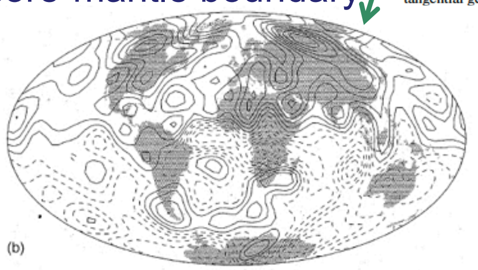


Fig. 7.2. Radial component of the geomagnetic field at the Earth's surface (a) and at the core–mantle boundary (b). Full lines for inward magnetic flux and dashed lines for outward flux. Contour intervals are arbitrary and different in the two panels.

From accurate measurement of surface field:

1. Extrapolate to core-mantle boundary = dynamo

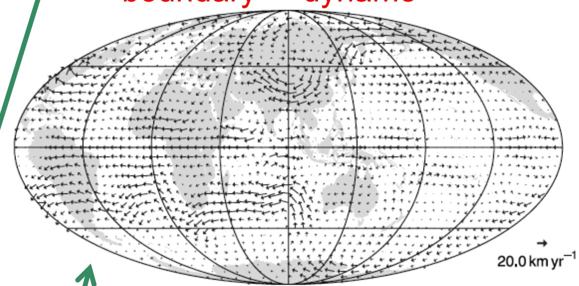


**Fig. 20** Large-scale core surface flow constructed by Holme and Olsen (2006) under the frozen-flux and tangential geostrophy assumptions from a satellite observation-derived secular variation model

*Hulot et al. 2010*

2. Derive core flows

$$\frac{\partial B_r}{\partial t} = -\nabla_h \bullet (\mathbf{u}_h B_r)$$

*h=horizontal*

3. Secular variation & reversals.....

# Secular variation

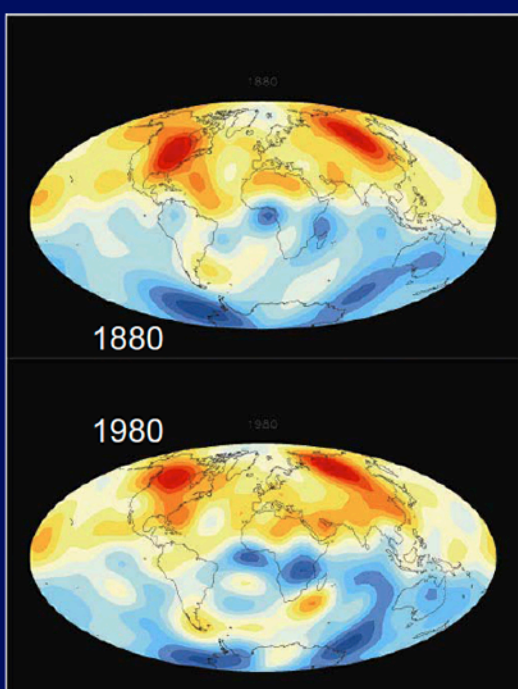


Dipole dropped by 9% since 1840
Reconstructions of core field morphology 1590 - now
Fluctuations of non-dipole parts on time scales 50 – 400 yrs
Stability of high-latitude flux lobes
Westward drift in Atlantic / Africa

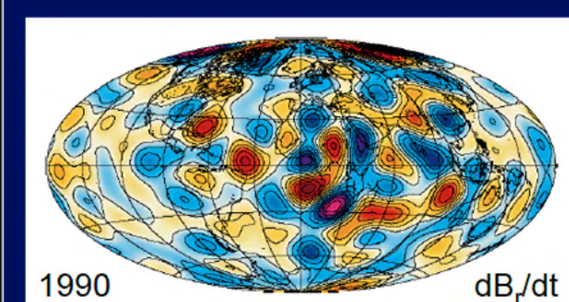

*Hulot et al. 2010*

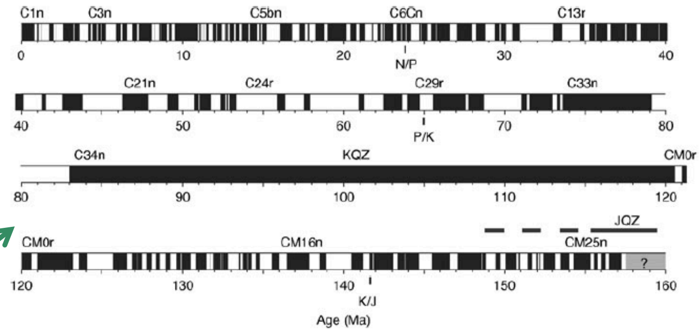


Polarity reversals:

1. variable in duration and

2. rate

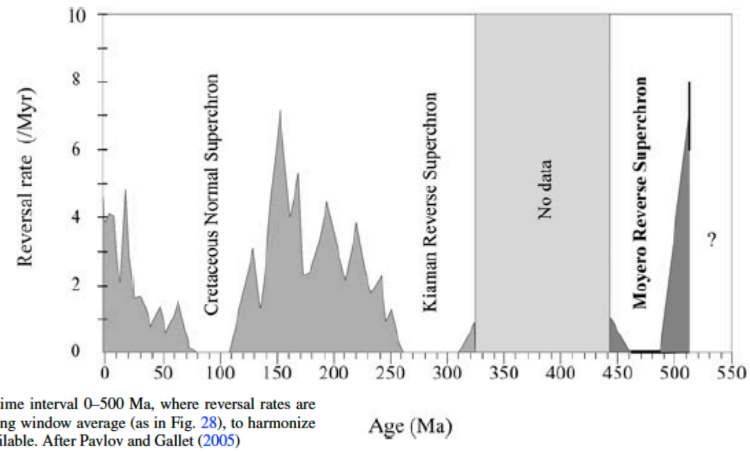


Fig. 29 Estimate of the reversal rate (in $My^{-1}$) for the time interval 0–500 Ma, where reversal rates are estimated by geological stage, rather than by using a moving window average (as in Fig. 28), to harmonize post- and pre- 150 Ma data for which much less data is available. After Pavlov and Gallet (2005)

## *Planetary Dynamos*

See vol. III ch. 7

**Volume of electrically conducting fluid (1) which is convecting (2) and rotating**

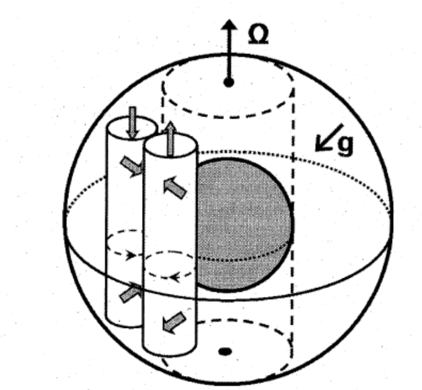


All planetary objects probably have enough rotation - the presence (or not) of a global magnetic field tells us about (1) and (2)

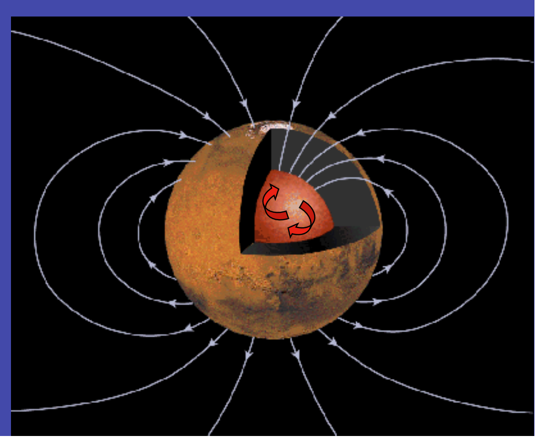

# Magnetic fields of solar system planets

Spacecraft detected magnetic fields at most (but not all) major planets

| Planet | Dynamo | $R_c/R_p$ | $B_s$ [μT] | Dip. tilt | Quadr / Dipole |
|---|---|---|---|---|---|
| Mercury | Yes (?) | 0.75 | 0.35 | <5° ? | 0.1-0.5 |
| [redacted] | | | | | |
| Earth | Yes | 0.55 | 44 | 10.4° | 0.04 |
| [redacted] | | | | | |
| Jupiter | Yes | 0.84 | 640 | 9.4° | 0.10 |
| Saturn | Yes | 0.6 ? | 31 | 0° | 0.02 |
| Uranus | Yes | 0.75 | 48 | 59° | 1.3 |
| Neptune | Yes | 0.75 | 47 | 45° | 2.7 |
| Ganymede | Yes | 0.3 ? | 1.0 | < 5° ? | ? |

V. dipolar

Irregular

**$R_c$/ $R_p$: core / planetary radius, $B_s$: Mean field at planet's surface, Quadr. / dipole power at $R_c$**



- Dipole – n=1
- Quadupole – n=2
- Quadrupole/Dipole ratio indicates irregular field

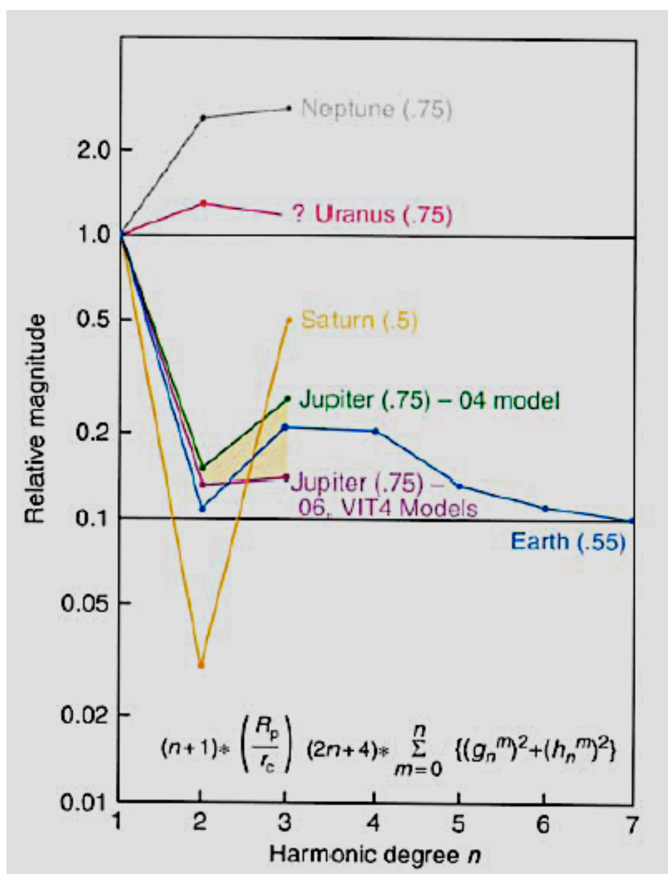


*Connerney 2007*

*Hulot et al. 2010*

# Moon & Mars: All Crustal Remanent Magnetization

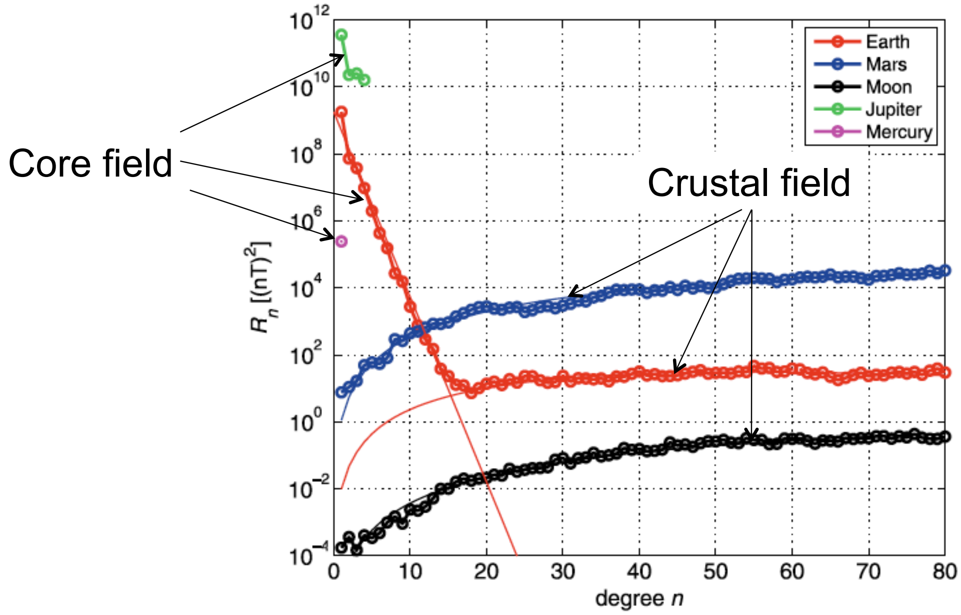


Power spectra of the field of internal origin for the Earth (after Olsen et al. 2009a and Maus et al. 2008), Mars (after Cain et al. 2003), Jupiter, Mercury (after Connerney 2008) and the Moon (after Purucker 2008) at their respective surface reference radius. Also shown are theoretical crustal spectra (thin curves, Voorhies et al. 2002) for the Earth, Mars and the Moon.

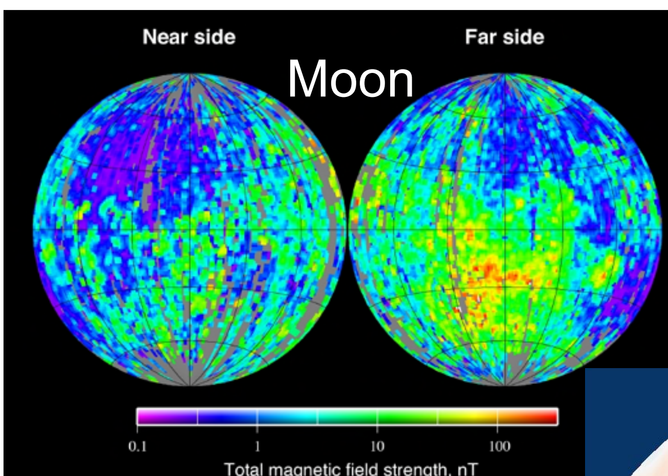


*From Wikapedia – Lunar Prospector observations*

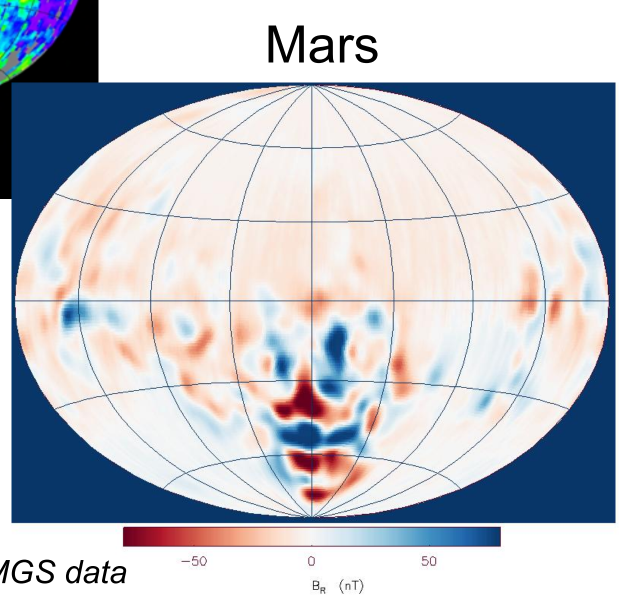


*From David Brain, MGS data*

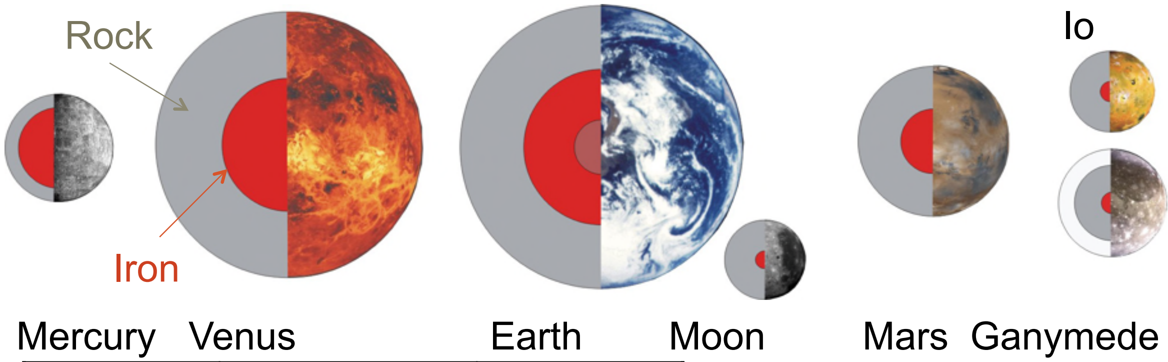


| ***Planet*** | ***Density** [g cm$^{-3}$]* | *$R_{core}$ / $R_{planet}$* |
|---|---|---|
| Mercury | 5.43 | 0.75 |
| Venus | 5.24 | 0.55 |
| Earth | 5.515 | 0.55 |
| Moon | 3.36 | 0.2 |
| Mars | 3.94 | 0.5 |
| Ganymede | 1.94 | 0.3 |

*Why don't Venus or Mars have dynamos?*

What drives the geodynamo

In words...
Vol. III
Ch. 7
p 192

Or by picture...

gravitational acceleration). In terrestrial planets, the adiabatic heat flow can be a large fraction of the actual heat flow, or it may exceed the actual heat flow, in which case at least the top layers of the core would be thermally stable. Near the top of Earth's core approximately 3–4 TW can be conducted along the adiabat (Lay *et al.*, 2008), i.e. close to the minimum estimates for the entire core heat flow. But even if all heat flux near the core–mantle boundary were carried by conduction, a convective dynamo can exist thanks to the inner core. At the inner core boundary, the adiabatic temperature profile of the convecting outer core crosses the melting point of iron. The latter increases with pressure more steeply than the adiabatic gradient, which is the reason why the Earth's core freezes from the center rather than from above. As the core cools, the inner core grows with time by freezing iron onto its outer boundary. This has two important implications for driving the dynamo. The latent heat that is released upon solidification is an effective heat source, which contributes to the heat budget approximately the same amount as the bulk cooling of the core. The heat flux that originates at the inner core decreases with radius as $r^{-2}$ in the spherical geometry of the fluid core. The adiabatic temperature gradient is roughly proportional to $r$, because gravity decreases towards the center. Therefore, even if the actual heat flux were slightly less than the adiabatic heat flux near the core–mantle boundary, it must be superadiabatic deeper down. A second, perhaps more important effect is that the light elements in the outer core are preferentially rejected when iron freezes onto the inner core. Hence, they become concentrated in the residual fluid near the inner core boundary. This layering is gravitationally unstable because of the reduced density, which leads to compositional convection that homogenizes the light elements in the bulk of the fluid core. Compositional convection contributes as much as, or more than, thermal convection to the driving of the geodynamo in recent geological times.

# Earth: Internal structure & energetics

- Seismology: Dense core with $R_c/R_p=0.55$
- Fe only cosmochemically abundant element matching density
- No shear waves in outer core, hence it is liquid
- Solid inner core with $0.35R_c$
- ~10% light element (Si, S, O, ...) in outer core, less in inner core
- Earth heat flow 44 TW. Core fraction estimated 3-15 TW
- Core heat flow mostly due to secular cooling

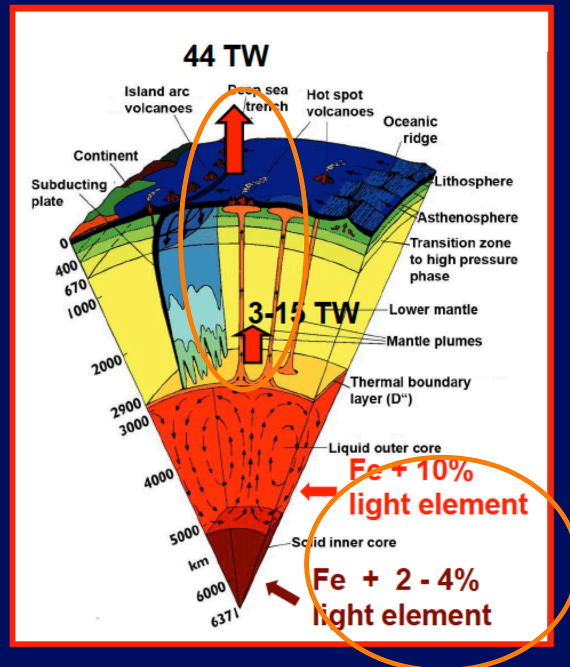




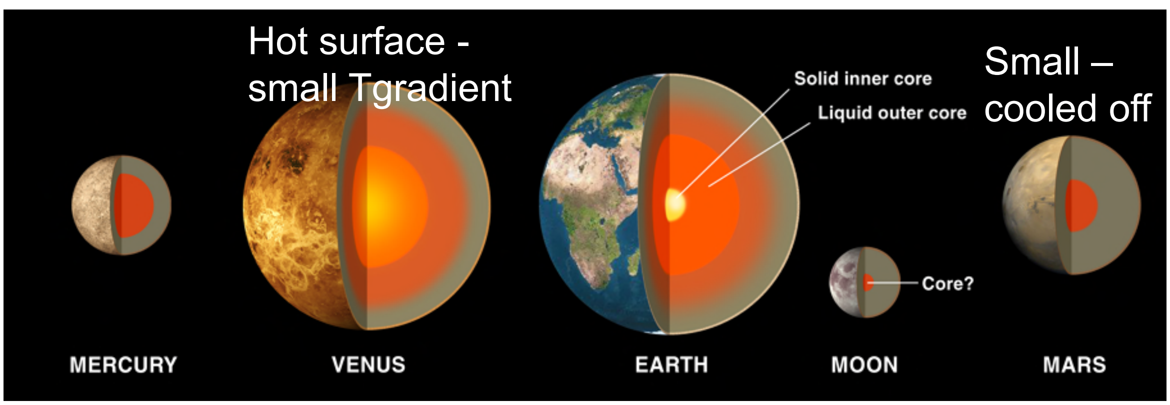


***Why Don't Venus or Mars have Dynamos?***

- Enough rotation – even for Venus
- Conducting fluid core – probably
- Lack of convection in core?
    - Mantle convection controls heat flow from core
    - Lack of plate tectonics suggests less efficient cooling of interior and lower heat flux from core
    - No inner core means no latent heat of solidification and no enhancement of lighter material in the outer core

# Giant Planets

| | | Distance *AU* | Mass *Earth Mass* | Radius *Earth Radii* | Density *1=water* | Composition % by mass |
|---|---|---|---|---|---|---|
|  | *Jupiter* | **5.20** | **318** | **11.2** | **1.33** | **90% H, He** |
|  | *Saturn* | **9.54** | **95** | **9.46** | **0.71** | **75% H, He** |
|  | *Uranus* | **19.2** | **14** | **3.98** | **1.24** | **10% H, He** Water Ammonia Methane |
|  | *Neptune* | **30.1** | **17** | **3.81** | **1.67** | **10% H, He** Water Ammonia Methane |

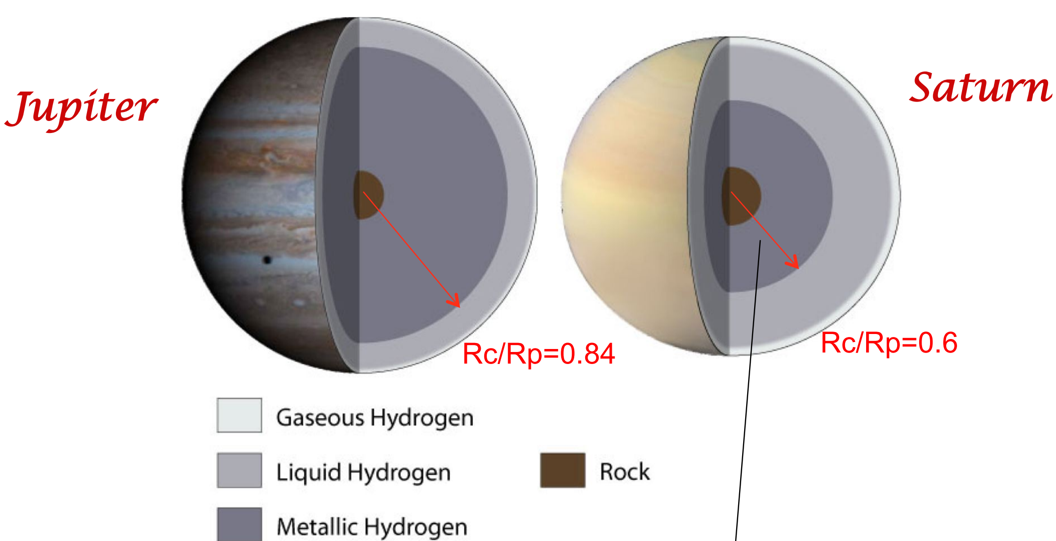


Saturn has lower mass

- ➢ lower pressures
- ➢ smaller region of metallic hydrogen
- ➢ weaker magnetic field

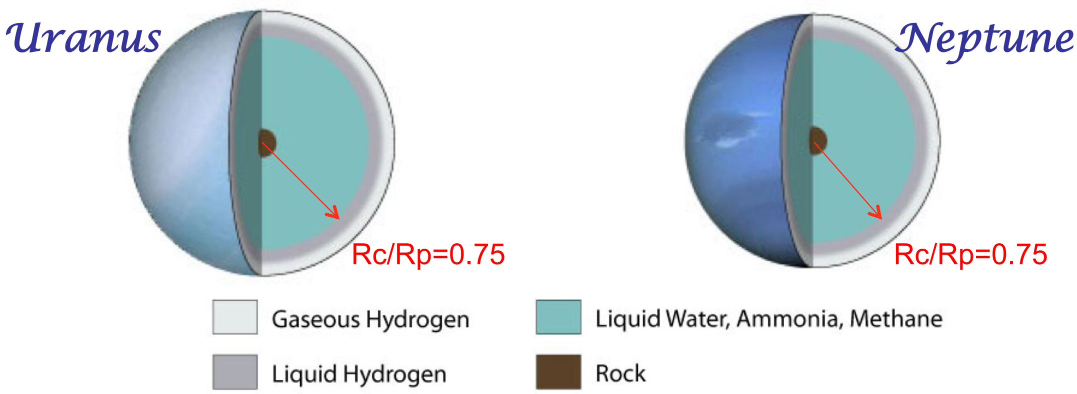


Uranus and Neptune have much less mass

- Lower pressures
- No metallic hydrogen
- Weak & irregular magnetic fields produced in water layer, deep below gas envelope

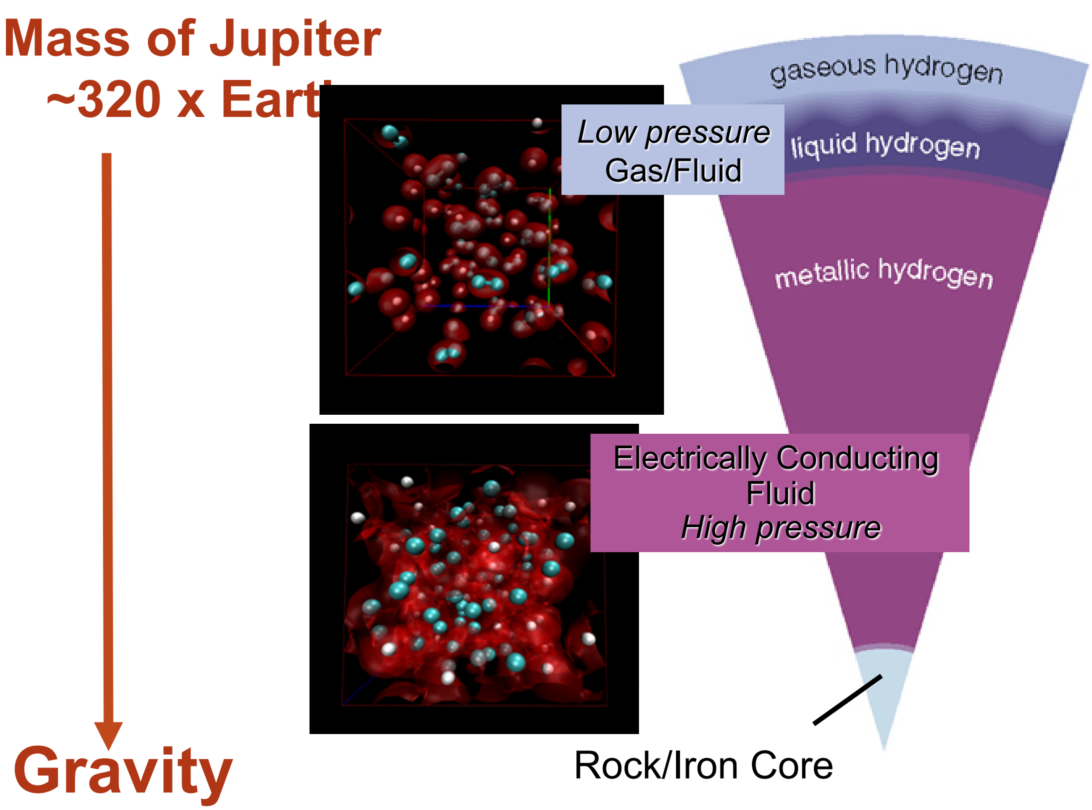

## Interior of Jupiter Using Best Equation of State

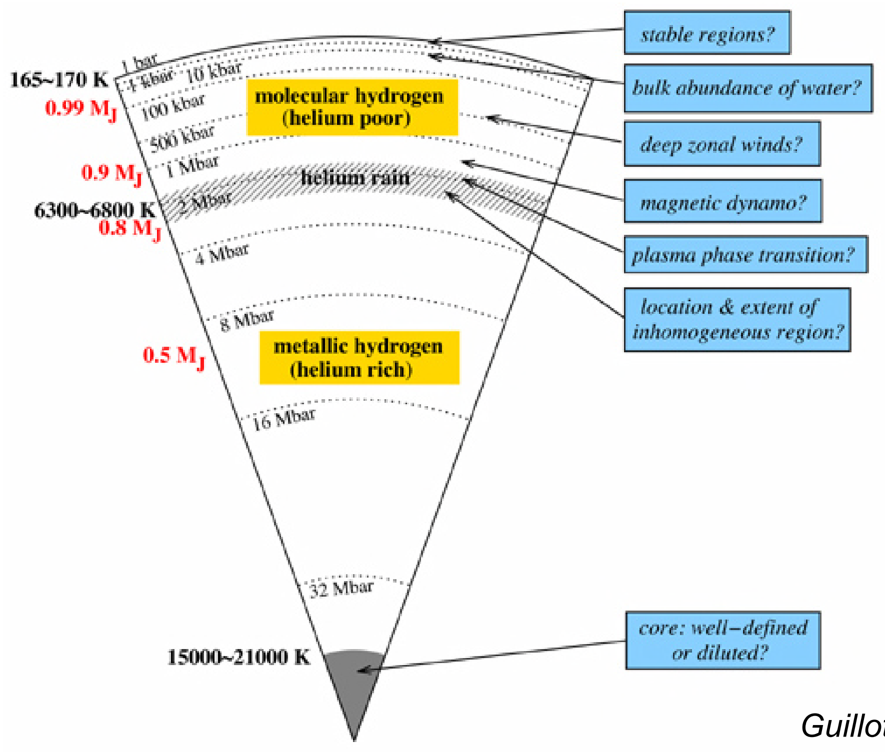


*Still lots of unknowns!!*

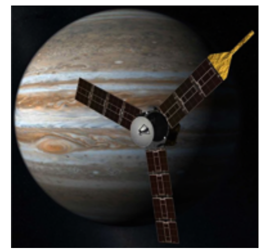

Juno

Launch Aug. 5th

*Guillot et al. 2004*

## Magnetic Spectra of Earth and Jupiter

- Current knowledge of Jupiter is limited to n < 4
- Earth dynamo at n >14 is hidden by crustal field
- Juno will measure out to n ~ 20
- Determine spectral shape, dynamo radius, and secular variations

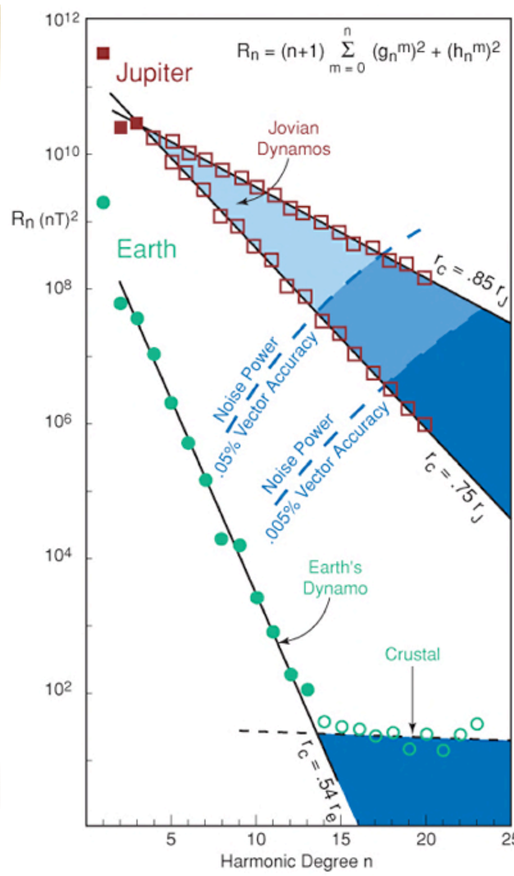

## *Dynamo Models – Lecture 1 Eqns. & discussion*

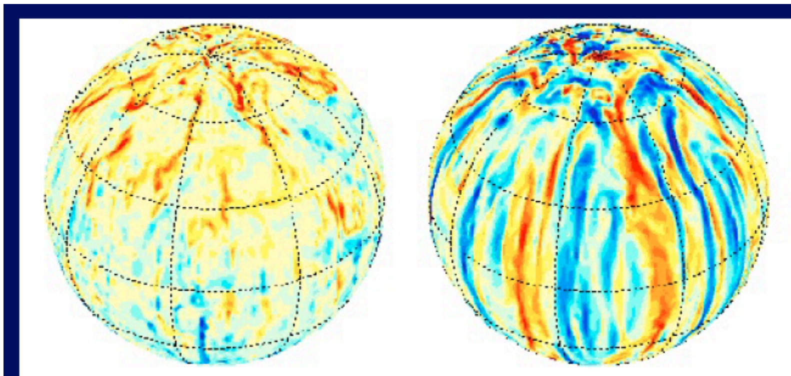

Radial magnetic field    Radial velocity

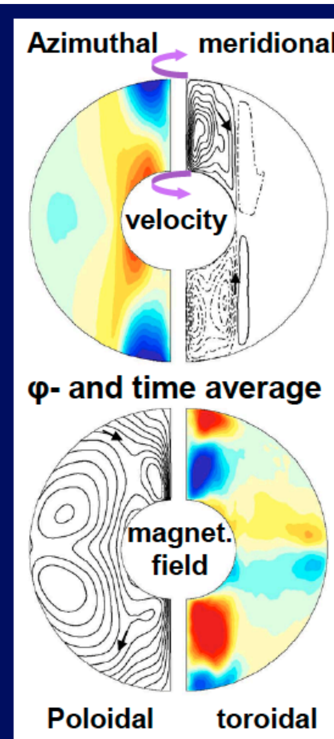


**$E=10^{-5}$  $Ra/Ra_c=114$  $Pm=0.8$  $Rm=914$**

- **Flow columnar outside tangent cylinder**
- **Vigorous flow inside tangent cylinder; polar plumes**
- **Strong toroidal field inside tangent cylinder**
- **$\alpha^2\Omega$ – dynamo ? (Ω-effect inside tangent cylinder)**



# Comparison with Earth: Field morphology

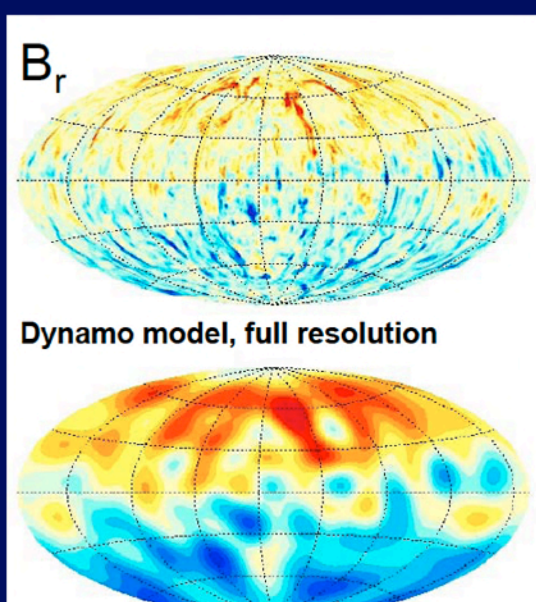


Dynamo model, full resolution

Dynamo model, filtered to n < 13

- Flux lobes at 60-70° latitude
- Weak flux at poles
- Flux spots of both polarities at low latitude. Expulsion of toroidal field bundles ?
- Westward vortex flow in polar cap

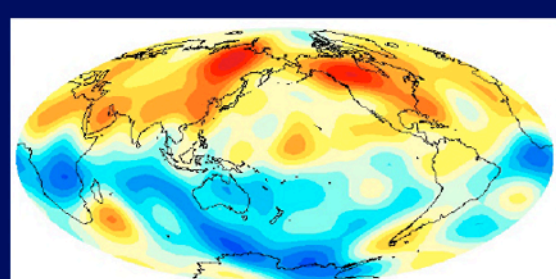

Earth's field at core mantle boundary

# Power-controlled field strength

**Hypothesis:** The magnetic energy density depends on thermodynamically available energy flux, that is the part of the energy flux that can be converted to magnetic energy and can balance ohmic dissipation The field strength is independent of rotation rate, conductivity, viscosity,...

$$B^2/2\mu_o \sim f_{ohm}\, \rho^{1/3}\, (L/H_T\, q_c)^{2/3}$$

$q_c$: convected heat flux, $H_T = c_p/(\alpha g)$: temp. scale height, L: charact. radial length scale, $\rho$: density, $f_{ohm}$: ratio ohmic dissipation / total dissipation



## *Dynamo Scaling Laws*

*Vol. III Ch. 7*

Fig 7.10 Earth Models

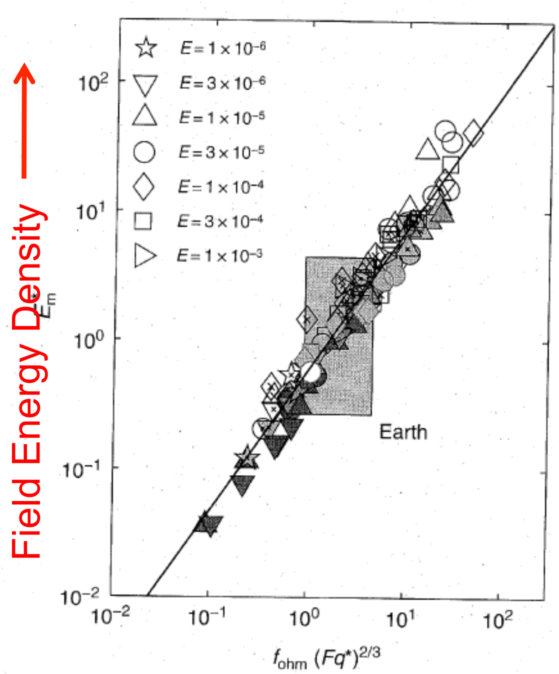


Fig 7.11 Planets & Stars

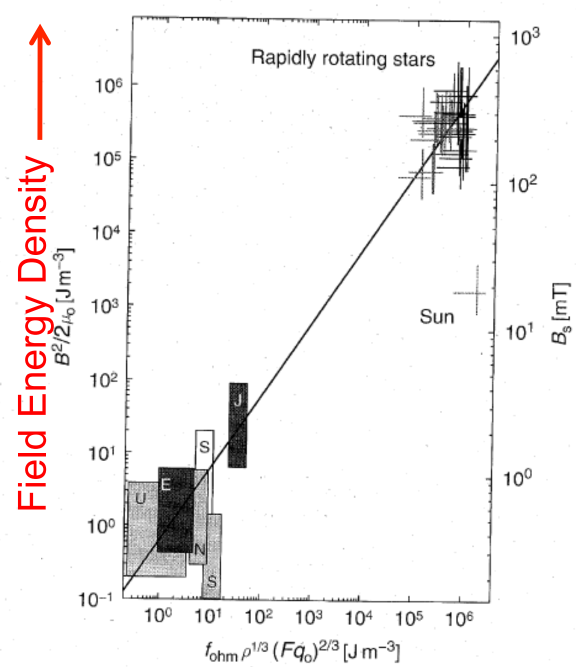


Core Heat Flux

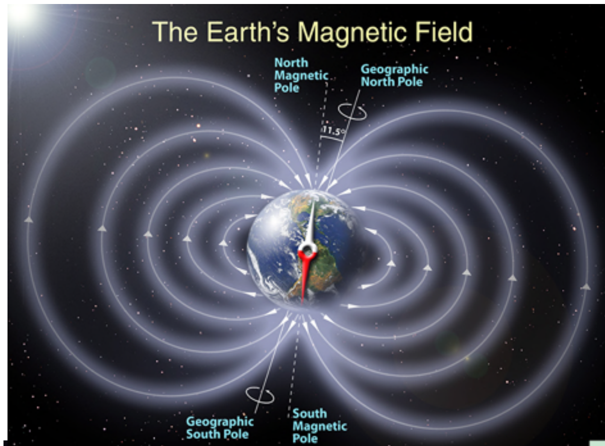


Now we have magnetic fields.... what about magnetospheres?

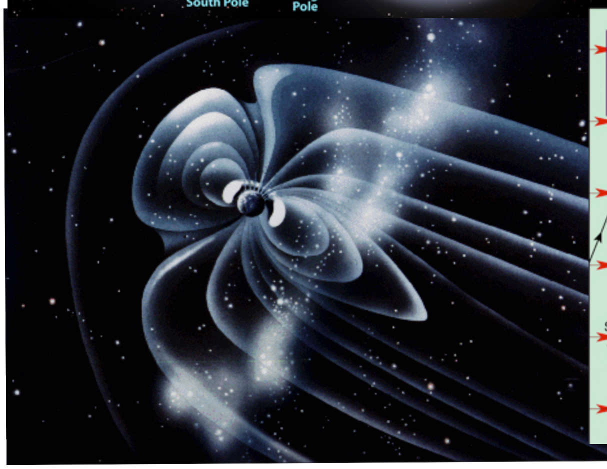

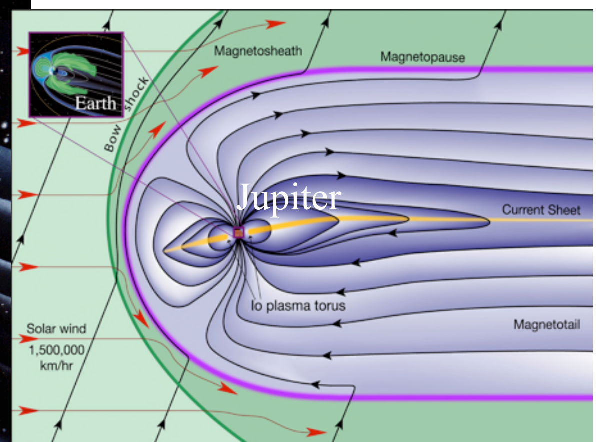


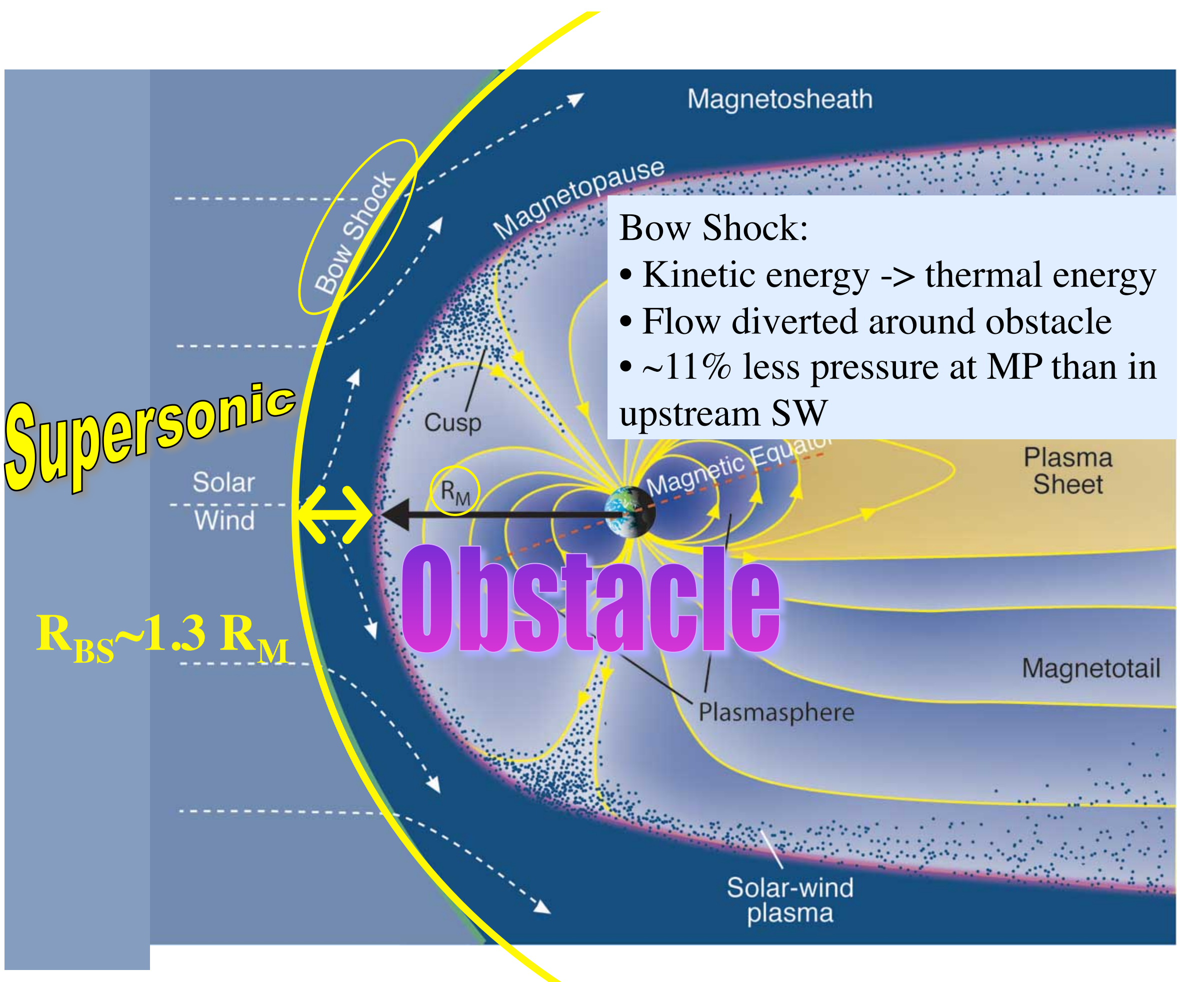

## *Dipole Magnetic Field in Solar Wind*

SW Ram Pressure ⟷ Magnetic Pressure

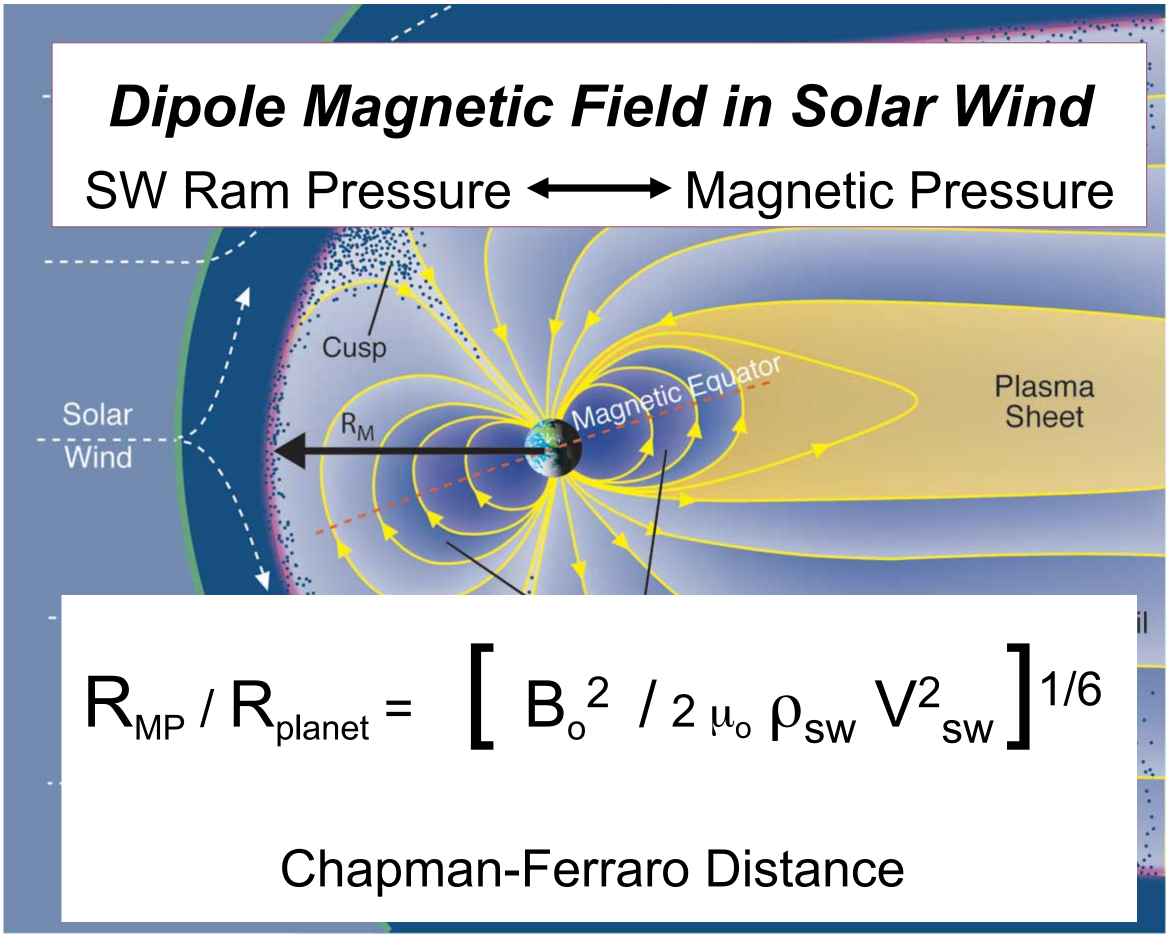


$$R_{MP} / R_{planet} = \left[ B_o^2 \; / \; 2 \, \mu_o \, \rho_{sw} \, V^2_{sw} \right]^{1/6}$$

Chapman-Ferraro Distance

$$\mathbf{R_{CF}}/R_p \sim \{\mathbf{B_o}^2 / 2 \, \mu_o \, \boldsymbol{\rho}_{\mathbf{sw}} \, V^2_{\mathbf{sw}}\}^{1/6}$$

| | Mercury | Earth | Jupiter | Saturn | Uranus | Neptune |
|---|---|---|---|---|---|---|
| $B_o$ Gauss | .003 | .31 | 4.28 | .22 | .23 | .14 |
| $R_{CF}$ Calc. | 1.4 $R_M$ | 10 $R_E$ | 42 $R_J$ | 19 $R_S$ | 25 $R_U$ | 24 $R_N$ |
| $R_M$ Obs. | 1.4-1.6 $R_M$ | 8-12 $R_E$ | 60-90 $R_J$ | 16-22 $R_S$ | 18 $R_U$ | 23-26 $R_N$ |

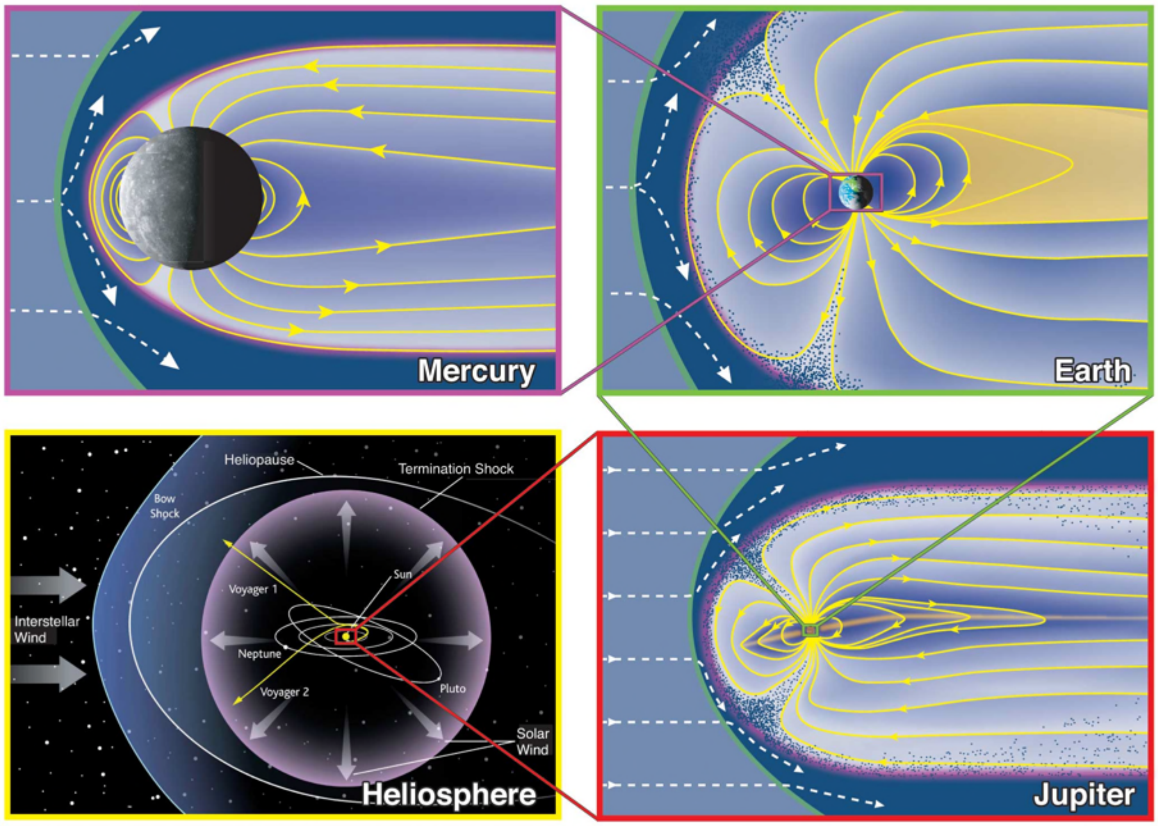


**Earth** ~ Dipole

$R_{mp} \sim (\rho V^2)^{-1/6}$

solar wind $\rho V^2$

**Jupiter**

$R_{mp} \sim (\rho V^2)^{-1/3}$

solar wind $\rho V^2$

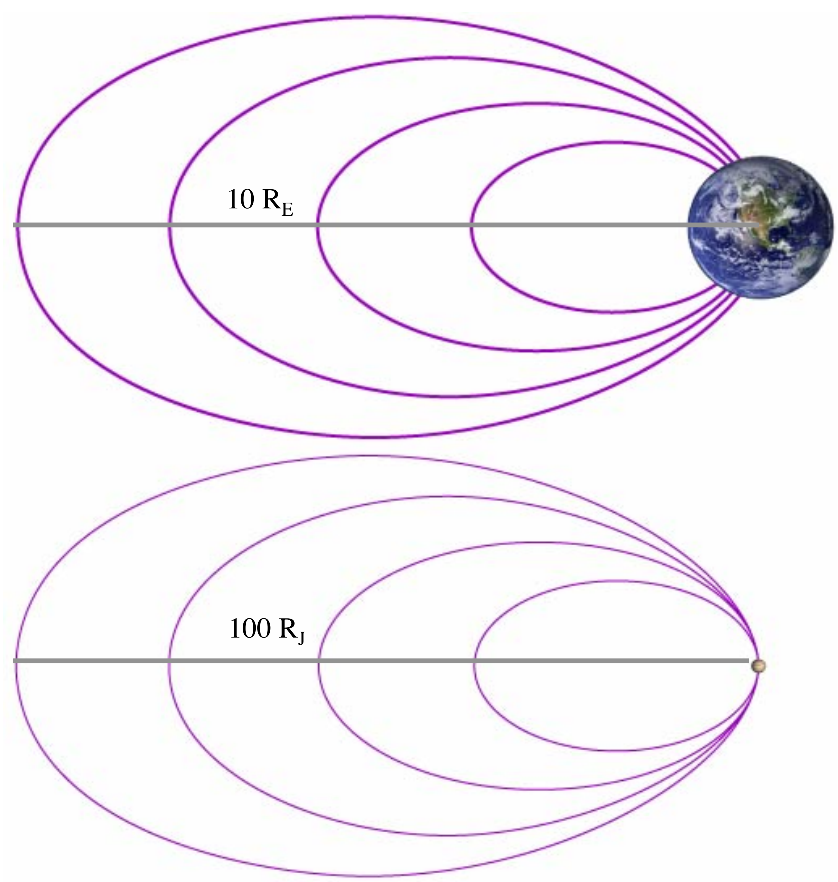

**Earth** ~ Dipole

$R_{mp}$ -> 0.7 $R_{mp}$

solar wind $\rho V^2$

x10 Solar wind pressure

**Jupiter**

$R_{mp}$ -> 0.5 $R_{mp}$

solar wind $\rho V^2$

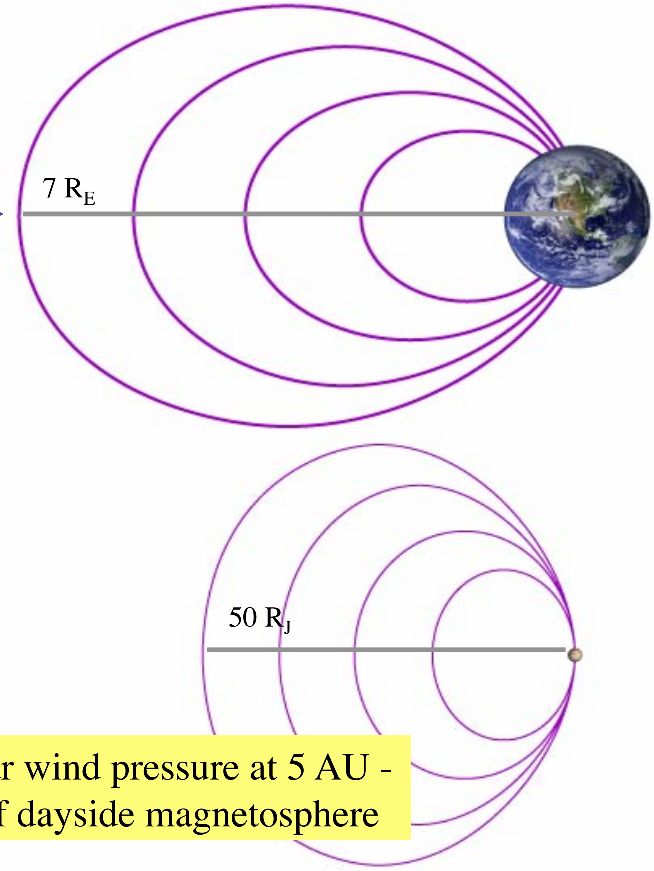


Factor ~10 variations in solar wind pressure at 5 AU -> observed 100-50 Rj size of dayside magnetosphere

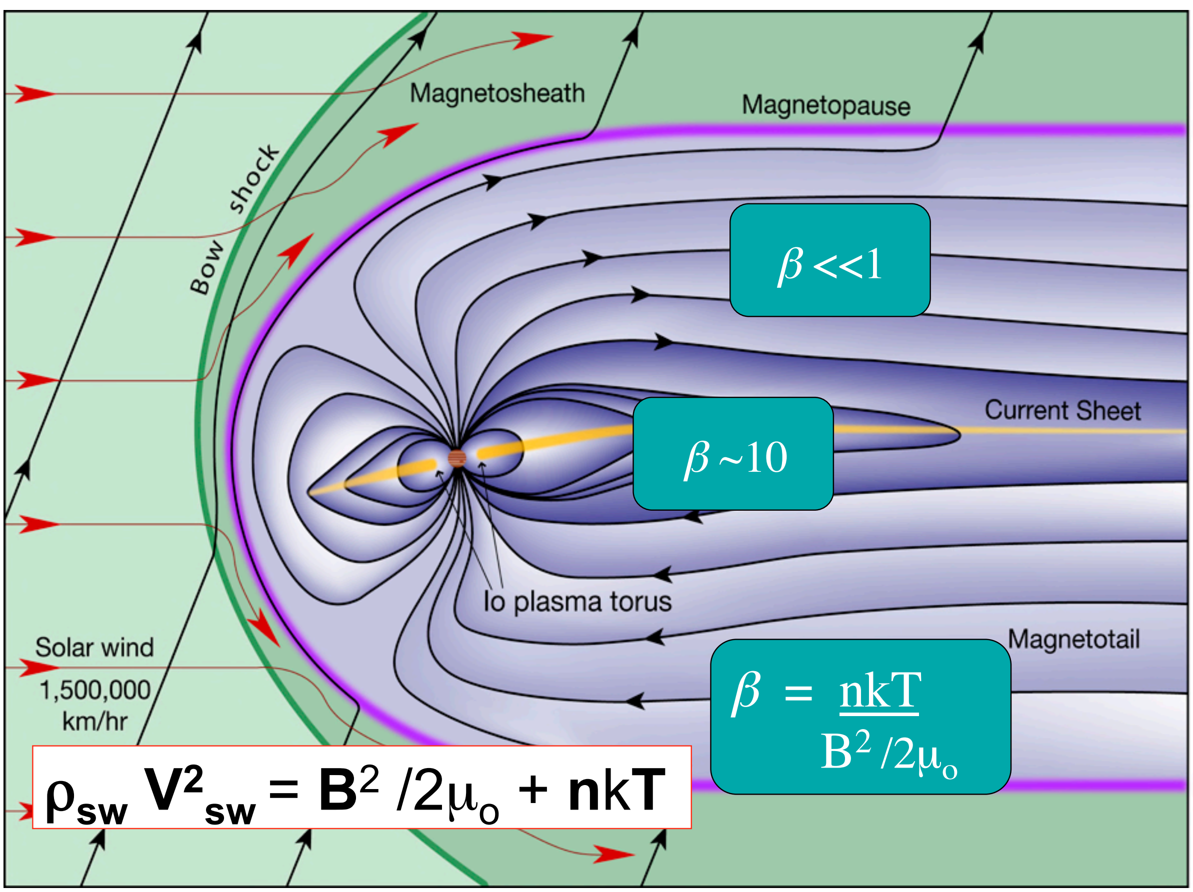

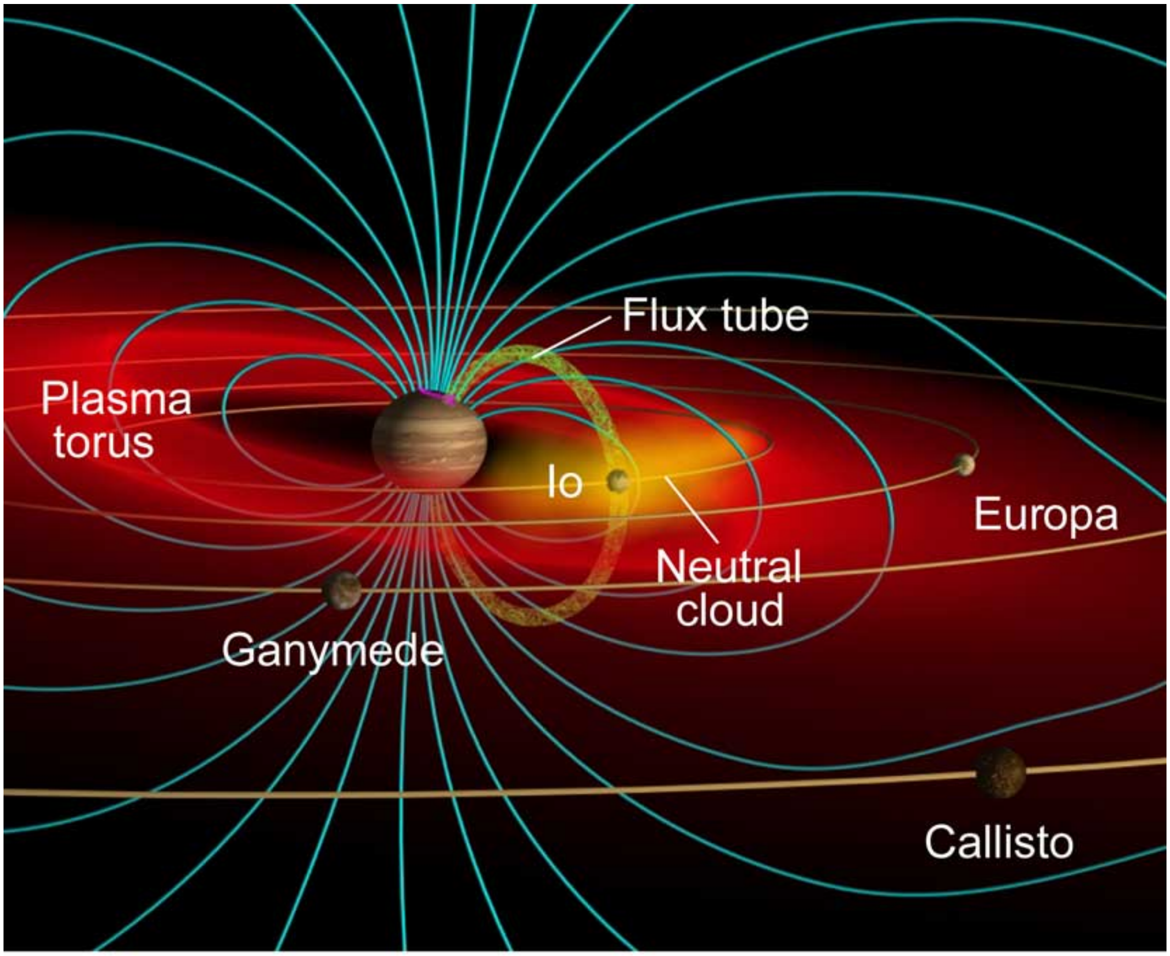
Flux tube
Plasma
torus
Io
Europa
Neutral
cloud
Ganymede
Callisto

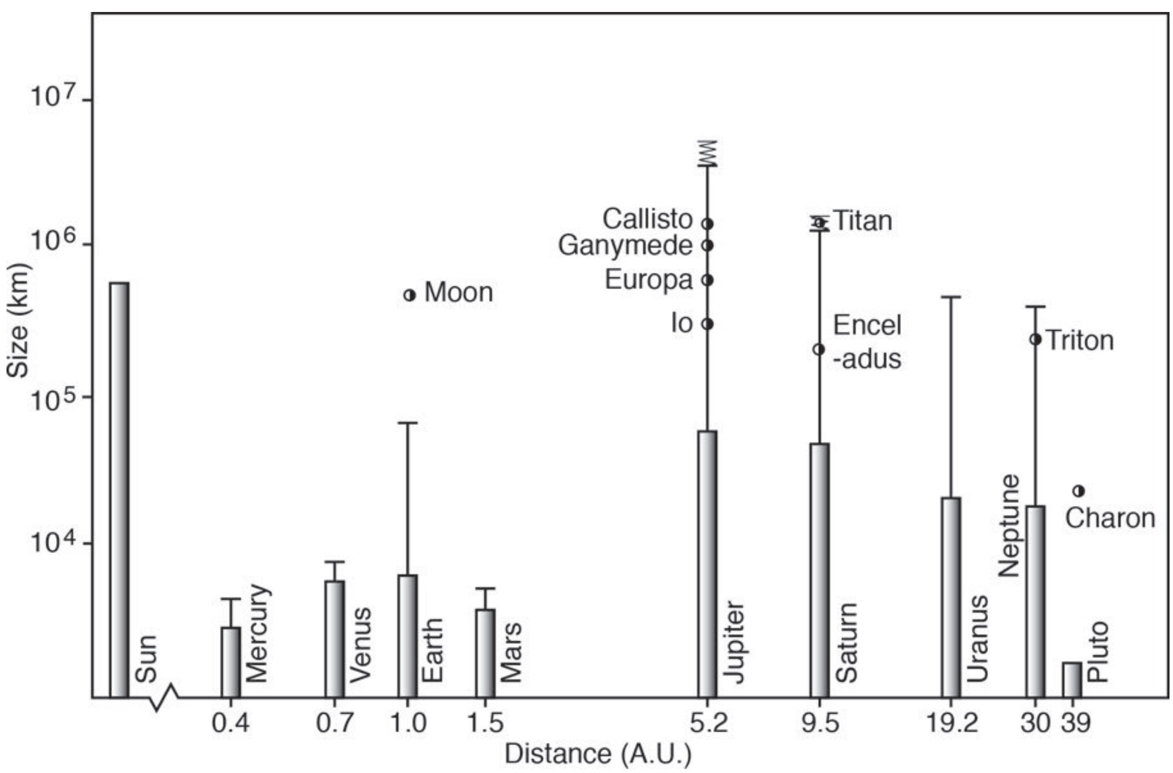
Size (km)
10^7
10^6
10^5
10^4
Sun
Mercury
Venus
Earth
Mars
Jupiter
Saturn
Uranus
Neptune
Pluto
Moon
Callisto
Ganymede
Europa
Io
Titan
Encel
-adus
Triton
Charon
0.4
0.7
1.0
1.5
5.2
9.5
19.2
30
39
Distance (A.U.)

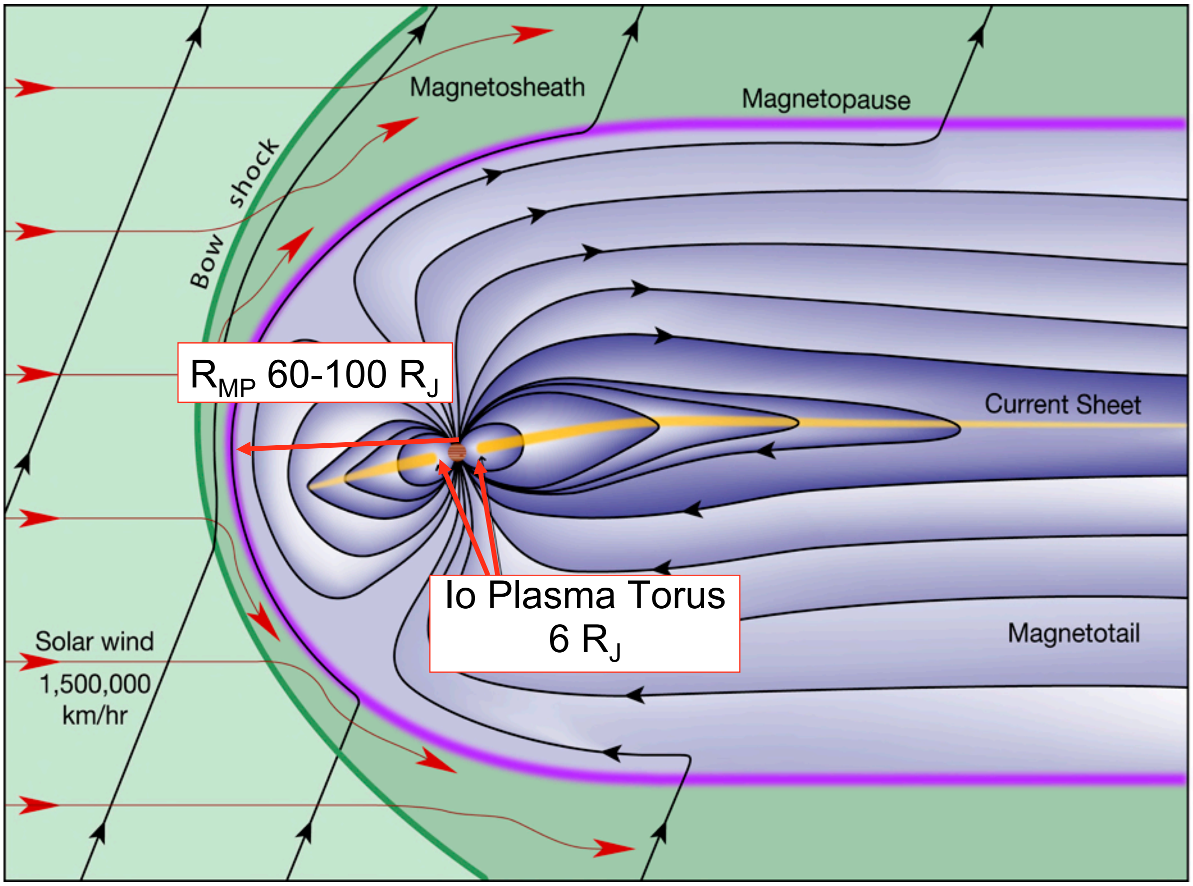


## Solar wind interaction with planets – Vol. I Ch. 13 *also Bagenal 2011*

| | Mercury | Venus | Earth | Mars | Jupiter | Saturn | Uranus | Neptune | Pluto |
|---|---|---|---|---|---|---|---|---|---|
| Distance from Sun, $a_P$ (A.U.)[a] | 0.39 | 0.72 | 1[b] | 1.52 | 5.2 | 9.5 | 19 | 30 | 40 |
| Solar Wind Density[b] ($cm^{-3}$) | 53 | 14 | 7 | 3 | 0.2 | 0.07 | 0.02 | 0.006 | 0.003 |
| IMF strength[c] (nT) | 41 | 14 | 8 | 5 | 1 | 0.6 | 0.3 | 0.2 | 0.1 |
| IMF azimuth angle[c] | 23° | 38° | 45° | 57° | 80° | 84° | 87° | 88° | 88° |
| Radius, $R_P$ (km) | 2,439 | 6,051 | 6,373 | 3,394 | 71,400 | 60,268 | 25,600 | 24,765 | 1,170 (±33) |
| Sidereal spin period (day) | 58.6 | -243 | 0.9973 | 1.026 | 0.41 | 0.44 | -0.72 | 0.67 | -6.39 |
| Magnetic Moment [d] ($M_E$) | 3-6 x $10^{-4}$ | <$10^{-5}$ | 1 | <$10^{-5}$ | 20,000 | 600 | 50 | 25 | ? |
| Surface Magnetic Field[e] $B_o$ (nT) | 250-290 | - | 30,600 | - | 430,000 | 21,400 | 22,800 | 14,200 | ? |
| $R_{CF}$[f] ($R_p$) | 1.6$R_M$ | - | 10 $R_E$ | - | 46 $R_J$ | 20 $R_S$ | 25 $R_U$ | 24 $R_N$ | ? |
| Observed $R_{MP}$ ($R_P$) | 1.5 $R_M$ | - | 8-12$R_E$ | - | 63-92 $R_J$ | 22-27 $R_S$ | 18 $R_U$ | 23-26 $R_N$ | ? |

[a] 1 A.U. = 1.5 x $10^8$ km

[b] The number density of the solar wind fluctuates by about a factor of 5 about typical values of $n_{SW}$ ~7 ($cm^{-3}$) / $a_p^2$]. The mass density of the solar wind is $\rho_{SW}$ = 1.04 $n_{SW}$ (amu $cm^{-3}$)

[c] Mean values for the interplanetary magnetic field (IMF) in units of nano-Tesla with spherical components $Br$, $B\theta$, $B\phi$. The azimuth angle is $\tan^{-1}(B\phi/Br)$. The radial component of the IMF, $Br$, decreases as $1/a_p^2$ while the transverse component, $B\phi$, increases with distance.

[d] $M_{Earth}$ = 7.9 x $10^{25}$ Gauss $cm^3$ = 7.9 x $10^{15}$ Tesla $m^3$

[e] Magnitude of dipole (see text for references).

[f] $R_{CF}$ is calculated using $R_{CF}=\xi\,(B_o^2/2\mu_o\,\rho\,V_{SW}^2)^{1/6}$ for typical solar wind conditions of $\rho_{SW}$ given above and $V_{SW}$ ~400 km $s^{-1}$ and $\xi$ an empirical factor of ~1.4 to match Earth observations (Walker and Russell 1995).

Magnetospheres scaled by stand-off distance of dipole field

| | $M/M_E$ | $MP_{Dipole}$ | $MP_{mean}$ | $MP_{Range}$ |
|---|---|---|---|---|
| Mercury | ~$8x10^{-3}$ | 1.4 $R_M$ | 1.4 $R_M$ | |
| Earth | 1 | 10 $R_E$ | 10 $R_E$ | |
| Saturn | 600 | 20 $R_S$ | 24 $R_S$ | 22-27* $R_S$ |
| Jupiter | 20,000 | 46 $R_J$ | 75 $R_J$ | 63-92# $R_J$ |

**Inflated magnetospheres of Jupiter & Saturn due to HOT PLASMAS**

Note bimodal average locations
* *Achilleos et al. 2008* # *Joy et al. 2002*

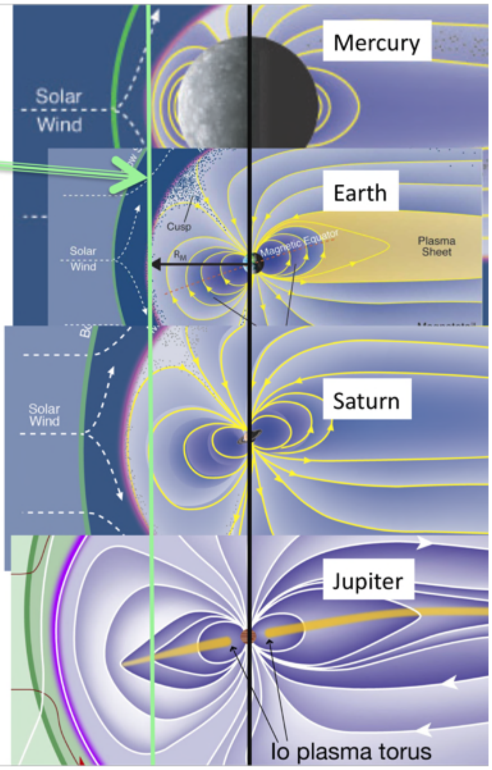


*Lecture 4*
*Vol. I Ch.10*

*Dungey Cycle*

Dynamics at Earth driven by the solar wind coupling the Sun's magnetic field to the Earth's field

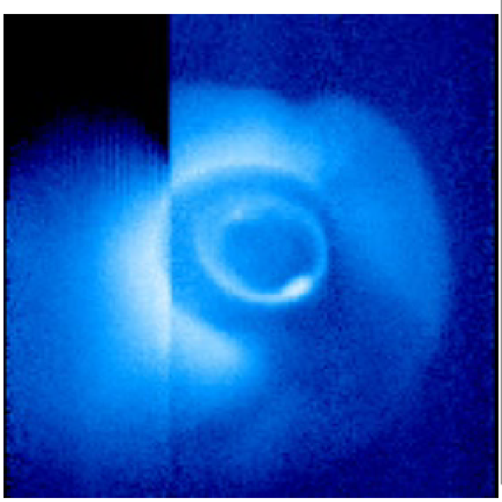

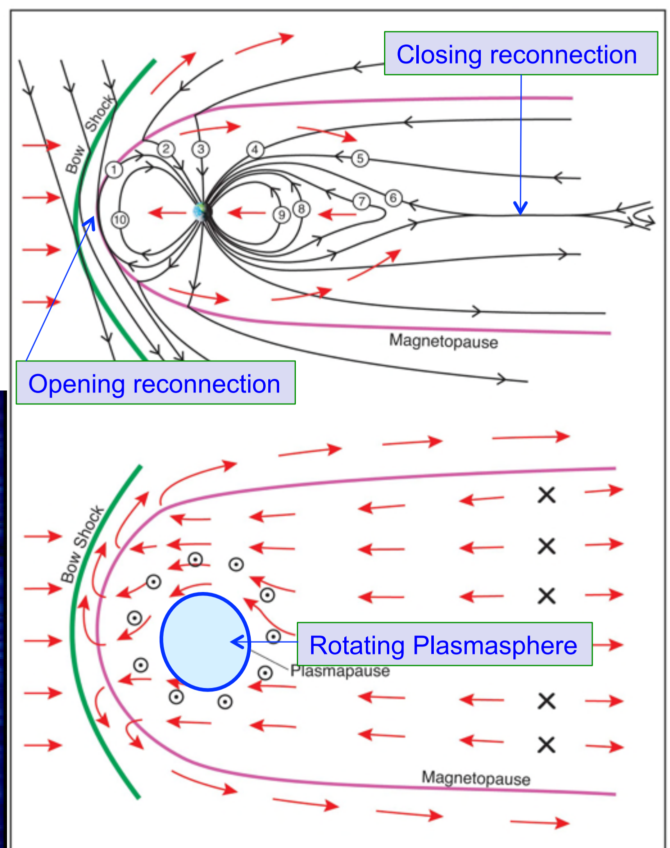

This is the conventional E-J approach. See Parker 1996; Vasyliunas 2005 for B-V approach

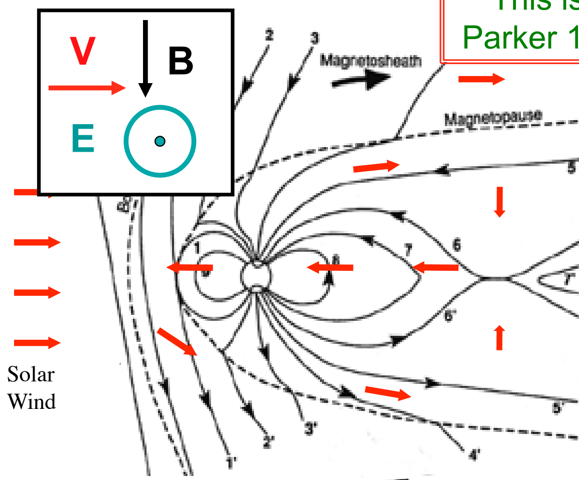


*The Dungey Cycle*

Solar wind driven magnetospheric convection*

$\mathbf{E}_{convection} = -\,\zeta\,\mathbf{V}_{SW} \times \mathbf{B}_{SW}$

$\zeta$~ efficiency of reconnection ~10-20%

crude approximation!!

$\mathbf{E}_{conv}$~ constant in m'sphere

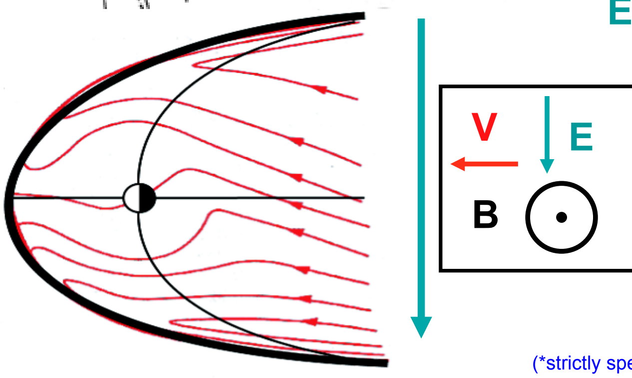


$\mathbf{V}_{convection}$

$\sim \zeta V_{SW}(R/R_{MP})^3$

(where 3 power assumes a dipole - in reality, the flow is not uniform and the power somewhat less)

(*strictly speaking not convection but advection or circulation)

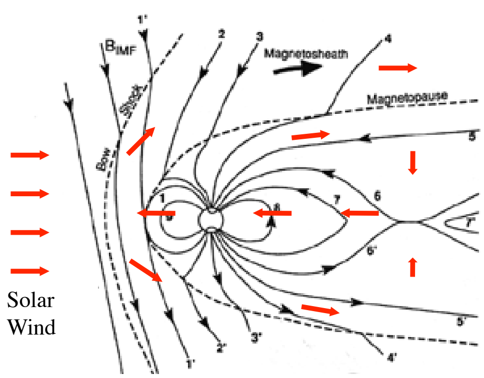


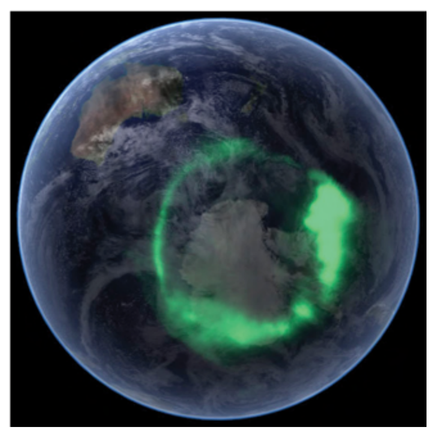

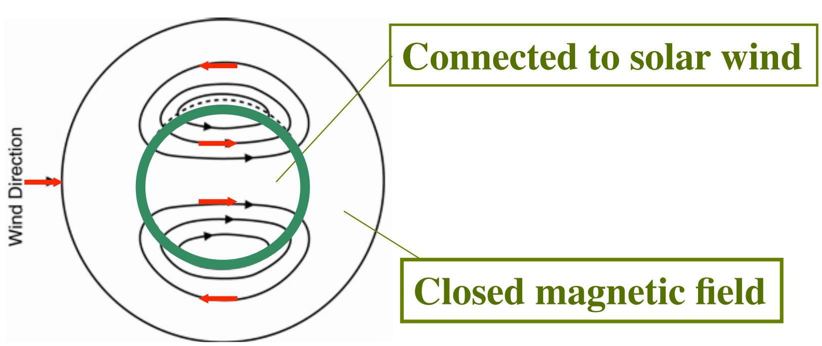


Polar view

# Reality = Messy & 3D

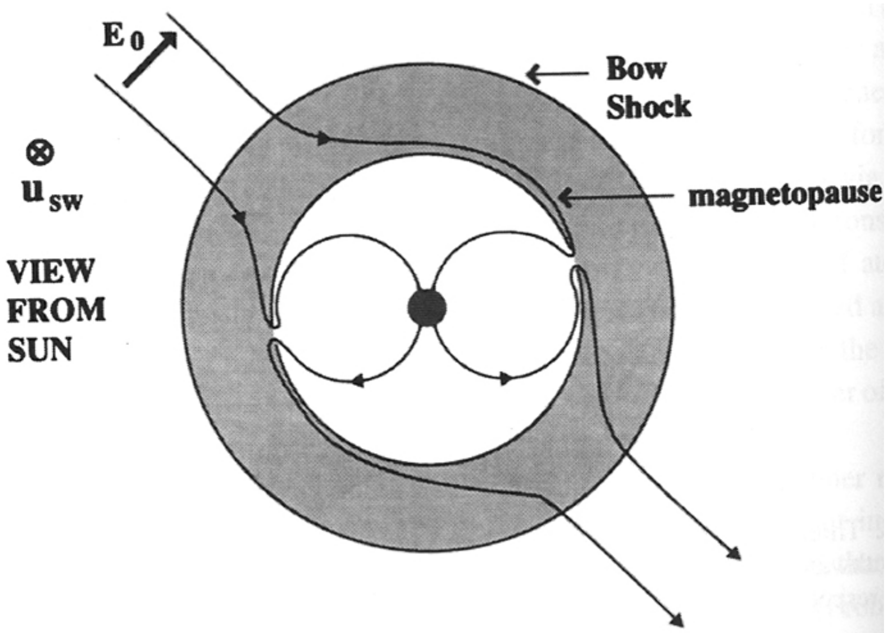


## *Dynamics*

*Dayside magnetopause*

- Response to $B_{SW}$ direction
- Solar wind ram pressure

*Tail Reconnection*

- Depends on recent history of dayside reconnection and state of plasmasheet

***Space Weather!***

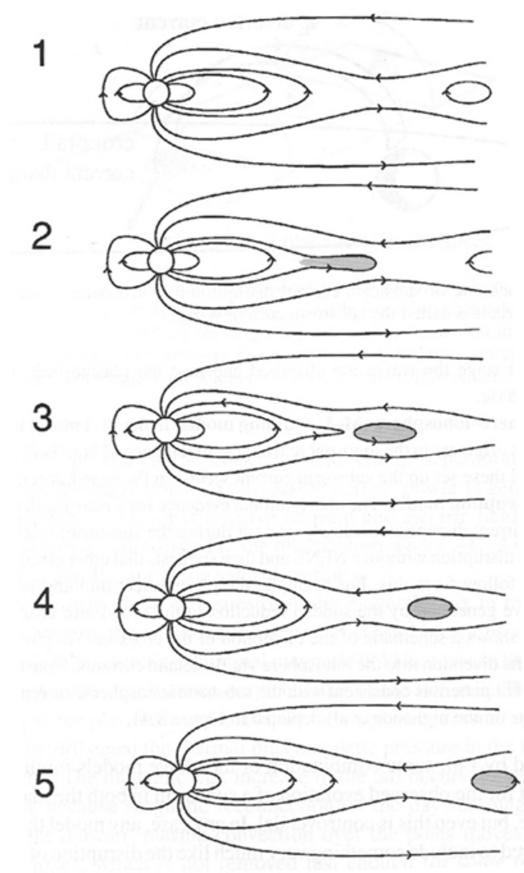

$$\mathbf{V}_{co} \sim \Omega \times \mathbf{R}$$

$$\mathbf{V}_{convection} \sim \zeta V_{SW}(R/R_{MP})^3$$

Fraction of planetary magnetosphere that is rotation dominated is…

$$R_{pp}/R_{MP} \sim [\, r_p R_{MP}\, \Omega \,/\, \zeta V_{SW}]^{1/2} \propto \Omega^{1/2}\mu^{1/6}/(\rho_{sw})^{1/12}\, V_{sw}^{2/3}$$

Where $r_p$=planetary radius

$\mu$= magnetic moment of planet $B_o R_p^3$

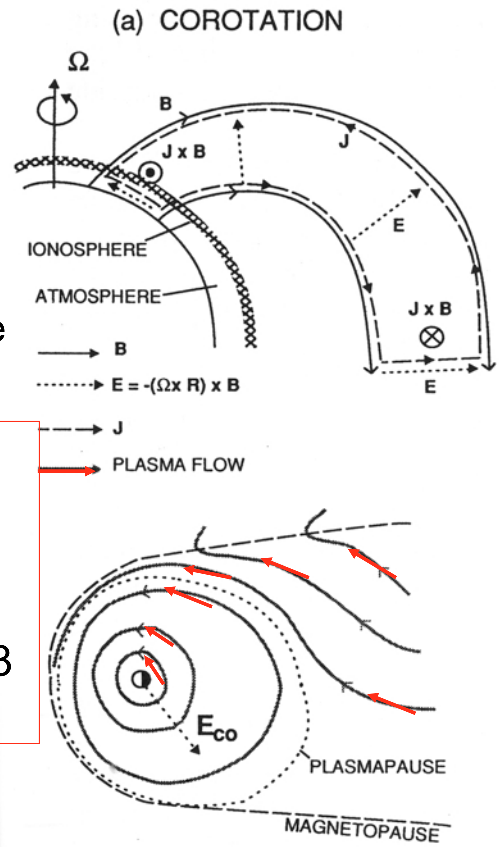


## Magnetospheric Dynamics – Vol. I Ch. 13 *also Bagenal 2011*

| | Mercury | Earth | Jupiter | Saturn | Uranus | Neptune |
|---|---|---|---|---|---|---|
| $R_{MP}$[a] (km) | 4000 | $6.5 \times 10^4$ | $6 \times 10^6$ | $1 \times 10^6$ | $6 \times 10^5$ | $6 \times 10^5$ |
| $V_{SW}$[b] (km/s) | 370 | 390 | 420 | 430 | 450 | 460 |
| $t_{N-T}$[c] | 10 s | 3 min | 4 hr | 45 min | 20 min | 20 min |
| $R_T$[d] ($R_p$) | 3 | 20 | 170 | 40 | 50 | 50 |
| $R_T$[d] (km) | 8000 | $1.3 \times 10^5$ | $1.2 \times 10^7$ | $2.3 \times 10^6$ | $1.3 \times 10^6$ | $1.2 \times 10^6$ |
| $V_{rec,1}$[e] (km/s) | 40 | 22 | 16 | 16 | 16 | 16 |
| $V_{rec,2}$[f] (km/s) | 37 | 39 | 42 | 43 | 45 | 46 |
| $t_{rec}$[g] | 3 min | 1 hr | 80 hr | 15 hr | 8 hr | 7 hr |
| $d_X$[h] ($R_p$) | 30 | 200 | 1700 | 400 | 500 | 500 |
| $V_{co}/V_{rec2}$[i] | $4 \times 10^{-5}$ | 0.04 | 8 | 1.3 | 0.4 | 0.4 |
| $R_{pp}$[j] ($R_p$) | 0.03 | 6.7 | 350 | 95 | 70 | 70 |

a Sub-solar magnetopause distance.

b $V_{SW}=387\,(a_p/a_E)^{0.05}$ (km/s) from Belcher et al. (1993)

c Solar wind nose-terminator time: $t_{N-T} = R_{MP} / V_{SW}$

d Radius of cross section of magnetotail, approximated as $R_T = 2R_{MP}$.

e Reconnection speed assuming 20% reconnection efficiency and $v_{rec} \sim 0.2\, v_{SW} B_{SW}/ B_{MP}$ km/s (e.g. Kivelson 2007)

f Reconnection speed assuming 10% reconnection efficiency and $v_{rec} \sim 0.1\, v_{SW}$ km/s

g Reconnection time $t_{rec} = R_T / v_{rec,2}$ (s)

h Distance to X-line $d_x \sim v_{SW}\, t_{rec}$

i Assumes rotation speed at the magnetopause is ~30% of rigid corotation

j Distance to plasmapause, where corotation is comparable to reconnection flow (e.g. Kivelson 2007)

## *Solar-wind vs. Rotation-dominated magnetospheres*

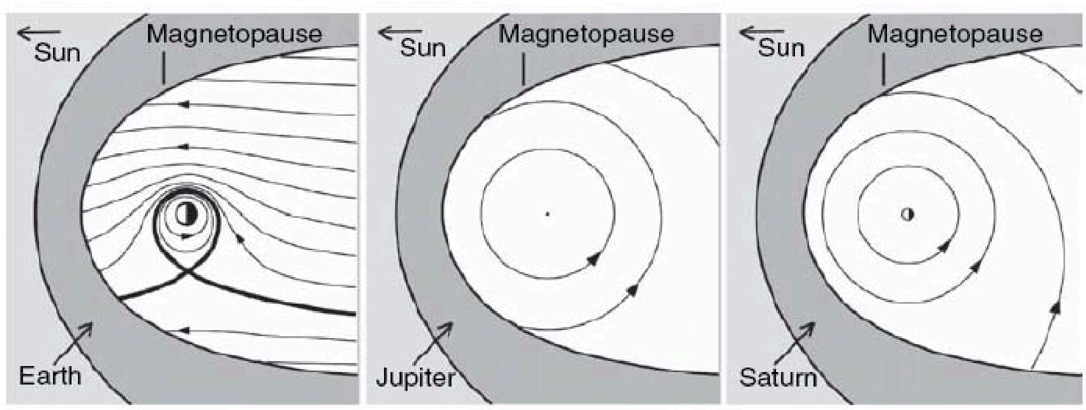


$R_{plasmapause} / R_{Planet} =$

6.7 350 95

# Plasma Sources

| | Mercury | Earth | Jupiter | Saturn | Uranus | Neptune |
|---|---|---|---|---|---|---|
| $N_{max}$ $cm^{-3}$ | ~1 | 1-4000 | >3000 | ~100 | ~3 | ~2 |
| Comp-osition | $H^+$ Solar Wind | $O^+$ $H^+$ Iono-sphere | $O^{n+}$ $S^{n+}$ Io | $O^+$ $H_2O^+$ $H^+$ Enceladus | $H^+$ Iono-sphere | $H^+$ $N^+$ Triton Iono-sphere |
| Source kg / s | ? | 5 | 700-1200 | ~20 70-700? | ~0.02 | ~0.2 |

Sources of Plasma:
Solar Wind + ionosphere mixed (over the poles) into magnetotail and convected sunward

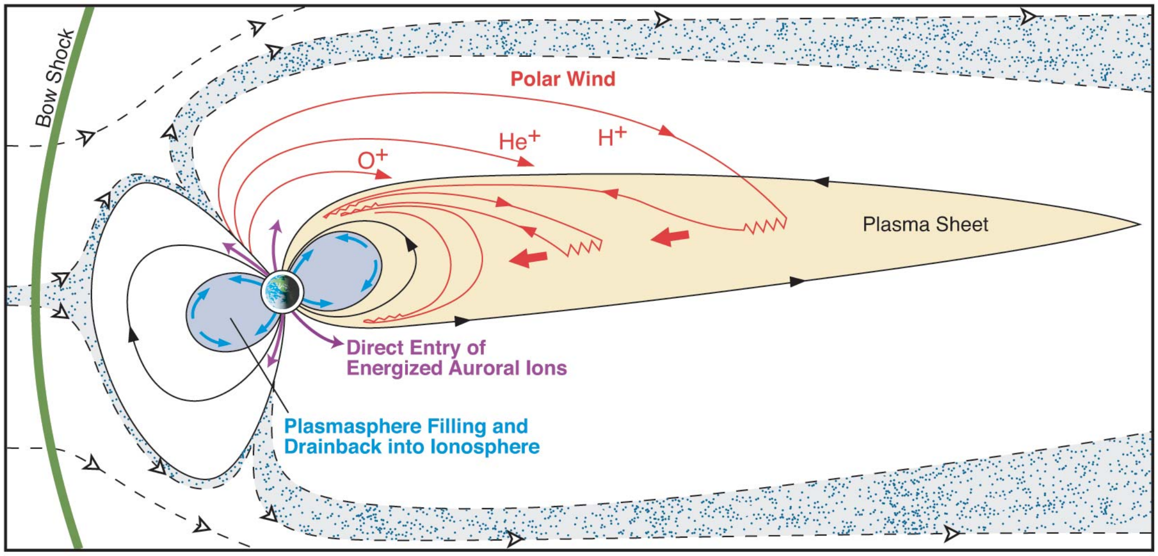


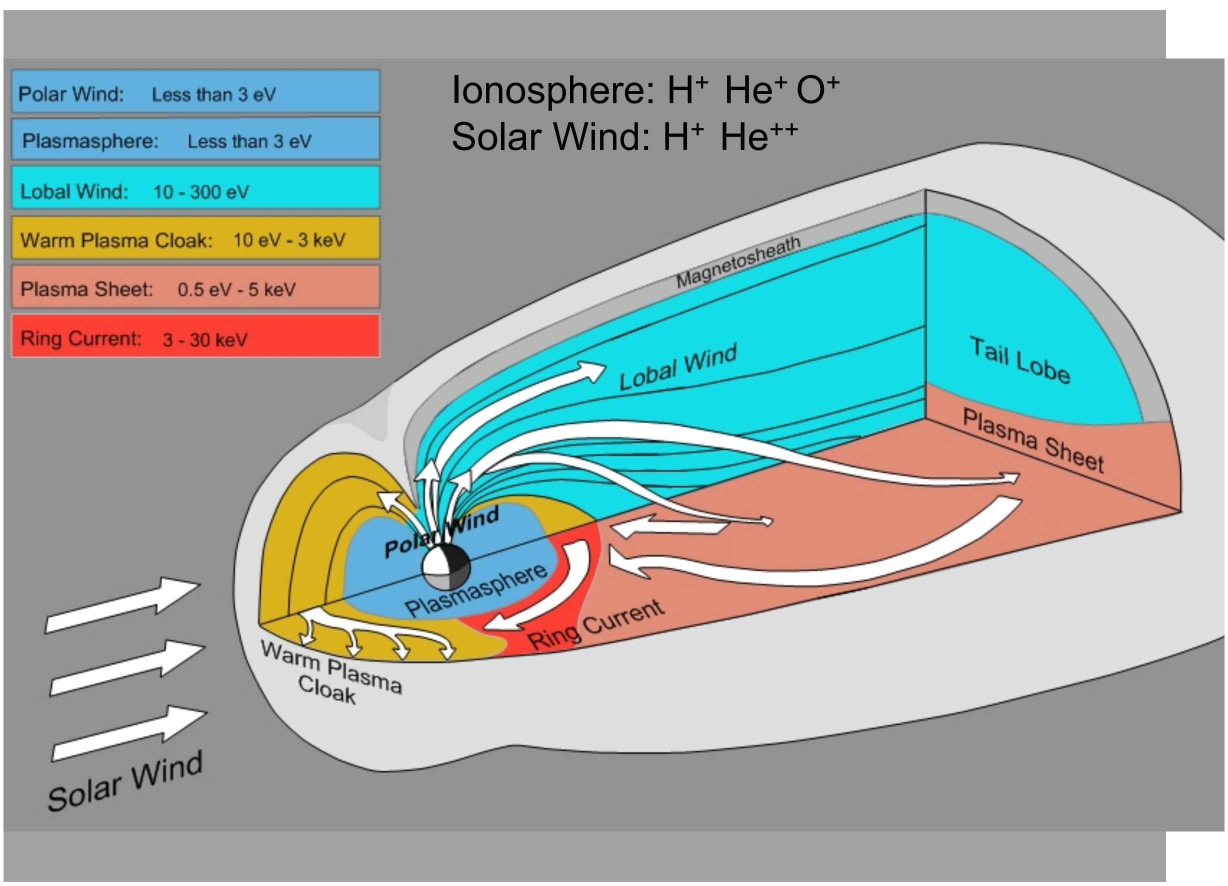

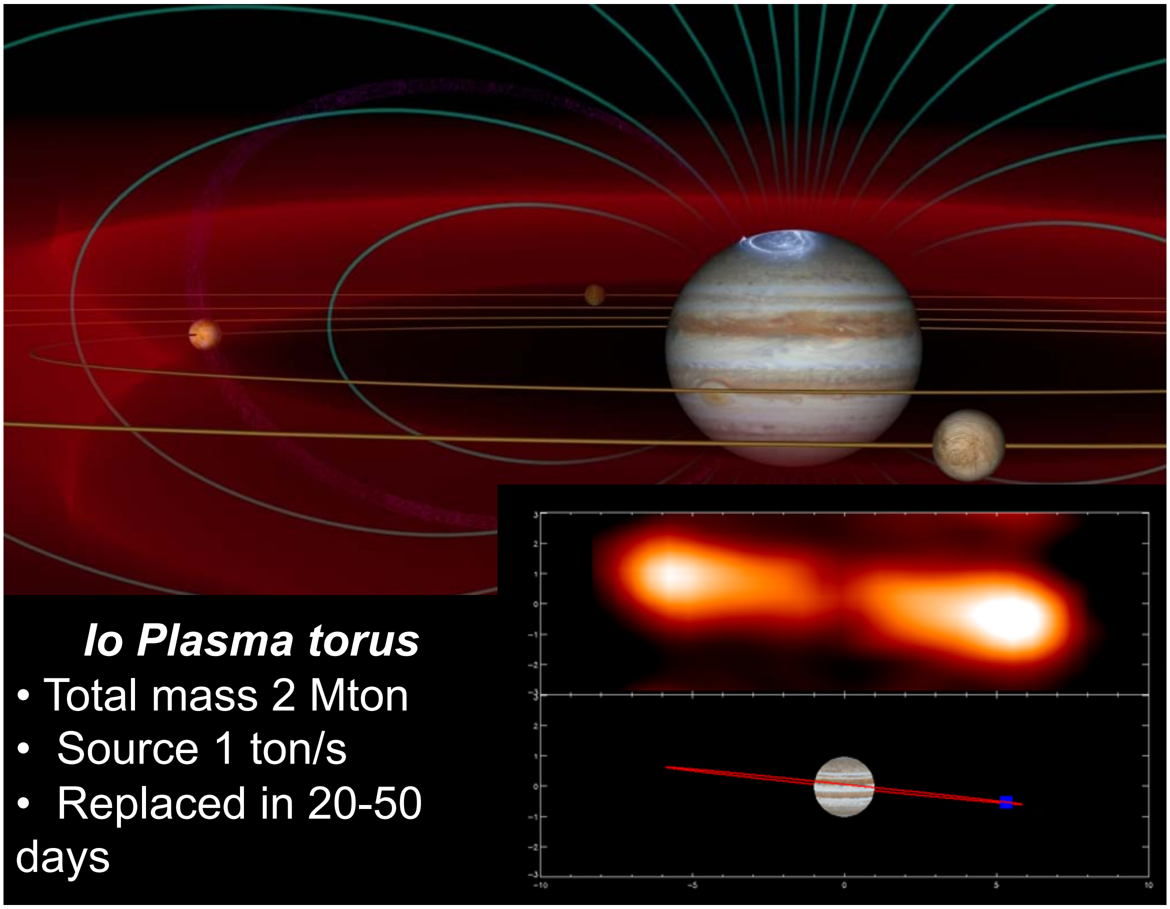


## Ion Pick Up

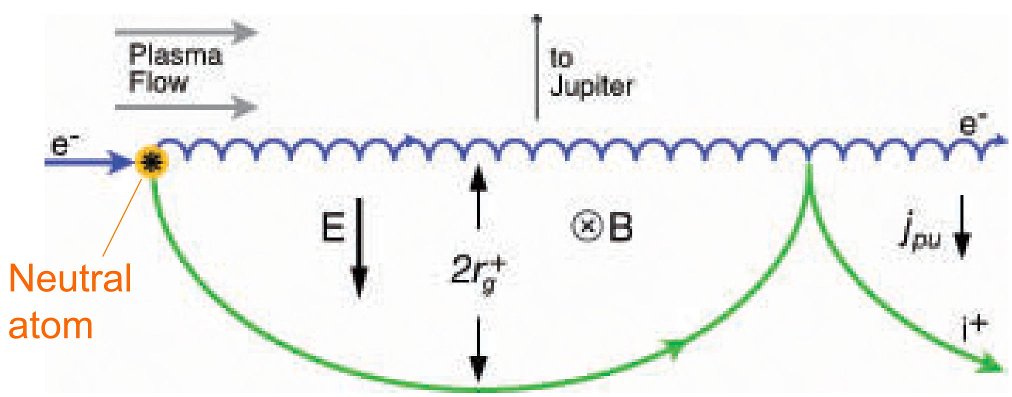


The magnetic field couples the plasma to the spinning planet

**_Cassini_**
**_UVIS_**

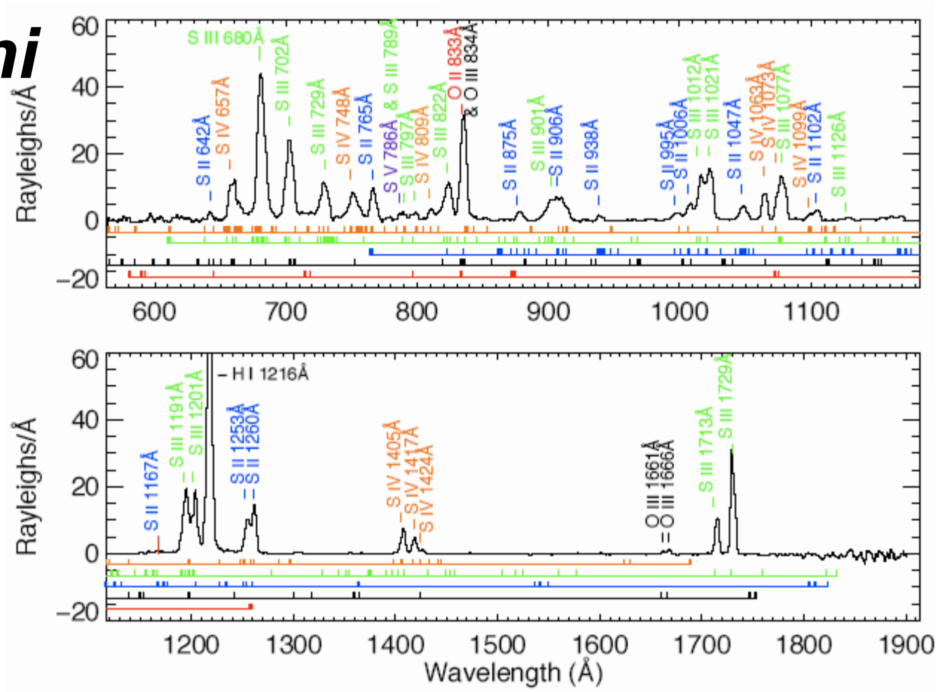


*Andrew Steffl*

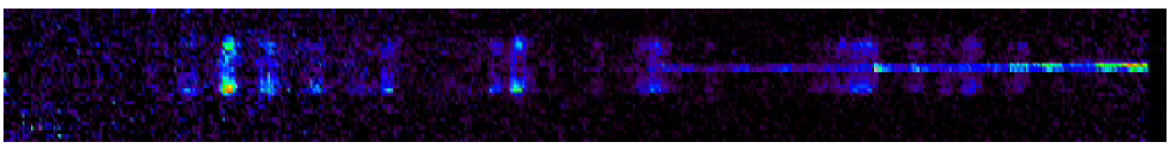

***Energy Crisis!***

- Total thermal energy ~6 x $10^{17}$ J
- Ion pick-up source takes 4 days
- UV power cools electrons ~7 hrs
- Extra source of hot electrons

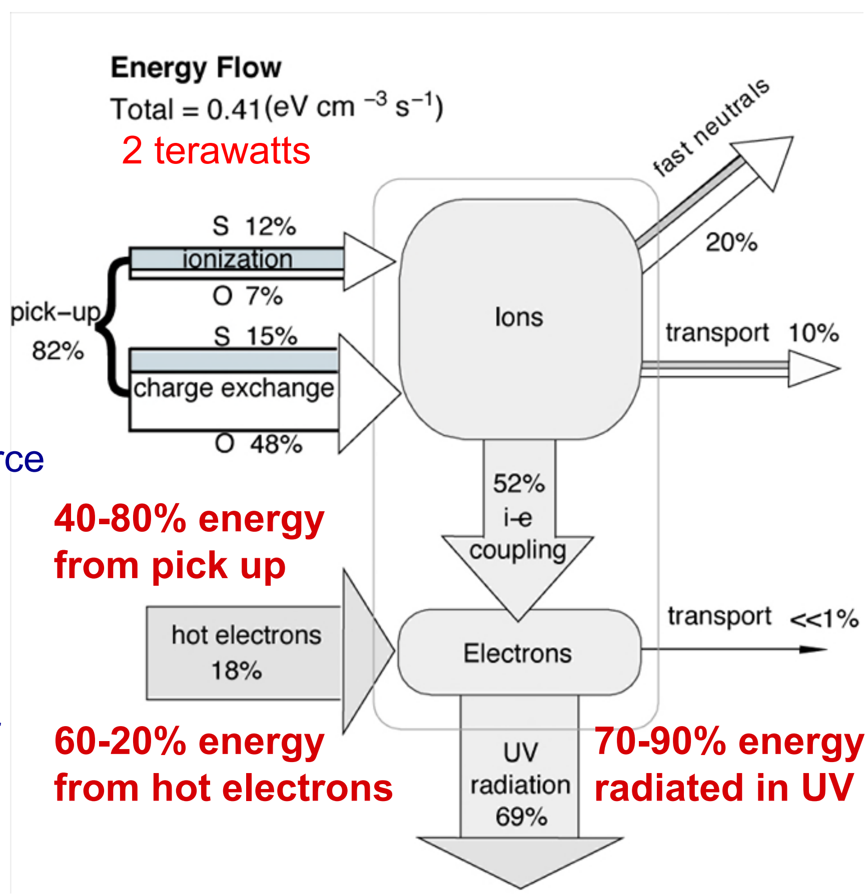

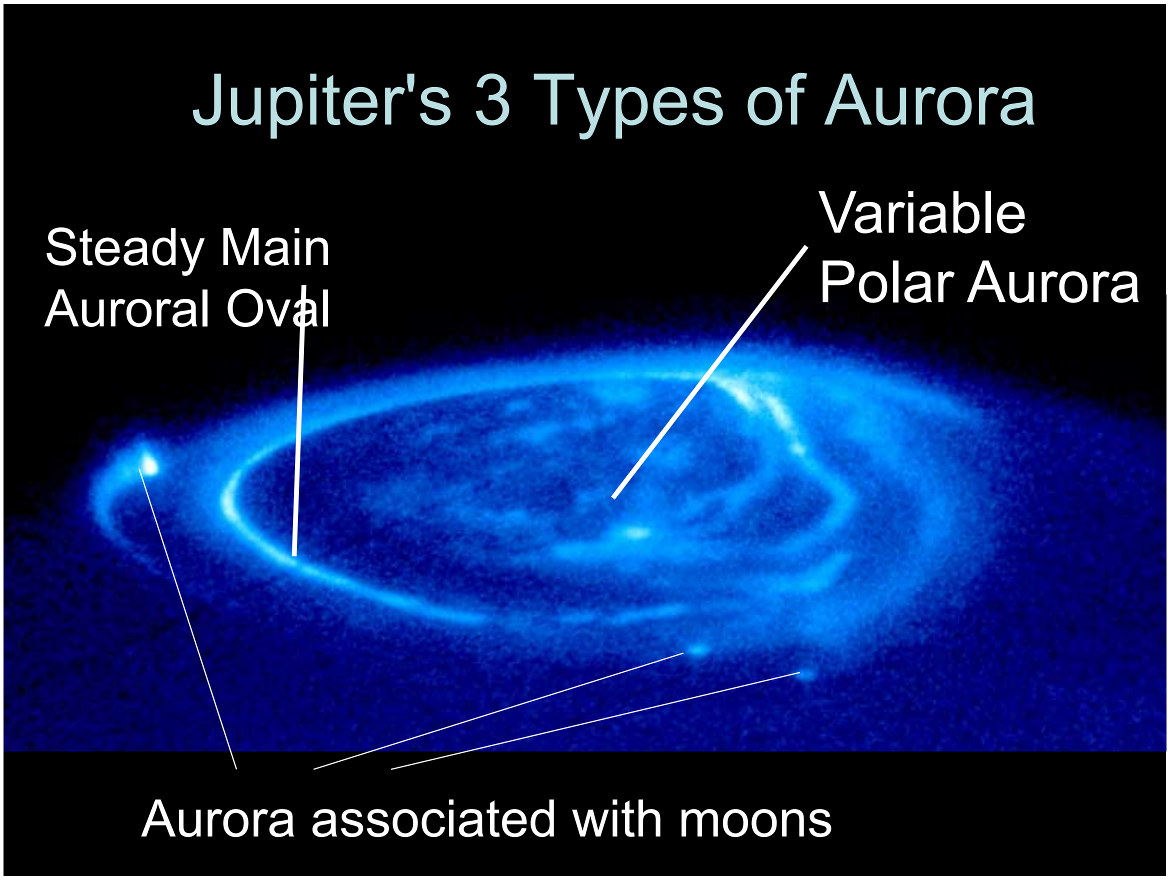
Jupiter's 3 Types of Aurora
Steady Main
Auroral Oval
Variable
Polar Aurora
Aurora associated with moons

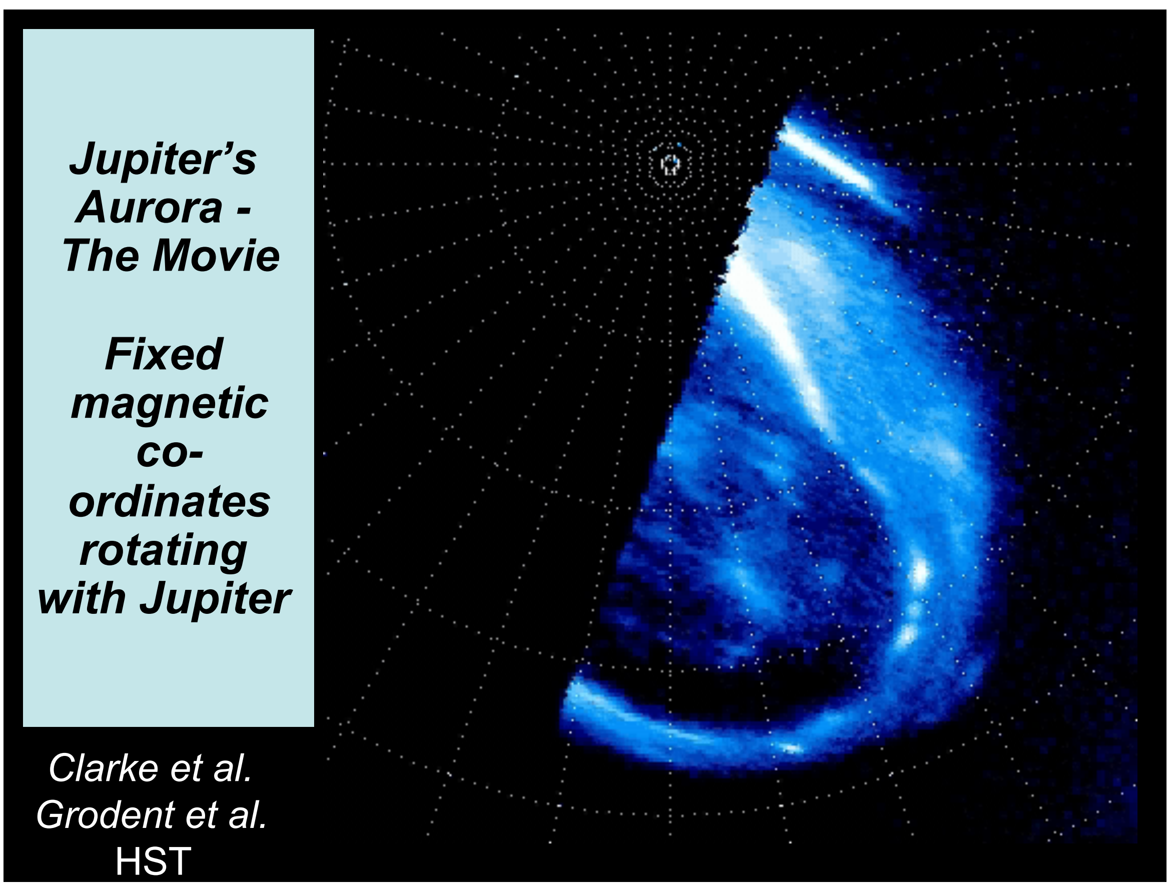
Jupiter's
Aurora -
The Movie
Fixed
magnetic
co-
ordinates
rotating
with Jupiter
Clarke et al.
Grodent et al.
HST

## *Main Aurora*

- Shape constant, fixed in magnetic co-ordinates
- Magnetic anomaly in north
- Steady intensity
- ~1° Narrow

*Clarke et al*., *Grodent et al*. HST

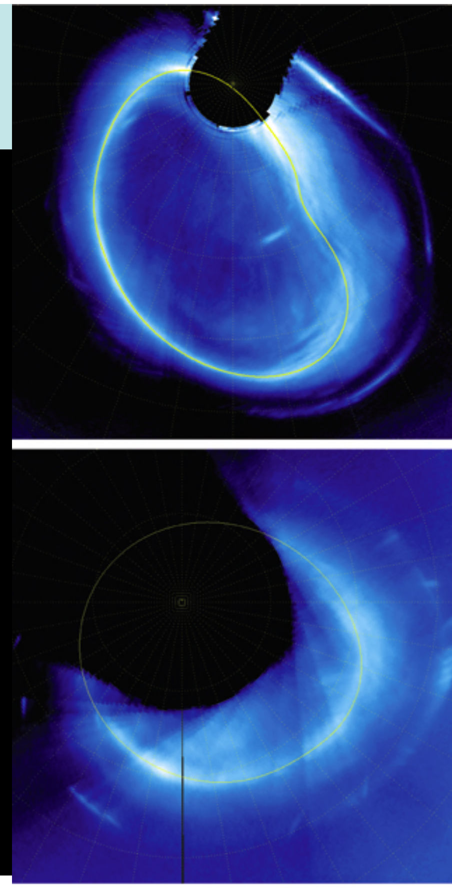

## *The aurora is the signature of Jupiter's attempt to spin up its magnetosphere*

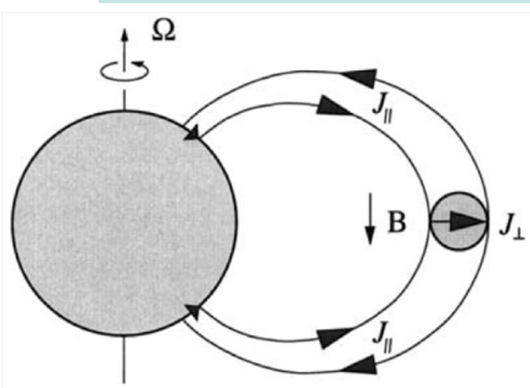


*Hill 1979*

- Outward transport of Iogenic plasma
- $J_{||}$ transfers load to ionosphere
- Transfer of angular momentum limited by ionospheric conductivity Σ

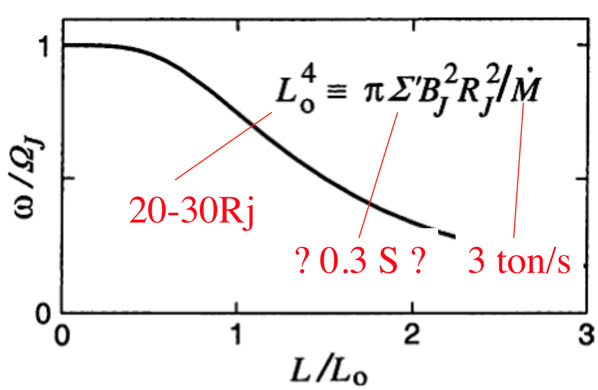


*N.B. Lo has units*

## *Coupling the Plasma to the Flywheel*

*Khurana 2001*

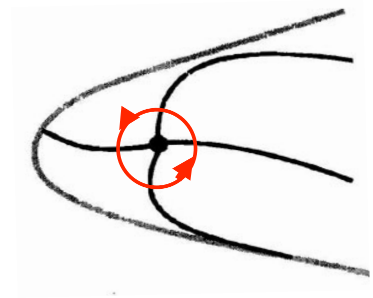

- As plasma from Io moves outwards its rotation decreases (conservation of angular momentum)
- Sub-corotating plasma pulls back the magnetic field
- Curl **B** -> radial current $J_r$
- $J_r$ x **B** force enforces rotation

**Field-aligned currents couple magnetosphere to Jupiter's rotation**

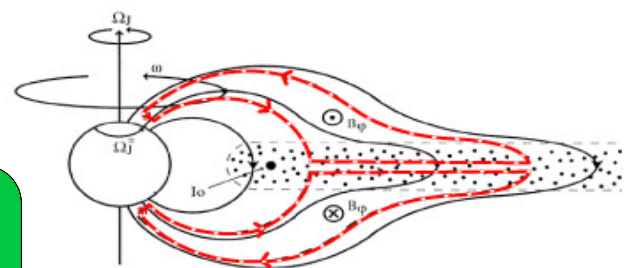



*Cowley & Bunce 2001*

## ***The aurora is the signature of Jupiter's attempt to spin up its magnetosphere***

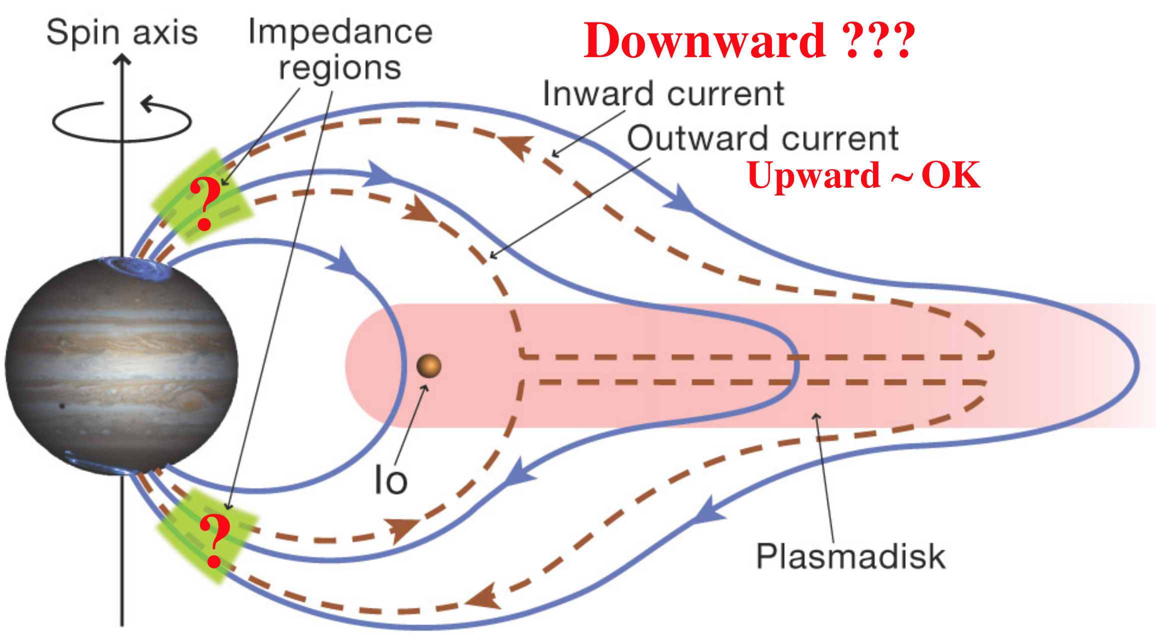

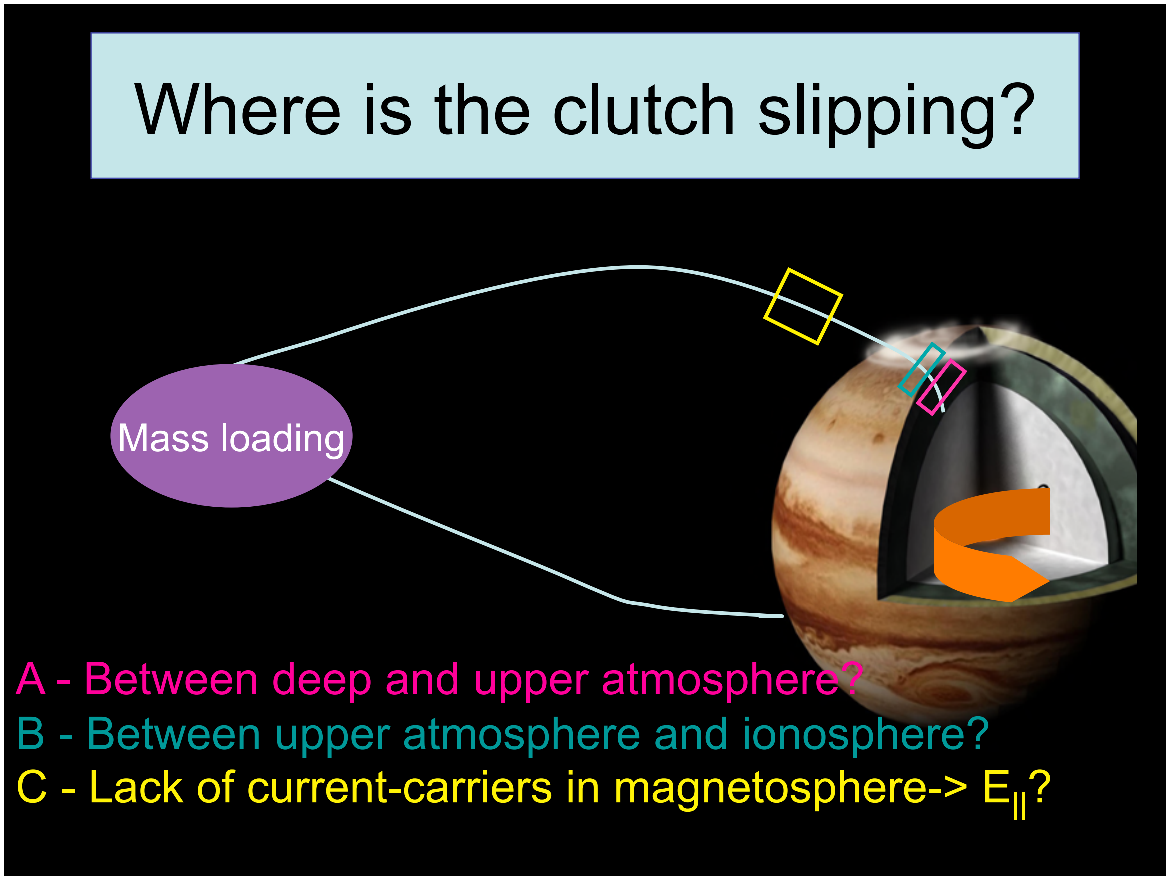

Where is the clutch slipping?
Mass loading
A - Between deep and upper atmosphere?
B - Between upper atmosphere and ionosphere?
C - Lack of current-carriers in magnetosphere-> $E_{||}$?


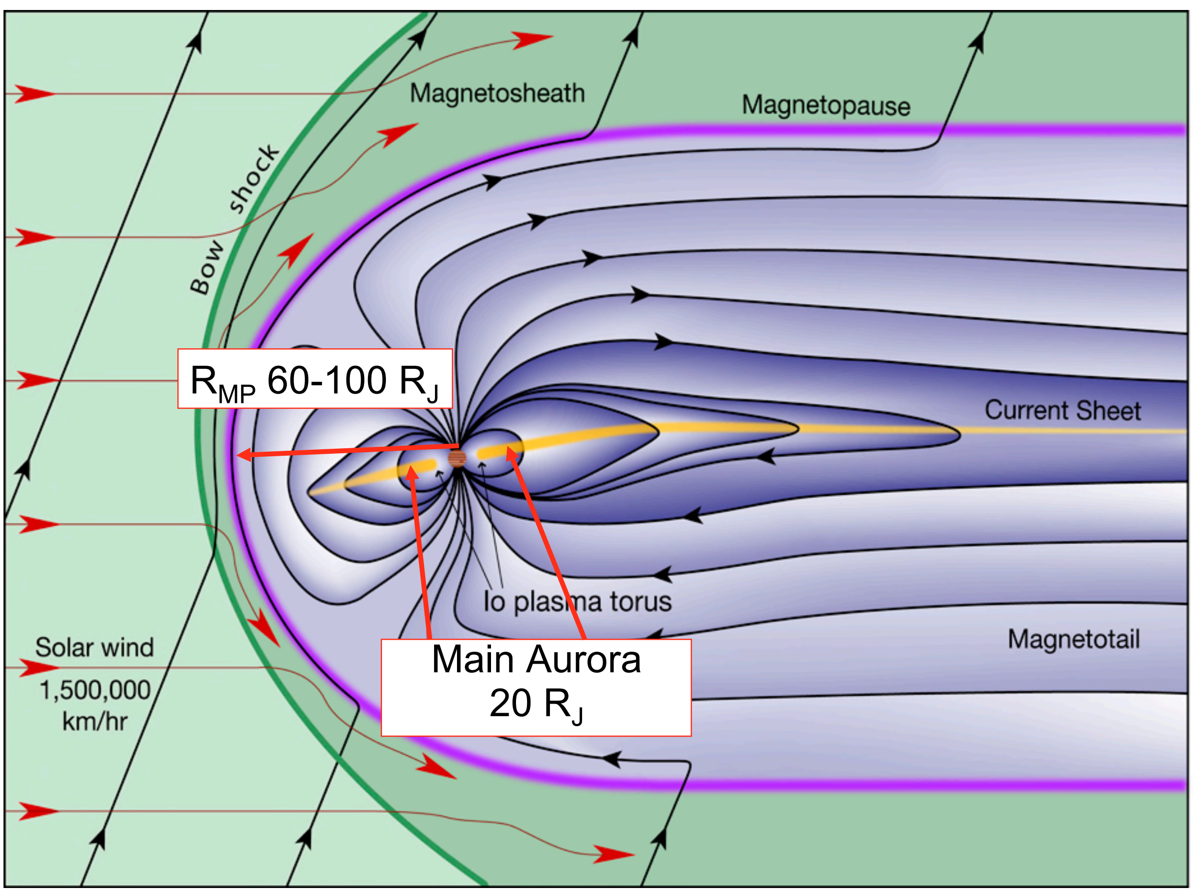

Magnetosheath
Magnetopause
Bow shock
$R_{MP}$ 60-100 $R_J$
Current Sheet
Io plasma torus
Main Aurora
20 $R_J$
Solar wind
1,500,000
km/hr
Magnetotail

*Magnetic field model of Khurana*

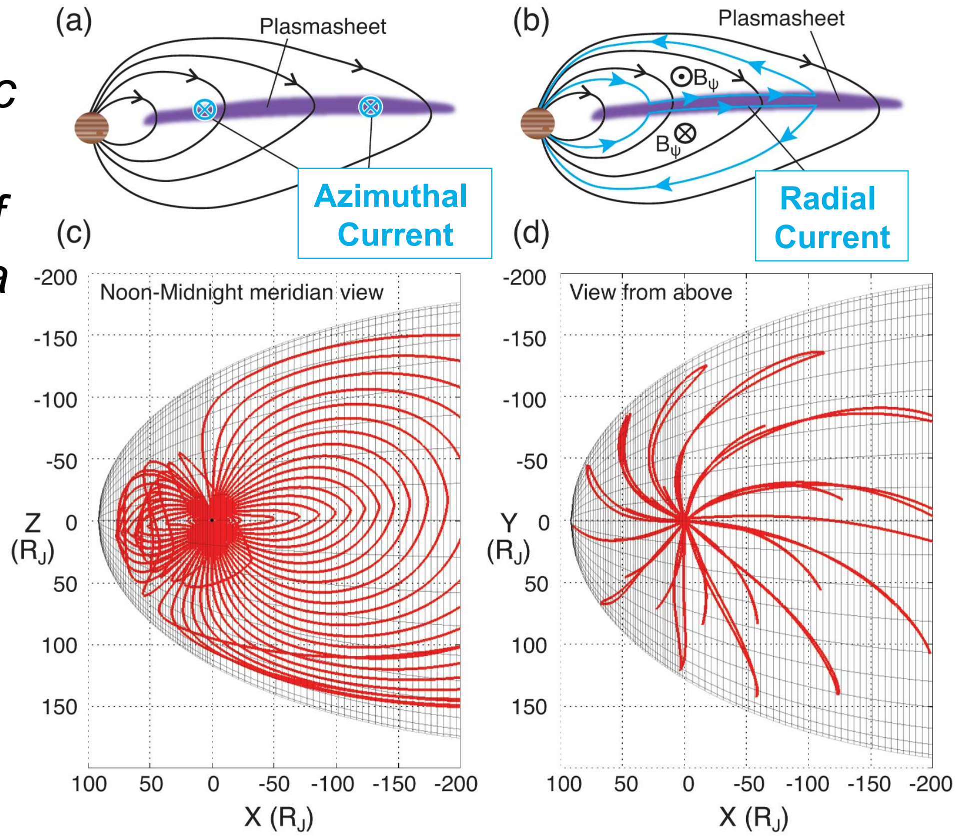


Magnetospheres scaled by stand-off distance of dipole field

| | $M/M_E$ | $MP_{Dipole}$ | $MP_{mean}$ | $MP_{Range}$ |
|---|---|---|---|---|
| Mercury | ~8x$10^{-3}$ | 1.4 $R_M$ | 1.4 $R_M$ | |
| Earth | 1 | 10 $R_E$ | 10 $R_E$ | |
| Saturn | 600 | 20 $R_S$ | 24 $R_S$ | 22-27* $R_S$ |
| Jupiter | 20,000 | 46 $R_J$ | 75 $R_J$ | 63-92# $R_J$ |

**Inflated magnetospheres of Jupiter & Saturn due to HOT PLASMAS**

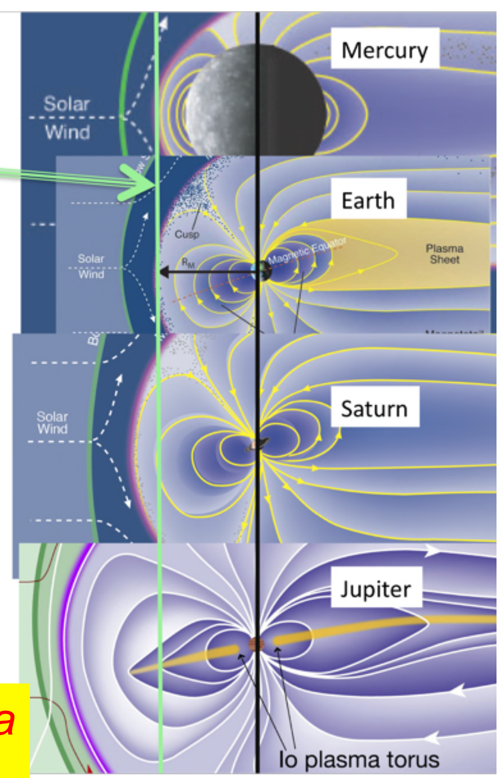


*What process heats the plasma as it moves outwards????*

# Vasyliunas Cycle

*Vasyliunas*
*Cowley et al.*
*Southwood & Kivelson*

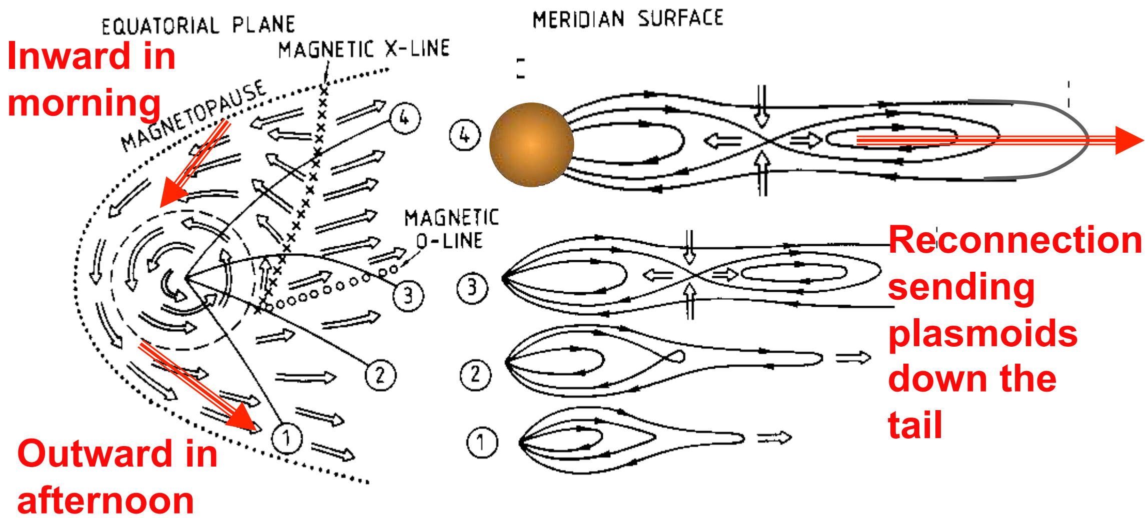


*Vogt et al. 2010*

Observations of plasmoid events in *Galileo* data

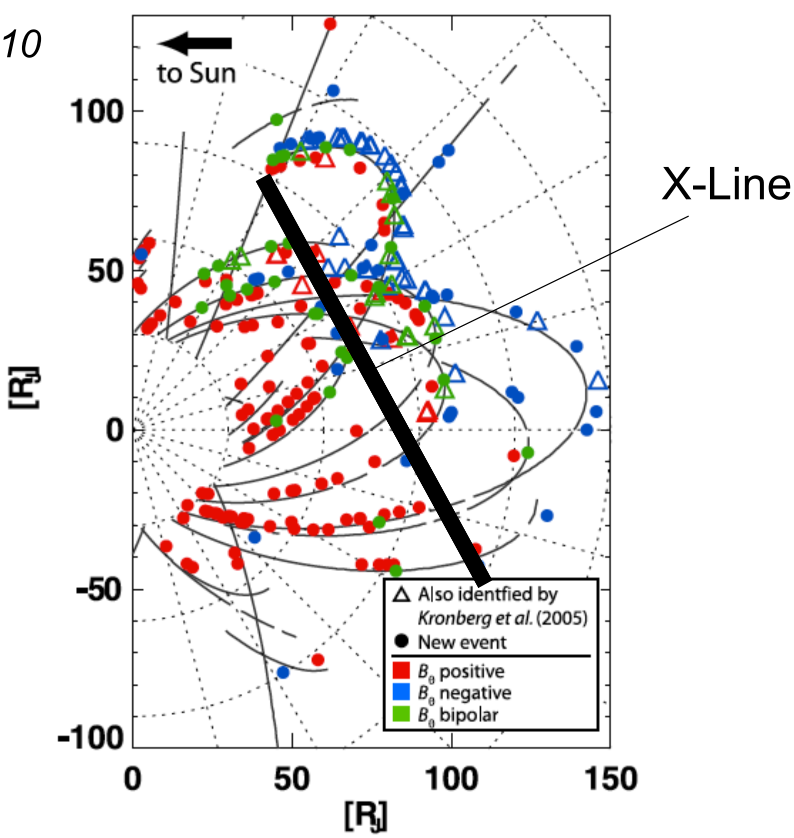

*Delamere & Bagenal (2011)*

Solar wind interaction:

- More of a plasma-plasma interaction

- Less of an interaction between magnetic fields

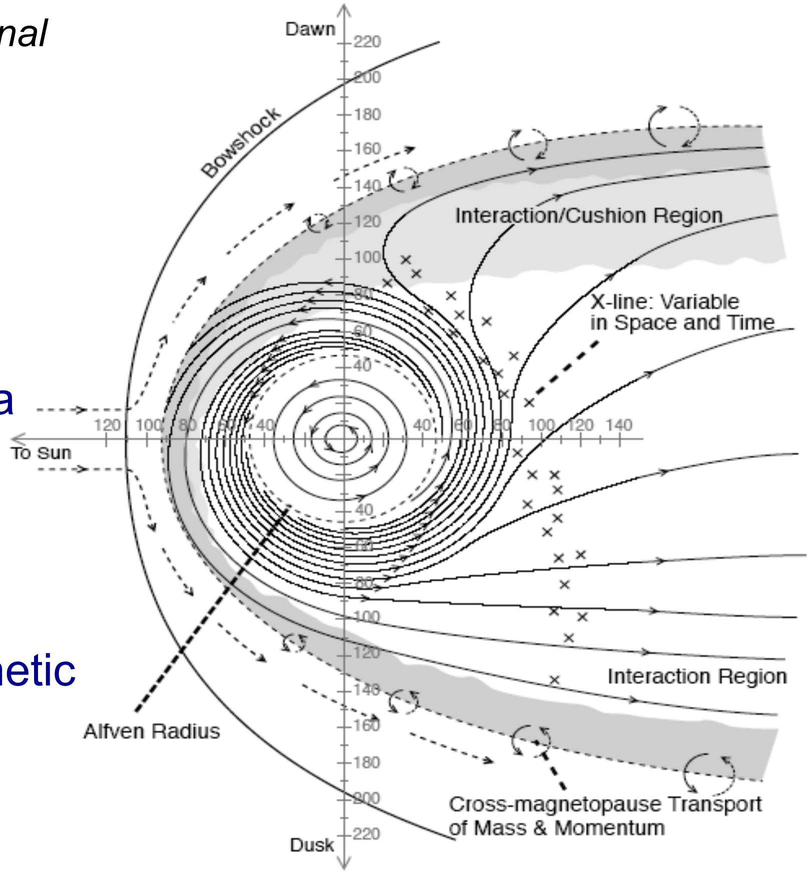


Can small-scale boundary-layer processes act like viscosity?

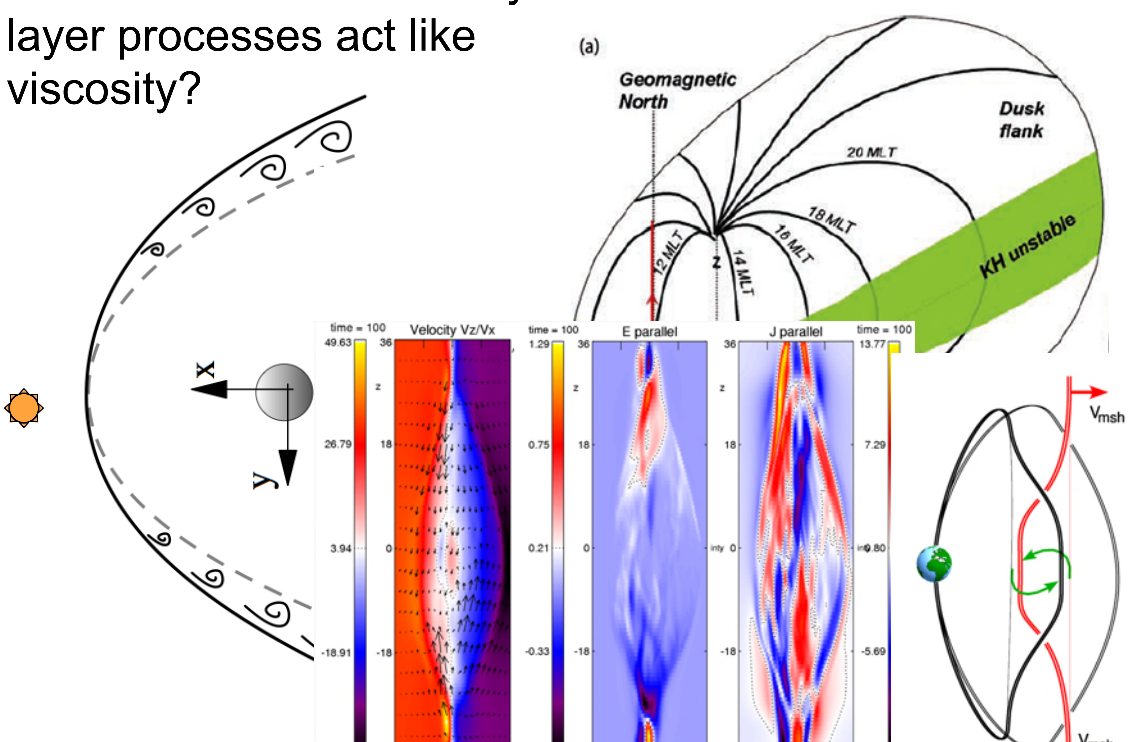


*Otto & Fairfield 2001*

Hybrid simulations of Kelvin-Helmholtz instability
- ions=particles
- electrons=fluid

*Peter Delamere, CU*

Bx

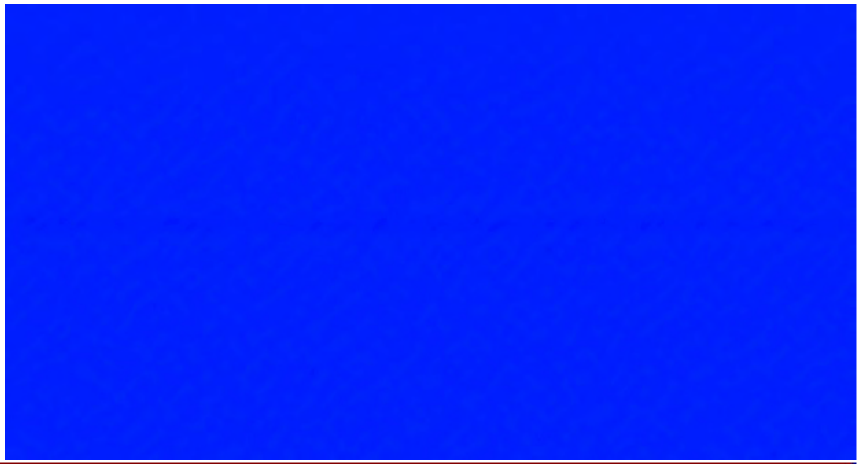

Heavy Light

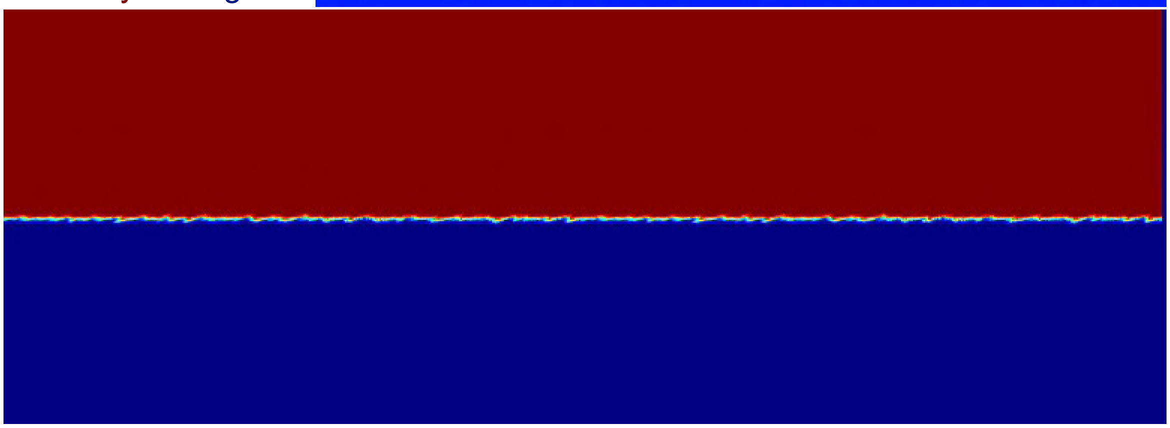

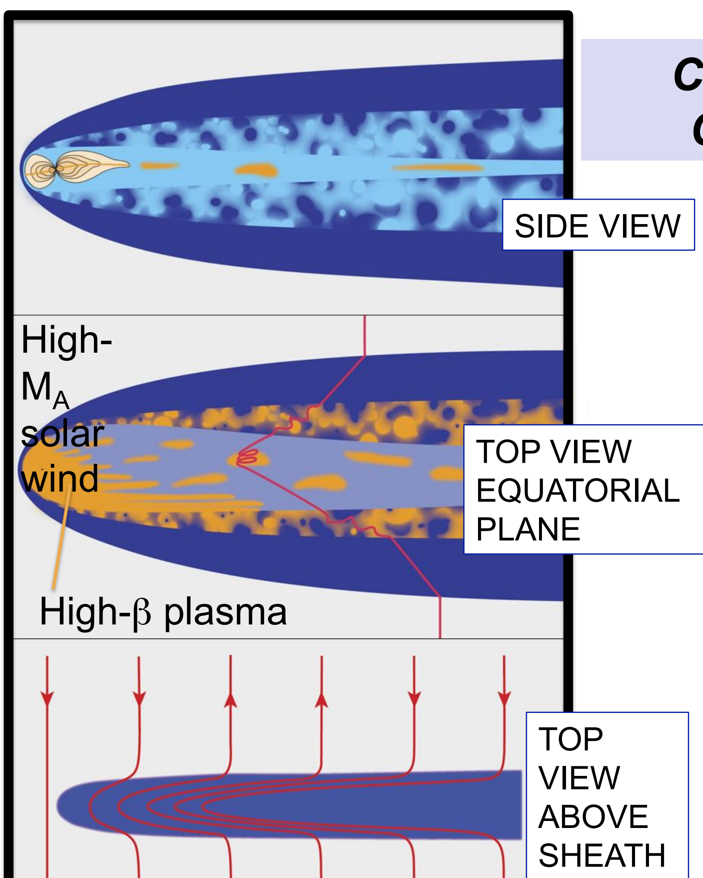


## ***Could Jupiter be a Colossal Comet?***

- *Plasma-plasma interaction with magnetic field playing less of a role than at Earth*
- Solar wind hung up on the boundary layers
- Venus- or comet-like rather than field-controlled terrestrial tail.

## Polar Magnetosphere

Juno passes directly through auroral field lines

Measures particles precipitating into atmosphere creating aurora

Plasma/radio waves reveal processes responsible for particle acceleration

UV & IR images provides context for *in-situ* observations

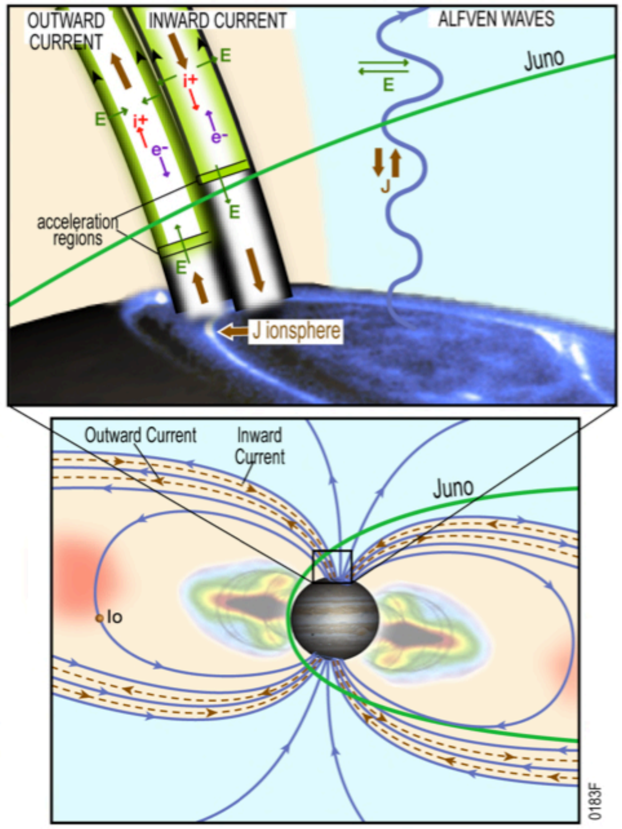


## *Saturn:*

Strong satellite & ring sputtering, weak ionization

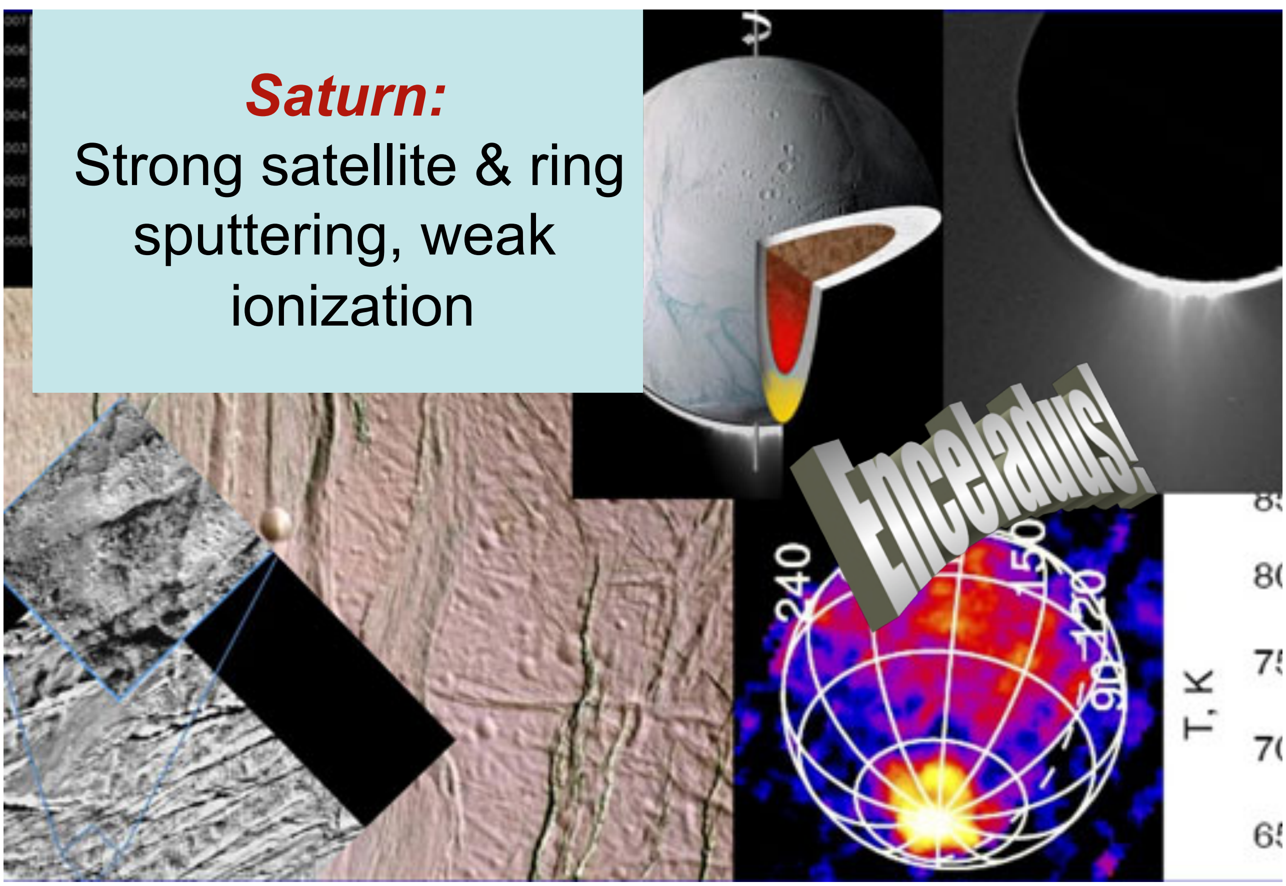

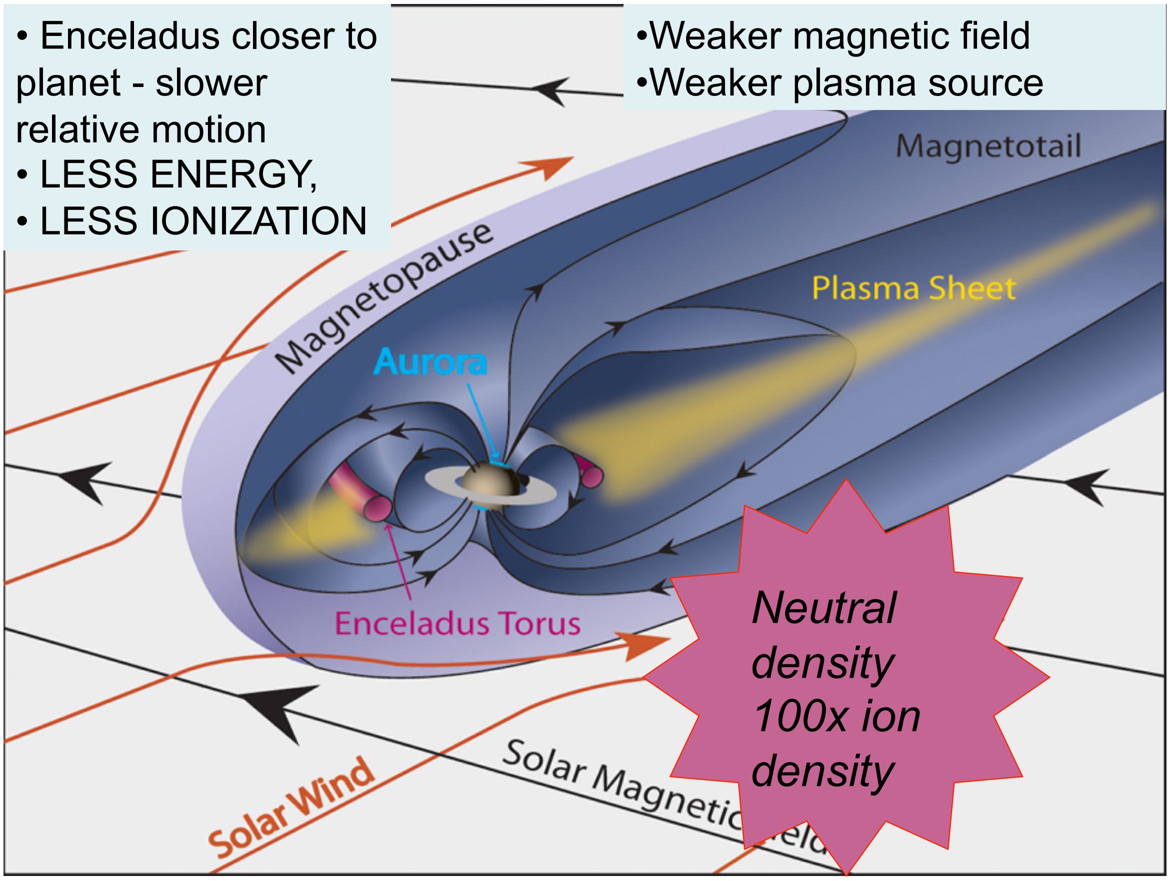


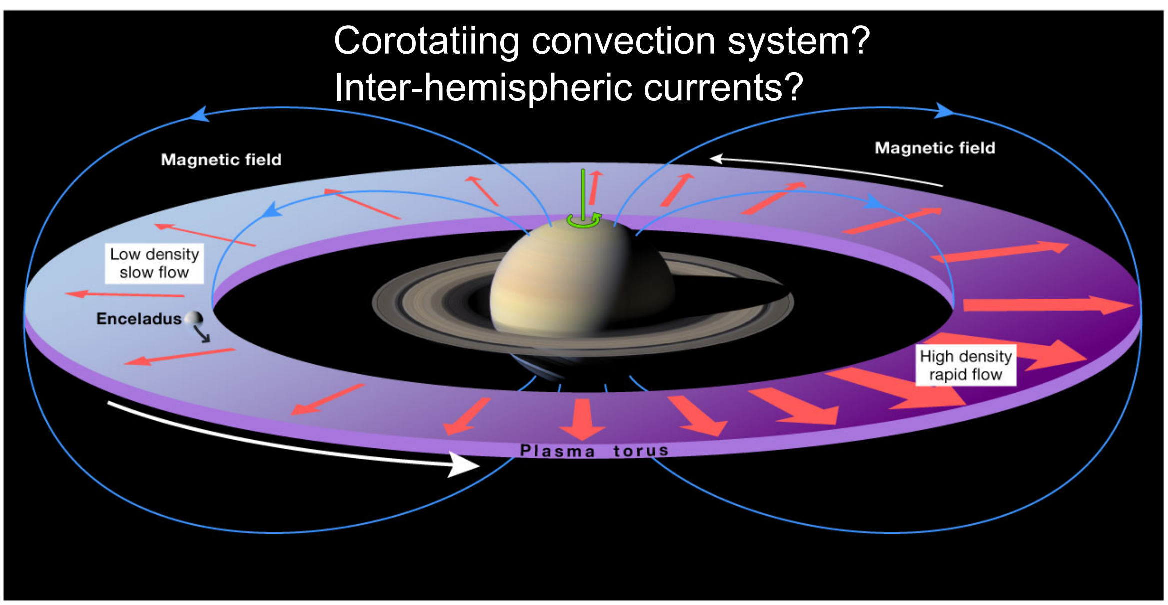


- Saturn's magnetic field is very symmetric – why are there periodic variations?
- Variable rotation rate?? Changes over “season”
- Current system between poles modulating ionization? Slowly changing with illumination of ionosphere / thermospheric winds??
- North & South ionospheres rotate at different rates??

# Plasma sheet shape: forcing

- Global shape of the current and plasma sheet is determined by:
  - Diurnal motion (dipole tilt) / other periodic mechanisms.
  - Centrifugal forcing on plasma offset from the rotational equator.
  - Stresses imposed on the magnetosphere from the solar wind.

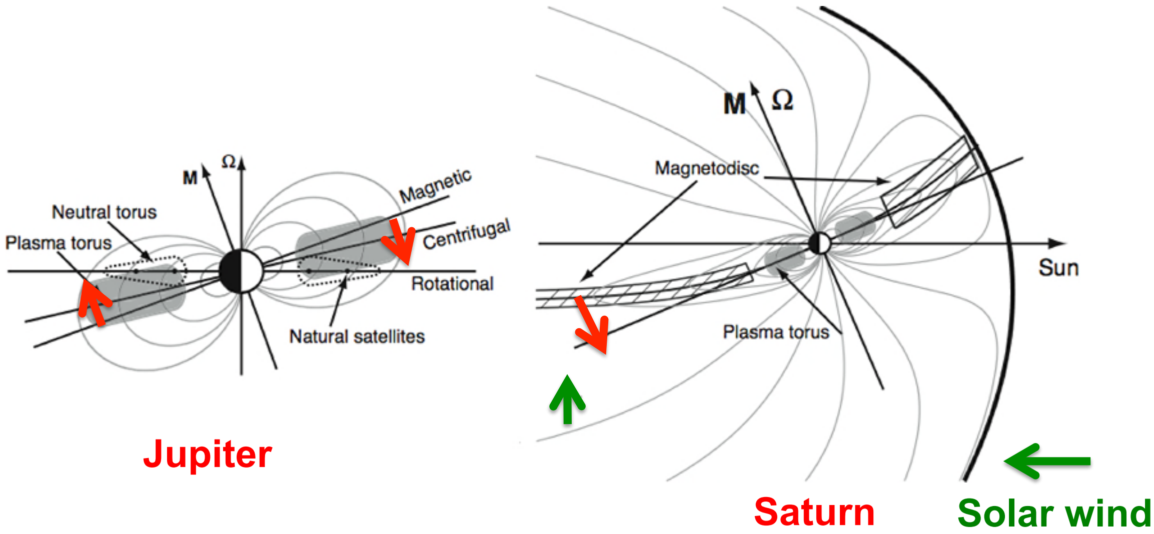


Arridge et al. (2011)

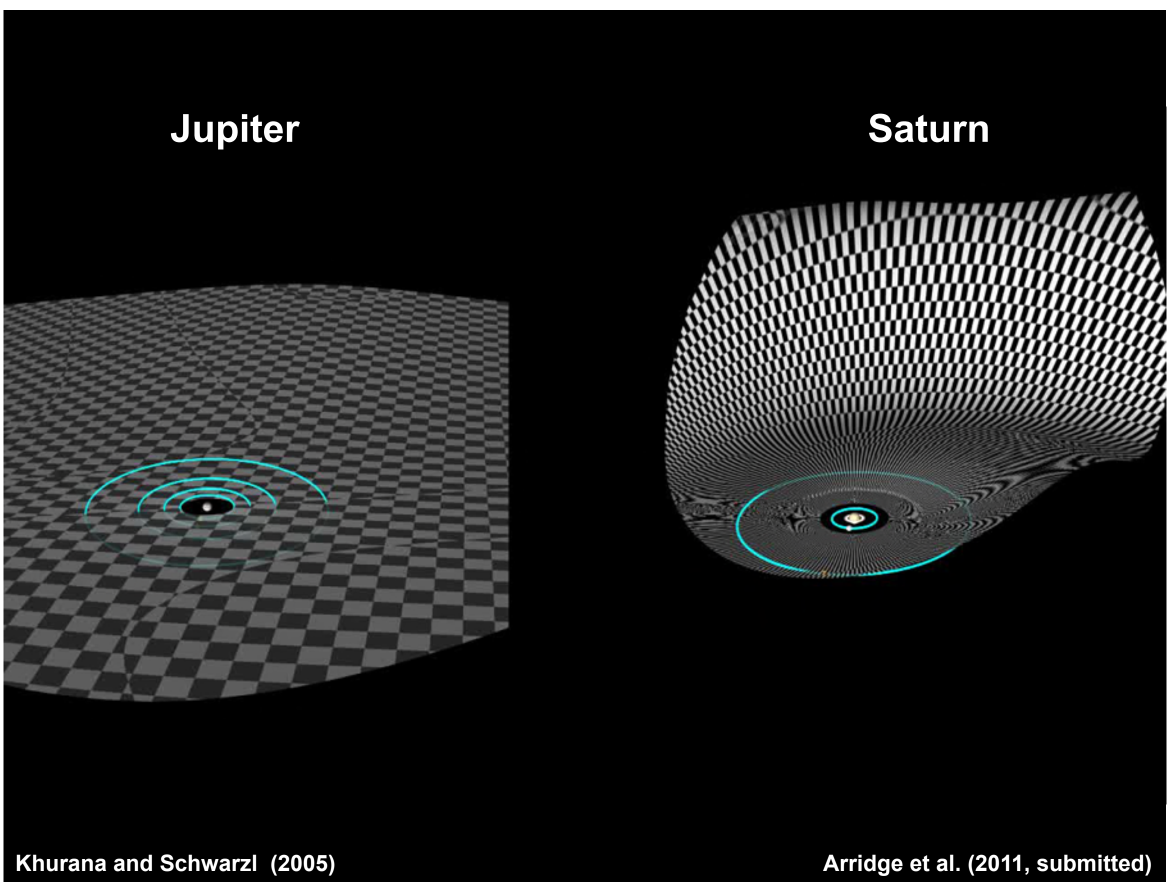

## Magnetospheres scaled by stand-off distance of dipole field

| | $M/M_E$ | $MP_{Dipole}$ | $MP_{mean}$ | $MP_{Range}$ |
|---|---|---|---|---|
| Mercury | ~$8 \times 10^{-3}$ | 1.4 $R_M$ | 1.4 $R_M$ | |
| Earth | 1 | 10 $R_E$ | 10 $R_E$ | |
| Saturn | 600 | 20 $R_S$ | 24 $R_S$ | 22-27* $R_S$ |
| Jupiter | 20,000 | 46 $R_J$ | 75 $R_J$ | 63-92# $R_J$ |

**Inflated magnetospheres of Jupiter & Saturn due to HOT PLASMAS**

Note bimodal average locations
* *Achilleos et al. 2008* # *Joy et al. 2002*

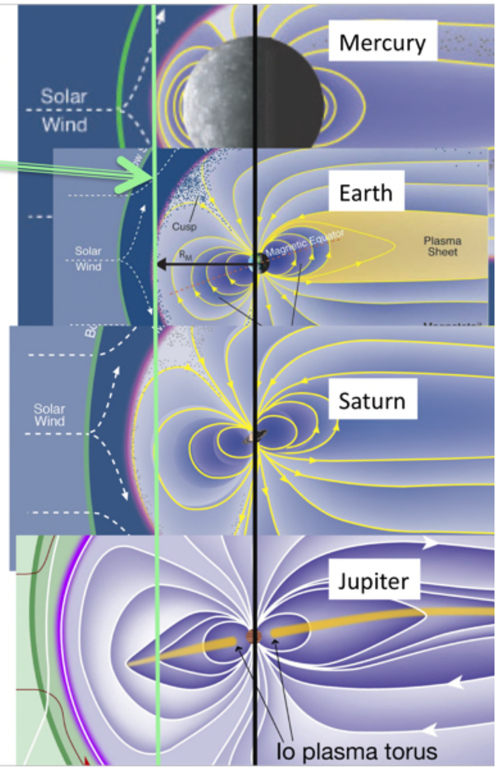


Saturn's aurora

- strongly modulated by the solar wind
- open-closed boundary

*Clarke et al.*

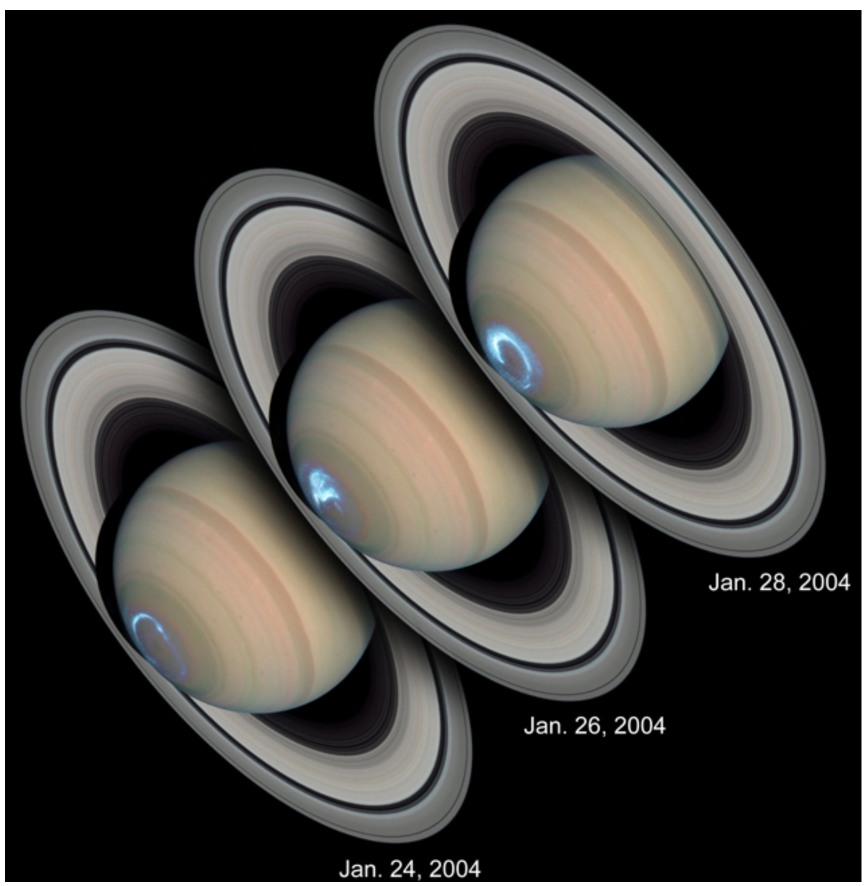

# Uranus

- -Highly asymmetric,
- -Highly non-dipolar
- -Complex transport (SW + rotation)
- -Multiple plasma sources (ionosphere + solar wind + satellites)

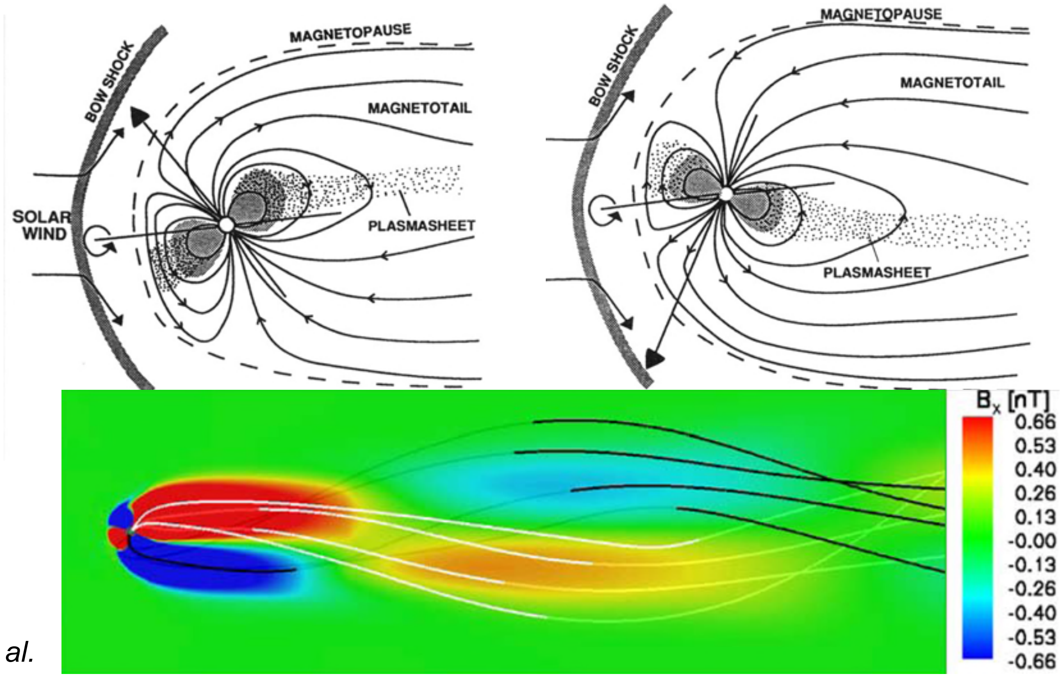


*Toth et al.*

# Neptune

Similarly complex as Uranus

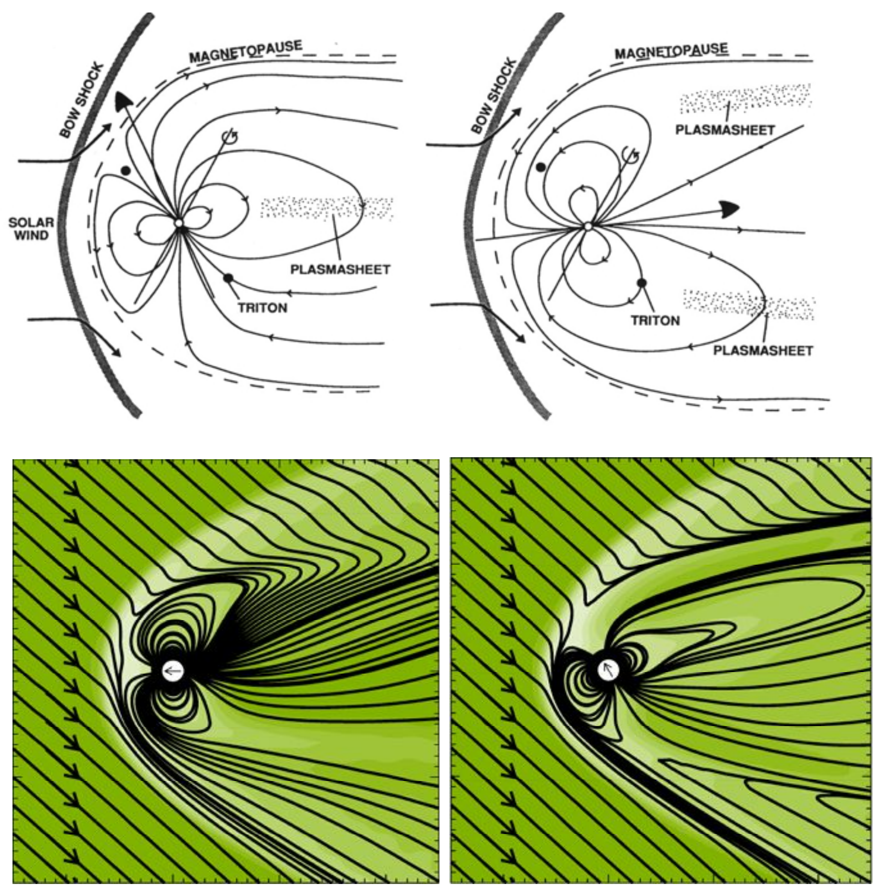


*Zieger et al.*

# *Mercury & Ganymede*

Mercury - Magnetic field detected by *Mariner 10* in 1974

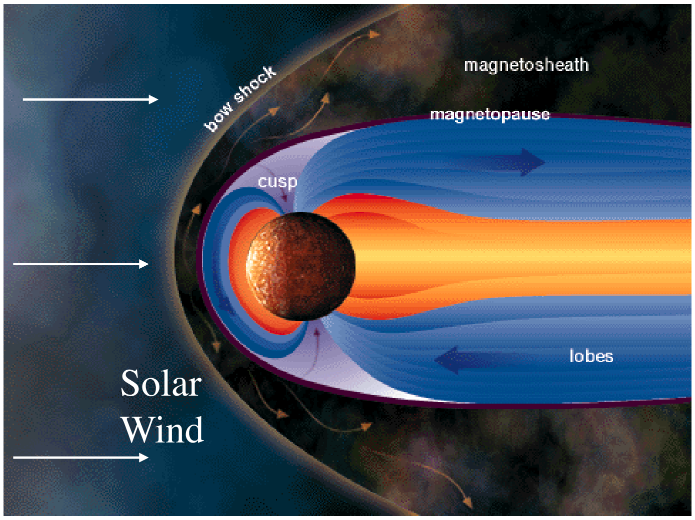


Ganymede - Magnetic field detected by *Galileo* in 1996

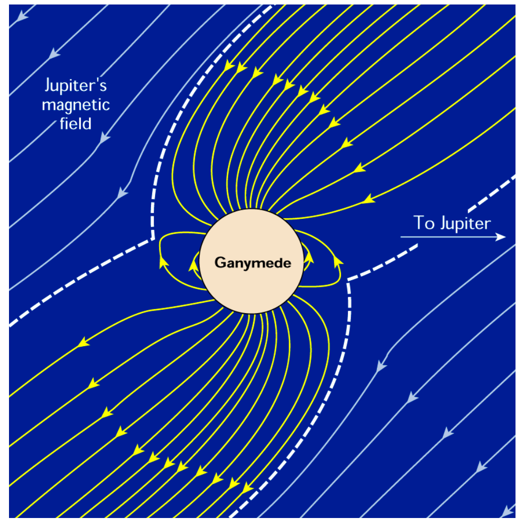


**$B_{surface}$ ~ 1/100 Earth** **Diameter of Earth**

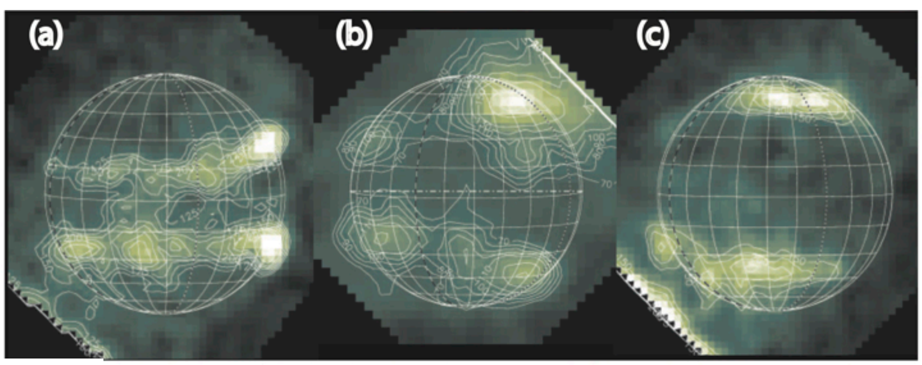


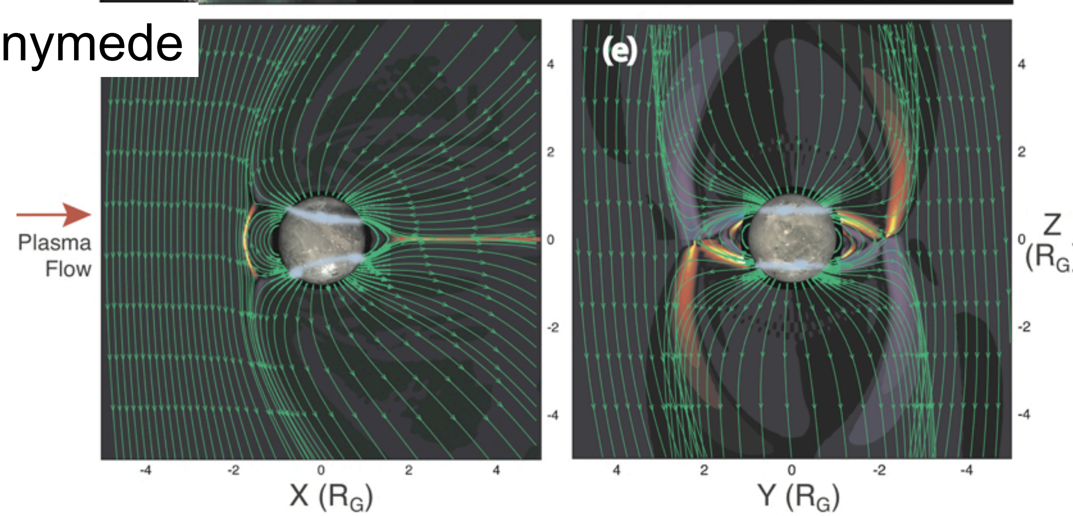

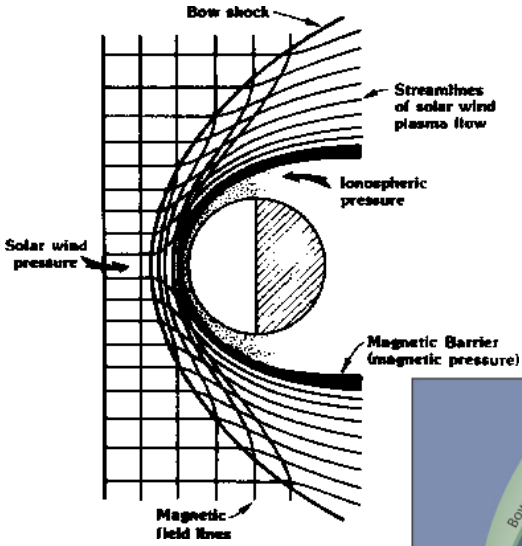


*Pressure Balance:*
Solar wind ram pressure
-> compressed IMF
-> magnetic pressure
vs. ionospheric thermal pressure

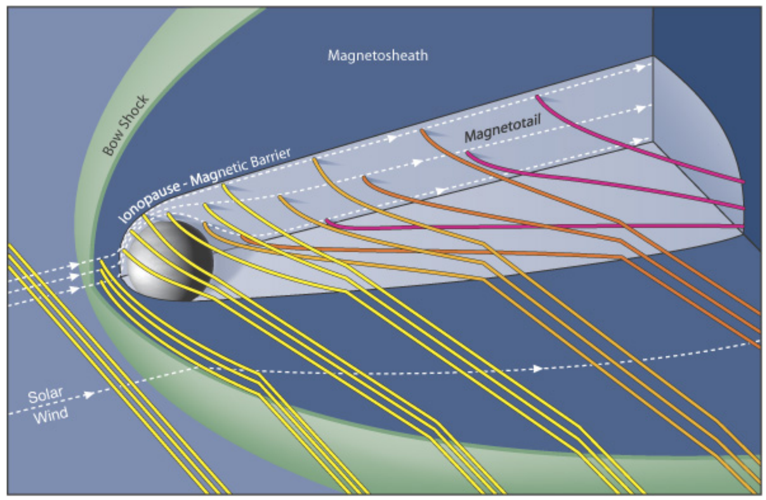


***VENUS***

Mars

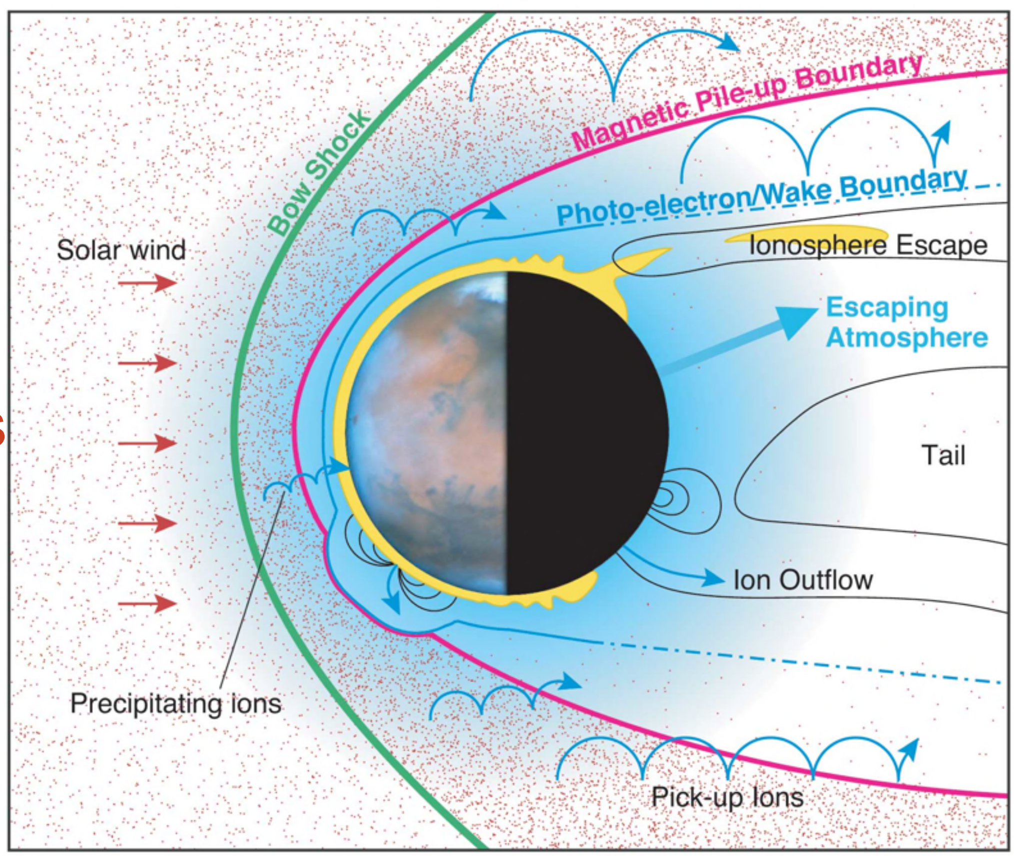

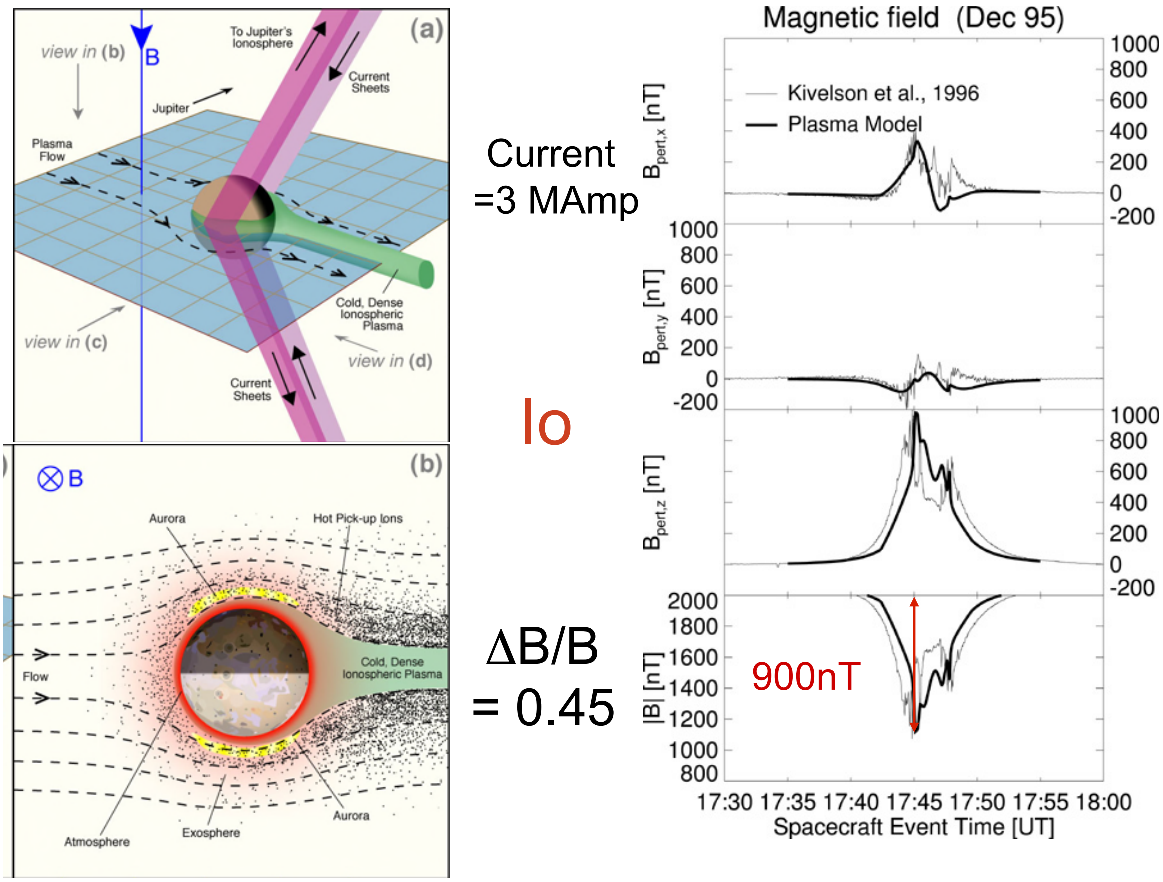


# Summary

- Diverse planetary magnetic fields & magnetospheres
- Dynamo primarily requires region of liquid conducting material that is convecting – generally limited by heat flow in core
- Earth, Mercury, Ganymede magnetospheres driven by reconnection
- Jupiter & Saturn driven by rotation & internal sources of plasma
- Uranus & Neptune are complex – *need to be explored!*